La réparation par excision de nucléotides à la croisée des chemins avec la transcription

Elena Cerutti

N° d'ordre NNT : 2019LYSE1057

THESE de DOCTORAT DE L'UNIVERSITE DE LYON
opérée au sein de
l' Université Claude Bernard Lyon 1

École Doctorale N° 340
Biologie Moléculaire Intégrative et Cellulaire

Spécialité de doctorat : Réparation de l'ADN

Soutenue publiquement le 10/05/2019, par :
Elena CERUTTI

Nucleotide Excision Repair at the crossroad with transcription

---

Devant le jury composé de :

Orioli, Donata – PA – IGM, Università di Pavia	Rapporteure
Coin, Frédéric – DR – IGBMC, Université de Strasbourg	Rapporteur
Schaeffer, Laurent – PU – INMG, Université Lyon 1	Examinateur
Giglia-Mari, Giuseppina – DR – INMG, Université Lyon 1	Directrice de thèse
Mari, Pierre-Olivier – CR – INMG, Université Lyon 1	Co-directeur de thèse
Diaz, Jean-Jacques – DR – CRCL, Université Lyon 1	Invité

UNIVERSITE CLAUDE BERNARD - LYON 1

Président de l'Université	M. le Professeur Frédéric FLEURY
Président du Conseil Académique	M. le Professeur Hamda BEN HADID
Vice-président du Conseil d'Administration	M. le Professeur Didier REVEL
Vice-président du Conseil Formation et Vie Universitaire	M. le Professeur Philippe CHEVALIER
Vice-président de la Commission Recherche	M. Fabrice VALLÉE
Directrice Générale des Services	Mme Dominique MARCHAND

COMPOSANTES SANTE

Faculté de Médecine Lyon Est – Claude Bernard	Directeur : M. le Professeur G. RODE
Faculté de Médecine et de Maïeutique Lyon Sud – Charles Mérieux	Directeur : Mme la Professeure C. BURILLON
Faculté d'Odontologie	Directeur : M. le Professeur D. BOURGEOIS
Institut des Sciences Pharmaceutiques et Biologiques	Directeur : Mme la Professeure C. VINCIGUERRA
Institut des Sciences et Techniques de la Réadaptation	Directeur : M. X. PERROT
Département de formation et Centre de Recherche en Biologie Humaine	Directeur : Mme la Professeure A-M. SCHOTT

COMPOSANTES ET DEPARTEMENTS DE SCIENCES ET TECHNOLOGIE

Faculté des Sciences et Technologies	Directeur : M. F. DE MARCHI
Département Biologie	Directeur : M. le Professeur F. THEVENARD
Département Chimie Biochimie	Directeur : Mme C. FELIX
Département GEP	Directeur : M. Hassan HAMMOURI
Département Informatique	Directeur : M. le Professeur S. AKKOUCHE
Département Mathématiques	Directeur : M. le Professeur G. TOMANOV
Département Mécanique	Directeur : M. le Professeur H. BEN HADID
Département Physique	Directeur : M. le Professeur J-C PLENET
UFR Sciences et Techniques des Activités Physiques et Sportives	Directeur : M. Y. VANPOULLE
Observatoire des Sciences de l'Université de Lyon	Directeur : M. B. GUIDERDONI
Polytech Lyon	Directeur : M. le Professeur E. PERRIN
École Supérieure de Chimie Physique Électronique	Directeur : M. G. PIGNAULT
Institut Universitaire de Technologie de Lyon 1	Directeur : M. le Professeur C. VITON
École Supérieure du Professorat et de l'Éducation	Directeur : M. le Professeur A. MOUGNIOTTE
Institut de Science Financière et d'Assurances	Directeur : M. N. LEBOISNE

« Dans la vie, rien n'est à craindre, tout est à comprendre. »

Marie Skłodowska-Curie

ACKOWLEDGEMENTS/REMERCIEMENTS/RINGRAZIAMENTI

It has been almost 4 years since I started my PhD and I would like to thank all the people that, in one way or another, helped me to get here.

First, I would like to thank Laurent Schaeffer, Donata Orioli and Frederic Coin for accepted to be part of my defence jury and to read and correct my manuscript. Thank you for the kind remarks about my work and for the comments that helped me improve my thesis.

I would like to thank my thesis director, Ambra. I have started my first internship in your group in 2013, when I didn't even know what a pipette was, and, since then, you have never stopped to teach me, science or not, something that have certainly enriched me as a person and a scientist. I also would like to thank my thesis co-director, Pierre-Olivier. I really thank you for your patience explaining me over and over again all the microscopy stuffs, even when I was looking at you with by best "fish face". I am pretty sure that your teaching skills, and your persistence, have borne its fruits; thank you a lot.

Je voudrais aussi remercier tous les membres de l'équipe, qui se sont succédés pendent ces presque 4 ans. En particulier, je voudrais remercier Laurianne, qui m'a introduit en première au sujet du nucléole et de l'ARN Pol I et qui a partager avec moi ses connaissances au début de ma thèse. Merci beaucoup pour ton aide et pour avoir beaucoup discuter avec moi, de science et non, toujours en essayant de comprendre mon française « bizarre ». Ensuite, je voudrais ainsi remercier Anna, qui a débarquée en France au même temps que moi. T'as toujours été très gentille avec moi et ça été très enrichissant pour moi de faire ta connaissance. Parmi les membres présentes de l'équipe, un merci très spécial va surement à Lise-Marie. Merci pour m'avoir aidé, expliqué, supporté, réexpliqué, soutenu, réexpliqué, appris, réexpliqué, montré, écouté, compris… et je ne connais pas d'autres mots pour t'exprimer toute ma reconnaissance. Ça été un très grand plaisir de travailler avec toi et je suis sûre que tu seras une excellente chercheuse. Ensuite, je voudrais dire un grand merci à Damien. Ça été très drôle d'avoir fait ta connaissance et je te remercie vivement pour m'avoir fait rigoler autant. Surtout dans les moments plus difficiles, tu m'as toujours remonté le moral avec tes blagues, et ça c'était tous ce qu'il fallait, donc merci beaucoup. Je veux remercier aussi Charlène, qui est une super technicienne. Ça ne fait pas longtemps que t'es là et probablement t'as fait ma connaissance dans une période pas très facile pour moi, mais t'as toujours été très compréhensive avec moi et ton aide a été très précieux. Je te remercie et j'espère qu'on aura encore l'occasion de passer du temps ensemble et mieux se connaitre. Finalement, je voudrais remercier tous les stagiaires que j'ai pu rencontrer pendent ces presque 4 ans. Ceux que j'ai encadré ou ceux que j'ai juste aidé, vous m'avez tous appris à être

aussi patient que je voudrais que les autres soient avec moi et à vous transmettre mes connaissances comme je voudrais qu'elles me soient transmises. Je ne sais pas si j'ai fait un bon boulot avec vous, mais surement vous l'avez fait avec moi.

Vorrei ringraziare ora la mia famiglia. Quando ho deciso di passare quasi 4 anni in un altro Paese, che per quanto vicino resta comunque un altro mondo, non sapevo cosa sarebbe successo. Ora posso dirvi che l'ancora di sicurezza che voi rappresentate mi è mancata molto. Ciononostante, vi ringrazio per essere sempre stati dalla mia parte e avermi sempre incoraggiato in questa decisione. Vi ringrazio perché, senza il vostro aiuto, molto probabilmente non avrei mai scritto questa tesi e non mi sarei mai resa conto di ciò che voglio veramente fare. Quindi vi ringrazio per questo. Ringrazio anche le mie amiche, Valentina, Veronica e Cristina, che nonostante la lontananza, hanno sempre fatto in modo che non mi perdessi niente delle loro vite, né loro della mia. Sarà un piacere immenso potervi vedere molto più spesso ed essere presente per tutto il bello che verrà. Infine vorrei ringraziare Filippo, che durante questi quasi 4 anni è sempre stato al mio fianco in ogni momento. Ti vorrei ringraziare per ogni piccola e grande cosa che hai fatto per me, ma sarebbe una lista infinita. Quindi ti dico che tutto quel che ho fatto e tutto quel che sono ora è perché ho te al mio fianco, e tutto ciò che farò e tutto quel che sarò, se avrò te al mio fianco, sarà sicuramente meraviglioso.

Merci à tous!

Elena

SUMMARY

Introduction

Cells are the units of organic life and store in their nuclei what constitutes the instruction manual for proper cellular functioning, in the form of the DNA molecule. There are different types of DNA, one of them is ribosomal DNA (rDNA), which is transcribed by RNA polymerase 1 (RNAP1) and is the first step of an important cellular function: ribosomal biogenesis. RNAP1 is responsible for more than 60 % of the total transcriptional activity of the cell and all transcription performed by RNAP1 takes place in a specific subcellular compartment: the nucleolus.

Unfortunately, the integrity of DNA is continuously challenged by a variety of endogenous and exogenous agents (e.g. ultraviolet light, cigarette smoke, environmental pollution, oxidative damage, etc.) that cause DNA lesions, which interfere with proper cellular functions resulting in aging or premature aging of the tissue and eventually, the organism as a whole.

To prevent the deleterious consequences of persisting DNA lesions, all organisms are equipped with DNA repair mechanisms. One of these systems is the Nucleotide Excision Repair (NER). NER removes helix-distorting DNA adducts such as UV-induced lesions (Cyclo-Pyrimidine Dimers and 6-4 Photoproducts, CPD and 6-4PP). NER exists in two distinct sub-pathways depending where DNA lesions are located within the genome. Global Genome Repair (GG-NER or GGR) will repair DNA lesion located on non-transcribed DNA. While, the second sub-pathway is directly coupled to transcription elongation and repairs DNA lesions located on the transcribed strand of active genes. This second sub-pathway is designated as Transcription-Coupled Repair (TC-NER or TCR).

The NER system has been linked to rare human diseases classically grouped into three distinct NER-related syndromes. These include the highly cancer prone disorders Xeroderma Pigmentosum (XP), Cockayne syndrome (CS), and trichothiodystrophy (TTD).

The objective of my thesis was to clarify some aspects of the repair mechanism at the crossroad with transcription. More particularly, my scientific objectives were:

- To concretely identify the players involved in the observed relocation of RNAP1 that occurs after UV irradiation. We identified two proteins involved in this relocation, which are specifically involved in the return of the RNAP1 within the nucleolus after completion of the DNA repair reaction.

- To clearly decipher the molecular mechanism of XAB2 function during DNA repair and to understand whether the function in transcription might be mechanistically similar to the function during DNA Repair.

Results

RNAP1

We have published in the PNAS journal, the article "Mechanistic insights in transcription-coupled nucleotide excision repair of ribosomal DNA", of which I am co-first author. Within this study, we have demonstrated the importance of a fully functional NER mechanism in order to repair UVC lesion on ribosomal genes and that during DNA repair of UV lesions, the RNAP1 is displaced at the periphery of the nucleolus and returns within the nucleolus after DNA repair completion. Furthermore, we have observed that, in a GGR deficient cell line, the RNAP1 transcription restart after repair was not coupled to the re-entry of RNAP1 within the nucleolus.

On these bases, we investigated possible proteins responsible for this re-entry of RNAP1 and that do not take part in the repair process.

We studied two candidate proteins because of their function in RNAP1 transcription and in the cell migration and organelle movement.

- Nuclear Actin: Actin was first described in the cytoplasm where it serves the functions of cellular shape maintenance, cell motility and muscle contraction. However, several studies identified its presence in the nucleus and, more importantly, its interaction with RNAP1.

- Nuclear Myosin I: In the cytoplasm, actin and myosin are part of the motor protein superfamily. In the nucleus, similarly to actin, Nuclear Myosin I has been described to correlate with RNAP1, but it interacts with the polymerase in an indirect way.

In the absence of these two proteins, we have demonstrated that 40h after UVC exposure transcription of ribosomal DNA restarts, but neither RNAP1 nor the rDNA do not relocate within the nucleolus, as it would be expected. In light of these results, we investigated the possibility of these two candidates playing a role in the repair mechanism of NER and we found that there is no evidence of their implication in the repair process, showing that these proteins control the re-entry of RNAP1 and rDNA within the nucleolus without interfering with the DNA repair reaction.

In light of these results, we wanted to investigate if the involvement of Nuclear Actin and Nuclear Myosin I in RNAP1 relocation after repair were transcription-dependent. To do so, we depleted these proteins in cells containing a LacO/LacR-GFP system that allow us to visualize rDNA and we performed RNA fish and RNAP1 Immunofluorescence experiments after Cordycepin

exposure. Cordycepin is an adenosine analogue that inhibits 47S rRNA synthesis in eukaryotic cells in a reversible way. The results we have obtained demonstrate that, in contrast with what happens for UV-irradiation, in the absence of Nuclear Actin and Nuclear Myosin I, 40 hours of recovery after a 2h of Cordycepin treatment, rDNA transcription restarts and the rDNA/RNAP1 relocate within the nucleolus. This result confirms that the rDNA/RNAP1 re-entry within the nucleolus after DNA repair is transcription-independent and that Nuclear Actin and Nuclear Myosin I are responsible for this UV-specific re-entry.

We have then investigated the possible interaction between Nuclear Actin and Nuclear Myosin I, known to be both implicated in different cellular events such as cell migration or muscle contraction, and RNAP1 by Co-Immunoprecipitation experiment on chromatin extracts. Furthermore, we explored the binding profile of Nuclear Actin and Nuclear Myosin I on the ribosomal DNA before and after UV-C exposure. The results we obtained suggest that Nuclear Actin and Nuclear Myosin I could work synergistically to bind rDNA and that both are needed in the same process of repositioning rDNA/RNAP1 within the nucleolus once repair is completed.

XAB2

The XPA-binding protein 2 was identified because of its ability to interact with XPA, a central factor to both GGR and TCR pathways. XAB2 is an 855 amino acids protein consisting of 15 tetratricopeptide repeats. IP experiments demonstrated that a fraction of XAB2 is able to interact with CSA and CSB as well as RNAP2. Since the XAB2 role in the TCR pathway has been poorly investigated so far, our aim was to decipher its function and its mechanism in both DNA repair and RNAP2 transcription.

XAB2 during DNA repair

Normally, 24h after UVC exposure, lesions on the active genes transcribed by RNAP2 are repaired and transcription restarts. In the absence of XAB2, transcription does not restart, suggesting that this protein plays a role in this process. However, it was not known whether XAB2 was implicated directly in the DNA repair reaction or whether it was playing a role in transcription restart after completion of DNA repair. Thanks to a technique developed in our research group, we could demonstrate that XAB2 plays a role in the repair reaction and this role induces a long lasting block of transcription after UV irradiation.

In addition, we investigated the dynamic behavior of XAB2 during repair. Surprisingly, we could show that XAB2 is released from the damaged area, while all the other NER proteins studied so far strongly accumulate on the local lesion.

Without any damage, XAB2 has certain mobility within the nucleus. This mobility is the result of XAB2 diffusion but also of the interactions with the chromatin. Interestingly, when we measured the mobility of XAB2 within CSA and CSB deficient cell lines and without any damage, we observed an increased immobile fraction in both CSA and CSB deficient cell lines, suggesting that CSA and CSB are responsible for the release of XAB2 from a more immobile substrate.

We then investigated, by Co-IP on nuclear extracts, the interaction between XAB2 and RNAP2 before and after UV-C exposure in WT cells and in CSA and CSB deficient cell lines, in order to decipher the mechanistic behavior of XAB2 during repair. The results we obtained demonstrated the presence of XAB2 in a pre-mRNA splicing complex before and after UV-C exposure and that a portion of XAB2 interacts with RNAP2 during the first steps of NER in WT cells, suggesting a role of XAB2 in the damage recognition by the repair machinery.

XAB2 during transcription

It has been demonstrated that XAB2 interacts with the RNAP2. In order to clearly understand the role of XAB2 in RNAP2 transcription we studied the mobility of RNAP2 in presence and absence of XAB2. For this purpose, we used a stable cell line produced in our lab expressing a RNAP2 tagged at the N-terminal with the Green Fluorescent Protein. Using the FRAP technique, we measured and compared the dynamic behavior of RNAP2 in the presence and in the absence of XAB2. The results of this analysis show that in absence of XAB2, RNAP2 bound fraction largely decreased, suggesting that XAB2 plays a role in keeping RNAP2 on the chromatin during the pause of transcription.

RESUMÉ

Introduction

Les cellules sont les unités de la vie organique et stockent dans leurs noyaux ce qui constitue le manuel d'instruction pour le bon fonctionnement cellulaire, sous la forme de la molécule d'ADN. Il existe différents types d'ADN, dont l'ADN ribosomique (ADNr), qui est transcrit par l'ARN Polymérase 1 (ARNP1) et est la première étape d'une fonction cellulaire importante : la biogenèse ribosomique. L'ARNP1 est responsable de plus de 60 % de l'activité transcriptionnelle totale de la cellule et toute transcription effectuée par l'ARNP1 a lieu dans un compartiment subcellulaire spécifique : le nucléole.

Malheureusement, l'intégrité de l'ADN est continuellement remise en question par une variété d'agents endogènes et exogènes (p. ex., la lumière ultraviolette, la fumée de cigarette, la pollution de l'environnement, les dommages oxydatifs, etc.) qui causent des lésions de l'ADN qui interfèrent avec les correctes fonctions cellulaires, entraînant le vieillissement ou le vieillissement prématuré du tissu et, finalement, de l'organisme dans son ensemble.

Afin de prévenir les conséquences néfastes des lésions persistantes de l'ADN, tous les organismes sont équipés de mécanismes de réparation de l'ADN. Un de ces systèmes est la réparation par excision de nucléotides (NER). NER supprime les adduits d'ADN déformant l'hélice tels que les lésions induites par les UV (dimères de cyclo-pyrimidine et 6-4 photo produits, CPD et 6-4PP). NER existe dans deux sous voies distinctes selon l'endroit où les lésions de l'ADN se trouvent dans le génome. Global Genome Repair (GG-NER ou GGR) réparera la lésion d'ADN située sur l'ADN non transcrit. Inversement, la deuxième sous voie est directement couplée à l'allongement de la transcription et répare les lésions de l'ADN situées sur le brin transcrit des gènes actifs. Cette deuxième sous voie est désignée Transcription-Coupled Repair (TC-NER ou TCR).

Le système NER a été associé à des maladies humaines rares classées généralement en trois syndromes distincts liés aux NER. Il s'agit notamment des troubles hautement cancéreux xeroderma pigmentosum (XP), du syndrome de Cockayne (CS) et de la trichothiodystrophie (TTD).

L'objectif de ma thèse était de clarifier certains aspects du mécanisme de réparation à la croisée des chemins avec la transcription. Plus particulièrement, mes objectifs scientifiques étaient les suivants :

- Identifier concrètement les acteurs impliqués dans la relocalisation observée de l'ARNP1 après l'irradiation UV. Nous avons identifié deux protéines impliquées dans cette relocalisation,

qui sont spécifiquement impliquées dans le retour de l'ARNP1 e du ADNr dans le nucléole après l'achèvement de la réaction de réparation de l'ADN.

- Décrypter clairement le mécanisme moléculaire de la fonction de la protéine XAB2 pendant la réparation de l'ADN et comprendre si sa fonction en transcription pourrait avoir un mécanisme similaire à la fonction pendant la réparation de l'ADN.

Résultats

ARNP1

Nous avons publié dans le journal PNAS un article intitulé « Mechanistic insights in transcription-coupled nucleotide excision repair of ribosomal DNA », dont je suis co-premier auteur. Dans le cadre de cette étude, nous avons démontré l'importance d'un mécanisme de NER entièrement fonctionnel afin de réparer les lésions UVC sur les gènes ribosomiques et que lors de la réparation des lésions UV à l'ADNr, l'ARNP1 est déplacé à la périphérie du nucléole et retourne dans le nucléole après la réparation de l'ADN. De plus, nous avons observé que, dans une lignée cellulaire déficiente en GGR, le redémarrage de la transcription par l'ARNP1 après réparation n'était pas couplée à la rentrée du RNAP1 dans le nucléole.

Sur ces bases, nous avons recherché les protéines possibles responsables de cette rentrée de l'ARNP1 et qui ne participent pas au processus de réparation.

Nous avons étudié deux protéines candidates en raison de leur fonction dans la transcription par l'ARNP1 et dans la migration cellulaire et le mouvement des organites.

- Actine nucléaire : l'actine a été décrite pour la première fois dans le cytoplasme où elle sert les fonctions de maintien de forme cellulaire, de motilité cellulaire et de contraction musculaire. Toutefois, plusieurs études ont identifié sa présence dans le noyau et, plus important encore, son interaction avec l'ARNP1.

- Myosine nucléaire I : Dans le cytoplasme, l'actine et la myosine font partie de la superfamille des protéines motrices. Dans le noyau, de la même manière que l'actine, la myosine nucléaire I a été décrite comme étant en corrélation avec l'ARNP1, mais elle interagit avec la polymérase de façon indirecte.

En l'absence de ces deux protéines, nous avons démontré que 40h après l'exposition aux UVC, la transcription de l'ADN ribosomique redémarre, mais ni l'ARNP1 ni l'ADNr ne se relocalise à l'intérieur du nucléole, comme on pouvait s'y attendre. À la lumière de ces résultats, nous avons examiné la possibilité que ces deux candidats jouent un rôle dans le mécanisme de réparation du NER et nous avons constaté que, dans nos conditions, il n'y a aucune preuve de leur implication

dans le mécanisme de réparation, montrant que ces protéines contrôlent la rentrée de l'ARNP1 et de l'ADNr dans le nucléole sans interférer avec la réaction de réparation de l'ADN.

À la lumière de ces résultats, nous voulions déterminer si l'implication de l'actine nucléaire et de la myosine nucléaire I dans la relocalisation de l'ARNP1 après réparation dépendait de la transcription. Pour ce faire, nous avons dépléter ces protéines dans des cellules contenant un système Laco/LacR-GFP qui nous permettent de visualiser l'ADNr et nous avons réalisé des expériences d'ARNfish et d'immunofluorescence contre l'ARNP1 après exposition à la cordycépine. La cordycépine est un analogue de l'adénosine qui inhibe la synthèse de l'ARNr 47S dans les cellules eucaryotes de manière réversible. Les résultats que nous avons obtenus démontrent que, contrairement à ce qui se passe pour l'irradiation aux rayons UV, en l'absence d'actine nucléaire et de myosine nucléaire I, 40 heures de récupération après 2h de traitement par cordycépine, la transcription de l'ADNr redémarre et l'ADNr et l'ARNP1 se relocalise à l'intérieur du nucléole. Ce résultat confirme que la rentrée de ADNr/ARNP1 dans le nucléole après la réparation de l'ADN est indépendante de la transcription et que l'actine nucléaire et la myosine nucléaire I sont responsables de cette rentrée spécifique aux UV.

Nous avons ensuite étudié l'interaction possible entre l'actine nucléaire et la myosine nucléaire I, connue pour être à la fois impliquée dans différents événements cellulaires tels que la migration cellulaire ou la contraction musculaire, et l'ARNP1 par une expérience de co-immunoprécipitation sur des extraits de chromatine. De plus, nous avons examiné le profil de liaison de l'actine nucléaire et de la myosine nucléaire I sur l'ADN ribosomique avant et après l'exposition aux UV-C. Les résultats que nous avons obtenus suggèrent que l'actine nucléaire et la myosine nucléaire I pourraient travailler de manière synergique pour lier l'ADNr et que les deux sont nécessaires dans le même processus de repositionnement de ADNr/ARNP1 à l'intérieur du nucléole une fois la réparation terminée.

XAB2

La protéine XPA-binding protein 2 a été identifiée en raison de sa capacité à interagir avec XPA, un facteur central des voies GGR et TCR. XAB2 est une protéine de 855 acides aminés composée de 15 répétitions de tétratricopeptides. Les expériences d'immunoprécipitation ont démontré qu'une fraction de XAB2 est capable d'interagir avec CSA et CSB ainsi qu'avec l'ARNP2. Depuis que le rôle de XAB2 dans la voie TCR a été peu étudié jusqu'à présent, notre but était de déchiffrer sa fonction et son mécanisme dans la réparation de l'ADN et la transcription par l'ARNP2.

XAB2 pendant la réparation de l'ADN

Normalement, 24h après l'exposition aux UVC, les lésions sur les gènes actifs transcrits par l'ARNP2 sont réparées et la transcription redémarre. En absence de XAB2, la transcription ne redémarre pas, ce qui suggère que cette protéine joue un rôle dans ce processus. Toutefois, on ne savait pas si XAB2 était directement impliqué dans la réaction de réparation de l'ADN ou s'il jouait un rôle dans le redémarrage de la transcription après la réparation de l'ADN. Grâce à une technique développée dans notre groupe de recherche, nous avons pu démontrer que XAB2 joue un rôle dans la réaction de réparation et ce rôle induit un bloc permanent de la transcription après irradiation UV.

De plus, nous avons étudié le comportement dynamique de XAB2 pendant la réparation. Étonnamment, nous avons pu montrer que XAB2 est libéré de la zone endommagée, tandis que toutes les autres protéines du NER étudiées jusqu'à présent s'accumulent fortement sur la lésion.

Sans aucun dommage, XAB2 a une certaine mobilité dans le noyau. Cette mobilité est le résultat de la diffusion de XAB2 mais aussi des interactions avec la chromatine. Il est intéressant de noter que lorsque nous avons mesuré la mobilité de XAB2 dans des lignées cellulaires déficientes par CSA et CSB et sans aucun dommage, nous avons observé une fraction immobile plus importante dans les lignées cellulaires déficientes par CSA et CSB, ce qui laisse entendre que CSA et CSB sont responsables du rejet de XAB2 à partir d'un substrat plus immobile.

Nous avons ensuite étudié, par Co-IP sur des extraits nucléaires, l'interaction entre XAB2 et l'ARNP2 avant et après l'exposition aux UV-C dans des cellules WT et dans des lignées cellulaire déficientes par CSA et CSB, afin de déchiffrer le comportement mécanistique de XAB2 pendant la réparation. Les résultats que nous avons obtenus ont démontré la présence de XAB2 dans un complexe d'épissage de pré-ARNm avant et après l'exposition aux UV-C et qu'une partie de XAB2 interagit avec l'ARNP2 pendant les premières étapes de la réparation de l'ADN dans les cellules WT, suggérant un rôle de XAB2 dans la reconnaissance des dommages par la machinerie de réparation.

XAB2 pendant la transcription

Il a été démontré que XAB2 interagit avec l'ARNP2. Afin de bien comprendre le rôle de XAB2 dans la transcription par l'ARNP2, nous avons étudié la mobilité de l'ARNP2 en présence et en absence de XAB2. À cette fin, nous avons utilisé une lignée cellulaire stable produite dans notre laboratoire exprimant une ARNP2 étiqueté au terminal N avec la GFP. En utilisant la technique de FRAP, nous avons mesuré et comparé le comportement dynamique de l'ARNP2 en présence et en absence de XAB2. Les résultats de cette analyse montrent qu'en absence de XAB2, la fraction

immobile de l'ARNP2 a largement diminué, ce qui suggère que XAB2 joue un rôle dans le maintien de l'ARNP2 sur la chromatine pendant la pause de transcription.

ABBREVIATIONS

5'ETS	5' External Transcribed Spacer
6-4PP	6-4 photoproducts
alt-EJ	alternative End Joining
AP site	Abasic site
APE1	AP-endonuclease 1
BER	Base Excision Repair
BPS	Branch-Point Sequence
BRCA2	Breast Cancer 2
BRE	TFIIB Recognition Element
CAF-1	Chromatin Assembly Factor-1
CAK	CDK-Activating Kinase
Cdk7	Cyclin-dependent kinase 7
Cdk9	Cyclin-dependent kinase 9
CHD1	Chromodomain-Helicase-DNA-binding protein 1
CK2	serine/threonine kinase
CPD	Cyclobutane Pyrimidine Dimers
CPSF	Cleavage and Polyadenylation Specificity Factor
CS	Cockayne Syndrome
CSA	Cockayne syndrome A
CSB	Cockayne syndrome B
CstF	Cleavage stimulatory Factor
CTD	C-Terminal Domain
CtIP	C-terminal binding protein-Interacting Protein
DDB1	DNA Damage-Binding protein 1
DDB2	DNA Damage-Binding protein 2
DFC	Dense Fibrillar Component
DJ	Distal Junction
Dna2	DNA2-like helicase
DNA-PK	DNA-dependant Protein Kinase
DNMT1	DNA Methyltransferase 1
DNMT3	DNA Methyltransferase 3
DNTT	DNA nucleotidyltransferase
DOT1L	Disruptor Of Telomeric silencing 1-Like
DPE	Downstream Promoter Element
DSB	Double Strand Break
DSIF	DRB Sensitivity Inducing Factor
EF	Elongating Factors
ELL	Eleven-nineteen Lysine-rich Leukemia protein
ERCC1	Excision Repair Cross-Complementation group 1
EXO1	Exonuclease 1
FACT	Facilitates Chromatin Transcription
FC	Fibrillar Center
GC	Granular Component
GG-NER	Global-Genomic Repair
HMG	High Mobility Group
HP1	Heterochromatin Protein 1
HR	Homologous Recombination
Inr	Initiator element
ITS	Internal Transcribed Spacers

LIG1/LIG3	DNA Ligase 1/3
MLH1	MutL homolog 1
MMR	Mismatch Repair
MSH2	MutS protein homolog 2
MSH6	MutS protein homolog 6
Nbs1	Nibrin
NELF	Negative Elongation Factor
NER	Nucleotide Excision Repair
NFR	Nucleosomal-Free Region
NHEJ	Non-Homologous End-Joining
NOR	Nucleolar Organizer Region
NoRC	Nucleolar Remodelling Complex
NTC	Nineteen Complex
NTIS	Non-Transcribed Intergenic Spacer regions
NTP	Nucleosides Triphosphate
NTR	Nineteen-Related
PAF1C	Pol II-Associated Factor 1 Complex
PAH	Polycyclic Aromatic Hydrocarbons
PARP-1	Poly [ADP-ribose] Polymerase 1
PCNA	Proliferating Cell Nuclear Antigen
PH	Pleckstrin Homology
PIC	Pre-Initiation Complex
PJ	Proximal Junction
PMS2	Mismatch repair endonuclease PMS2
PNBs	PeriNucleolar Bodies
Polβ	DNA polymerase β
P-TEFb	positive-Transcription Elongation Factor
PTM	Posttranslational Modification
PTRF	Pol 1 and Transcript Release Factor
rDNA	ribosomal DNA
RES	Retention and Splicing complex
RFC	Replication factor C
RNAP1	RNA Polymerase 1
RNAP2	RNA Polymerase 2
RNAP3	RNA Polymerase 3
ROS	Reactive Oxygen Species
RPA	Replication Protein A
RRN3	RNAP1-specific transcription initiation factor
rRNA	ribosomal RNA
SL1	Selectivity Factor 1
snRNA	small nuclear RNA
snRNA	small nuclear RNA
snRNP	small nuclear ribonucleoprotein
SSA	Single-Strand Annealing
SSB	Single Strand Brake
ssDNA	single strand DNA
TAFs	TBP-Associated Factors
TBP	TATA-Binding Protein
TC-NER	Transcription-Coupled Repair
TFIIA	Transcription Factor II A
TFIIB	Transcription Factor II B

TFIID	Transcription Factor II D
TFIIE	Transcription Factor II E
TFIIF	Transcription Factor II F
TFIIH	Transcription Factor II H
TFIIS	Transcription Factor II S
TSS	Transcription Start Site
TTD	Trichothiodistrophy
TTF-1	Transcription Termination Factor
UBF	Upstream Binding Factor
UCE	Upstream Control Element
USP7	Ubiquitin Specific Peptidase 7
UVSS	UV-sensitive Syndrome
UVSSA	UV Stimulated Scaffold protein A
XAB2	XPA-Binding protein 2
XLF	XRCC4-like factor
XP	Xeroderma Pigmentosum
XPA	Xeroderma Pigmentosum, Complementation group A
XPB	Xeroderma Pigmentosum, Complementation group B
XPC	Xeroderma Pigmentosum, Complementation group C
XPD	Xeroderma Pigmentosum, Complementation group D
XPF	Xeroderma Pigmentosum, Complementation group F
XRCC1	X-ray repair cross-complementing protein 1
XRCC4	X-ray repair cross-complementing protein 4
XRN2	5'-3' Exoribonuclease 2

TABLES AND FIGURES

TABLE OF CONTENTS

INTRODUCTION

1. DNA Damage and Repair

The DNA macromolecule enclosed in the nucleus of our cells represents the foundation of life for all organisms. It contains all the genetic information, which characterizes our phenotype, e.g. the colour of our eyes, as well as all the instructions that are required for the proper functioning of our physiological processes.

Unfortunately, the DNA structure is continuously challenged by an extended number of damaging agents, which are responsible for the production of a variety of DNA lesions. These DNA-damaging factors originate from three main sources (1):

a. Environmental agents such as UV light, ionizing radiation, air polluting agents and other genotoxic agents, e.g. cigarette smoke
b. Products of cellular metabolism such as reactive oxygen species (ROS) generated by oxidative respiration and products of lipid peroxidation
c. Spontaneous disintegration of DNA chemical bonds, e.g. hydrolysis of nucleotide residues or deamination of cytosine, adenine and guanine

The consequences of a defective DNA damage repair can be deleterious for the organism survival. In actively dividing cells, the damaged DNA strand can be replicated in a permanent mutated form, increasing the risk of cancer development (2). On the other hand, lesions may also block the transcription process, causing cell death or senescence and contributing to aging (3). In order to protect the DNA integrity and to prevent formation of deleterious mutations, cells developed several repair mechanisms able to eliminate DNA persisting lesions.

1.1. Types of DNA lesions

The most succinct, and at the same time complete, definition of DNA damage is: *"Damage to DNA consists of any change that introduces a deviation from the usual double-helical structure"*(4)

The various types of damages that our DNA can be subject to are listed below and their frequency rate is represented in Table 1.

Deamination: is a very common type of hydrolytic lesion and leads to the conversion of one base to another, resulting in a mismatch. For example, deamination of cytosine results in uracil, which preferentially pairs with adenine rather than guanosine, thus creating a mismatch. Then, when the cell undergoes replication, this will result in the substitution of a C:G pair with an A:T pair.

Depurination: is another very common lesion caused by hydrolytic loss of nitrogenous bases. Depurination is strongly affected by temperature and, among the total loss of nitrogenous bases, it occurs at a much higher rate compared to pyrimidine loss (5). In general, loss of nitrogenous bases leads to abasic sites, which may promote DNA strand breakage or base mismatch.

Alkylation: the most common alkylation reaction involves methylation of nitrogenous bases. It usually affects a nitrogen or an oxygen atom, thus resulting in a variety of modified bases, which have different pairing properties. Alkylated bases may also be subject to further modification, like for the 5-methylcytosine that is then deaminated to thymine, resulting in DNA mismatch. Furthermore, methylation has also a role in the alteration of chromatin architecture and deregulation of gene expression, through methylation of cytosine residues in CpG islands.

Oxidation: can affect the purine bases, as well as the pyrimidines. Oxidation of purines leads to 8-oxo-G or 8-oxo-A, while pyrimidine oxidation lead to glycol or -hydroxy compounds formation. Base oxidation is often coupled to strand breaks, both caused by ROS. Accumulation of oxidative damages is related to ageing (6).

Strand breaks: are the result of the disruption of the phosphodiester bond between two adjacent deoxyribose residues on one strand (Single-Strand Breaks, SSB) or on both strands (Double-Strand Breaks, DSB) of the DNA helix. Strand breaks frequently occur during normal DNA manipulations, such as transcription or replication, or genotoxic stresses caused by cell metabolism, such as ROS accumulation. DSB are less common in cells, since their presence is lethal; however, they are physiologically necessary for specific phases of cell cycle and only for some type of cells in order to allow homologous recombination of genetic information, e.g. they occur in germ cells during meiosis or in developing lymphocytes during V(D)J recombination. DSB can also be induced by exogenous agents like high-energy electromagnetic radiations (mostly ionizing radiations).

Dimerization: Dimers normally do not exist in DNA and their formation is most often caused by high-energy and short-wavelength UV light ranging between 280 and 350 nm (UV-B and UV-A). Dimerization can occur between two bases on the same strand or between bases from different DNA strands. There are two types of dimers in DNA: 6-4 photoproducts (6-4PP) that can involve T/C, C/C or T/T or Cyclobutane Pyrimidine Dimers (CPD) involving only T/T.

Bulky adducts and Inter/Intra-strand crosslinks: These lesions, as well as dimerizations, create physical impediments for processes such as transcription or replication of the DNA

double helix. Bulky lesions are formed by aromatic compounds, such as Polycyclic Aromatic Hydrocarbons (PAH), or by products of benzopyrene metabolism *in vivo* (a composite of cigarette smoke). Inter and Intra-strand crosslinks can be caused by intercalating agents, such as psoralen that is activated in presence of UV-A light, antibiotics as Mitomycin C, or even classic anticancer agents such as cisplatin derivatives (7).

Rate of DNA lesions per human cell per day	
Single strand break	55.000
Depurination	10.000
Deamination	400
Oxidation	1000
Alkylated bases	5000
Intra-strand crosslink	10
Double strand break	10-50
Dimerization (after a day of sun exposure)	100.000

Table 1. Rate of DNA damage per human cell per day
Information of different damages rates have been taken from (2, 8-11)

1.2. Repair mechanisms

All the repair mechanisms described below include a series of factors that participate in diverse and tightly regulated steps and some proteins are shared by different repair pathways. All these mechanisms are coupled to a signaling machinery communicating with the cell cycle in order to inhibit, when it is necessary, cell cycle progression and to give the cell the time for repair (12). Therefore, it has to be highlighted the intrinsic complexity of these repair mechanisms and the importance of their regulation.

1.2.1. Base Excision Repair

Base Excision Repair is responsible for the detection and repair of the most common type of DNA damages. Indeed, BER recognizes and removes small helix distorting lesions such as base oxidation by Reactive Oxygen Species (ROS), deamination and alkylation. ROS are generated, among others, as a product of the normal mitochondrial activity. Without BER, these lesions would potentially block DNA replication and increase the prevalence of disease causing mutations within the genome.

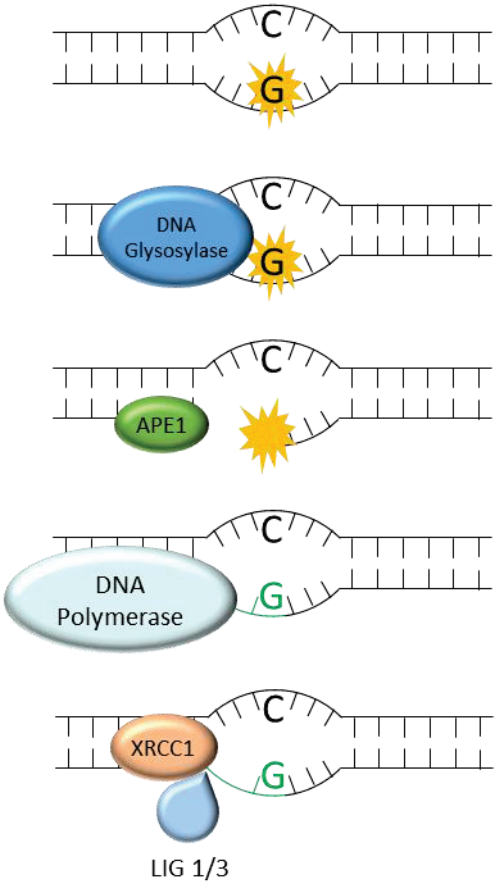

In the initiation step of BER, a damage specific DNA glycosylase identifies and removes the damaged base through cleavage of the bond between the target base and deoxyribose, leaving an intact abasic site (AP site). At least 11 different mammalian DNA glycosylases are known, which are sorted into four super families based on their structural characteristics. The intact AP site is then processed by a human AP-endonuclease 1 (APE1), which leads to the formation of a single strand break. A DNA polymerase (polβ) performs the removal of the sugar residue and the insertion of the new nucleotide. Finally, a Ligase (LIG1/LIG3) and the scaffolding protein XRCC1 seal the nick (13, 14).

Figure 1. Base Excision Repair mechanism

1.2.2. Mismatch Repair

The Mismatch Repair (MMR) pathway is involved in the correction of errors that escape polymerase proofreading during replication. MMR is responsible for the detection and repair of insertion/deletion loops and base-base mismatches; defects in this pathway result in a mutator phenotype leading to a strong cancer predisposition.

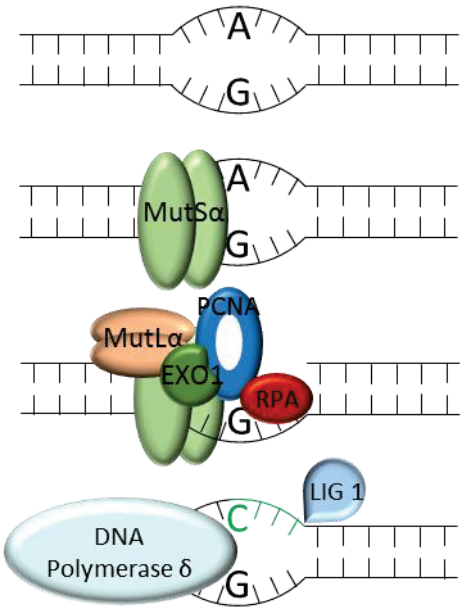

Figure 2. Mismatch Repair mechanism

The mismatch recognition process starts with the binding to the lesion of the MSH2/MSH6 heterodimer, named MutSα. MutSα undergoes an ATP-driven conformational change and recruits the MLH1/PMS2 complex, MutLα. This ternary complex can translocate in both directions along the DNA. When it encounters a strand discontinuity, it recruits the Proliferating Cell Nuclear Antigen complex (PCNA) and the EXO1 exonuclease to initiate degradation of the nicked strand. The resulting single strand is stabilized by Replication Protein A (RPA), then the gap is filled by DNA polymerase δ and the remaining nick is filled by DNA ligase 1 (LIG1) (15, 16).

1.2.3. Homologous Recombination

Homologous Recombination (HR) is one of two repair mechanisms for Double Strand Breaks (DSB). DSBs can arise from ionizing radiation, anticancer treatments, DNA replication errors leading to replication fork collapse, and even ROS. Even if the rate of DSBs is estimated at 10 per cell, per day, they are considered one of the most harmful lesions for the cell since even one unrepaired DSB can lead to deleterious mitosis or chromosome instability.

HR is a highly conserved, error-free mechanism that only occurs during the S or G2 phases of the cell cycle, when a homologous template *via* the sister chromatid is available. The first step of HR is defined by DSB end resection involving the MRN complex, formed by Mre11, Rad50 and Nbs1, and the C-terminal binding protein-Interacting Protein (CtIP), which activates the MRN complex to initiate the resection. More extensive resection, performed by the exonuclease 1 (EXO1) together with the Dna2/BLM complex, contributes to the formation of a 3’ single-strand DNA which is protected by the recruitment of RPA proteins. RPA competes with Rad51, such that a number of proteins termed mediators (Rad52, BRCA2 and Rad54) are necessary to displace RPA

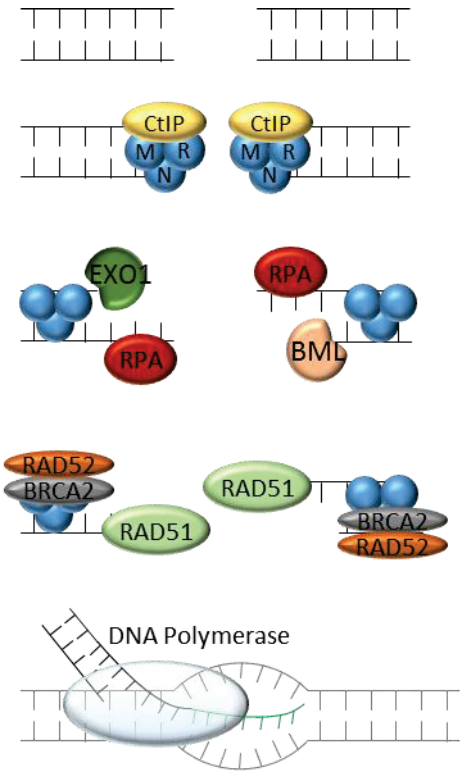

Figure 3. Homologous Recombination mechanism

and promote Rad51 binding. Actually, Rad51 drives the defining step of HR represented by the invasion of the 3' ssDNA into a homologous duplex. After strand invasion of the sister chromatid, a DNA polymerase can synthetize the new DNA on the damaged strand (17-19).

Another pathway responsible for DSBs processing is termed Single-Strand Annealing (SSA). SSA concerns DSBs occurring on genes containing sequence repeats, such as ribosomal DNA, and it requires a homology of at least 20 bp. SSA is a non-conservative mechanism since it requires deletion of several nucleotides. Similar to HR, the process starts with DNA end resection, but Rad52 aligns the two DNA repeated sequences and the generated ssDNA tails are removed by the ERCC1/XPF nuclease (20).

1.2.4. Non-Homologous End-Joining

DSB can also be repaired via an additional pathway termed Non-Homologous End-Joining (NHEJ). NHEJ mediates the direct ligation of the broken DNA molecule and, since it does not require a homologous template for repair, it is not confined to a certain phase of the cell cycle. Therefore, it is the major and faster mechanism that repairs DSB, but it is also potentially error-prone, due to the absence of a template.

The initial steps of NHEJ is the recognition and binding of the Ku heterodimer (Ku70/Ku80) to the DSB in a ring-shaped structure, which can accommodate the double strand DNA helix. The Ku heterodimer's function is to recruit the DNA-dependant protein kinase catalytic subunit (DNA-PKcs) and to stimulate its autophosphorylation. Upon DNA-PKcs phosphorylation, multiple DNA end-processing factors are also recruited to the break site to prepare the DNA ends for ligation, such as the endonuclease Artemis and the DNA nucleotidylexotransferase (DNTT) which catalyses the addition of nucleotides in the 3' terminus without a DNA template. These DNA end-processing steps make DNA ends compatible for ligation where the final phase is mediated by the complex DNA Ligase4/XRCC4/XLF (18, 21, 22).

Similar to NHEJ, DSBs can be processed by an alternative form of NHEJ, termed alt-EJ. This additional mechanism normally acts when the classical-NHEJ is compromised and it requires a

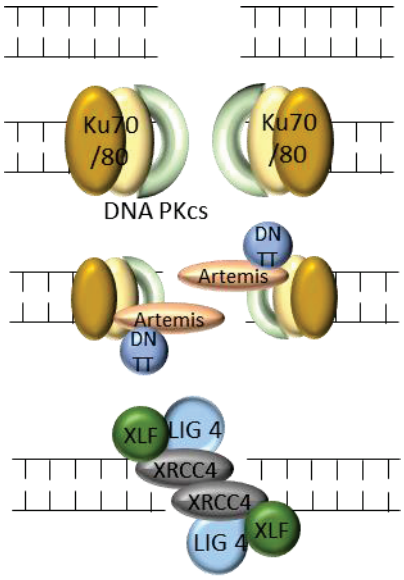

Figure 4. Non-Homologous End-Joining mechanism

homology between the double strands DNA of less than 20 bp. One of the first proteins implicated in alt-EJ is the Poly [ADP-ribose] Polymerase 1 (PARP-1) that binds the DSB in a competitive way with the Ku heterodimer, thus determining the choice between the c-NHEJ and alt-EJ. DNA ends are then processed by the MRN complex, stimulated by the phosphorylated CtIP. The DNA polymerase θ binds directly to resected DNA and synthetizes the new strand. DNA Ligase 1 or 3, with the recruitment or not of XRCC1, perform the end-ligation (18, 22).

1.3. Nucleotide Excision Repair

The Nucleotide Excision Repair mechanism (NER) was described for the first time in the early 1960s thanks to the work of Setlow, Howard-Flanders and Hanawalt (23-25). NER is the repair pathway responsible for detection and repair of a broad variety of helix-distorting DNA lesions, such as UV-induced Cyclobutane Pyrimidine Dimers (CPDs) or 6-4 Pyrimidine-pyrimidone Photoproducts (6-4PPs), but also of oxidative damage, bulky lesions and intrastrand crosslink formed by cancer chemotherapeutic drugs such as cisplatin (3, 26, 27).

The NER process starts with the recognition of the DNA lesion after which, the damaged strand is incised on both sides of the ≈ 30 nucleotide long stretch before it can be removed. A new DNA patch is synthetized using the undamaged complementary strand and is ligated with the contiguous filament. (28) The NER mechanism will be described in more details below.

1.3.1. Lesions recognition

The lesion detection step is a specific process that divides the NER mechanism into two sub-pathways: Global-Genome Repair (GG-NER), operating throughout the genome, and Transcription-Coupled Repair (TC-NER), which detects lesions on the transcribed DNA strand of transcriptionally active genes (29).

1.3.1.1. GGR

The UV light induced 6-4PPs and CPDs cause different distortions to the DNA double helix. 6-44PPs create a DNA alteration sufficient to be directly detected by the XPC/hRAD23b/Centrin2 complex, while CPDs cause a minor distortion of the double helix that is not detectable by the XPC complex but will be first recognized by the DNA Damage-Binding protein 2 complex (DDB2). It is for this reason that detection and repair of CPDs is slower than that of 6-4PPs (30, 31).

The DDB2 protein (encoded by the *xpe* gene) forms a heterodimeric complex with the DDB1 protein (also termed XPE binding-factors) and together are part of the CUL4-ROC1 ubiquitin ligase complex that ubiquitinates DDB2, XPC and histones upon DNA damage. DDB2 binds to the CPD lesion thanks to a hydrophobic pocket that accommodates the lesion and creates a protrusion that facilitates recognition of the damage by the XPC complex (31-33).

The XPC protein has been shown to bind to the strand opposite the lesion. Studies conducted on Rad4, the yeast orthologue of XPC, has demonstrated that a β-hairpin domain encircles two nucleotides opposite the damage, displaying increased ssDNA character due to the thermodynamic destabilization caused by the lesion (34). The hRAD23b protein stabilizes XPC by

protecting it from degradation by the ubiquitin–proteasome system and facilitates XPC binding to the damaged site, but it rapidly dissociates from XPC upon binding to damaged DNA strand (35, 36). The centrin2 protein is a calcium-binding protein of the calmodulin family and its interaction with XPC *via* its C-terminal domain has been shown to stimulate NER activity (37, 38). The XPC/hRAD23b/Centrin2 complex melts the DNA around the lesion and recruits the multiprotein complex TFIIH. Okuda et al. have recently demonstrated that XPC recruits TFIIH by binding to the pleckstrin homology (PH) domain of TFIIH subunit p62 (39).

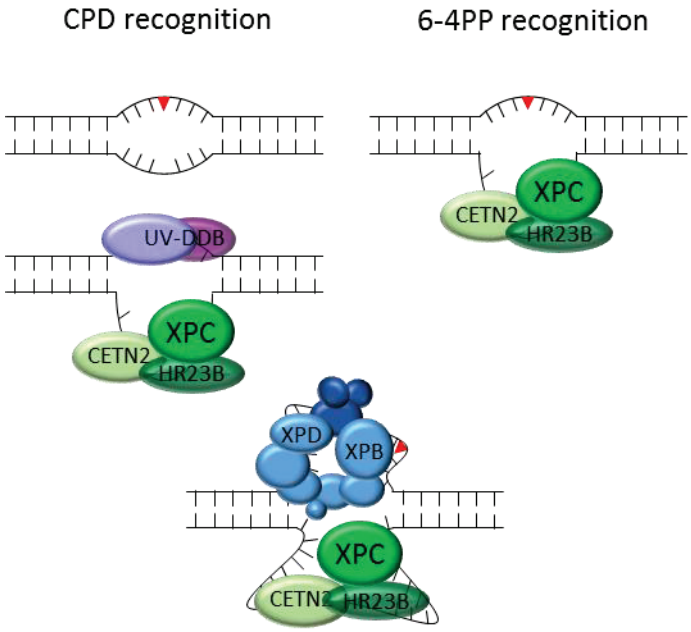

Figure 5. GGR recognition of UV lesions

1.3.1.2. TCR

The arrest of an elongating RNAPII by the lesion present on the transcribed strand is the damage recognition step in TCR. The fate of RNAPII and the way NER system has access to the lesion have not been clarified yet, but several scenarios have been proposed (40). Sarker et al. suggested that elements of the NER machinery might have access to the lesions upon polymerase remodelling (41). Alternatively, a translesional mechanism has been described, in order to clear the way for GGR to find and repair the lesion post-transcriptionally, but this could result in transcriptional mutagenesis (42, 43). Another hypothesis that is presented is that, since stalled RNAP2 can lead to cell death, RNAP2 may undergo degradation with transcript abortion (44). An additional scenario is represented by a backtracking mechanism of the RNAP2. Backtracking, or reverse translocation, can occur to allow space for the repair complex to operate and it could be

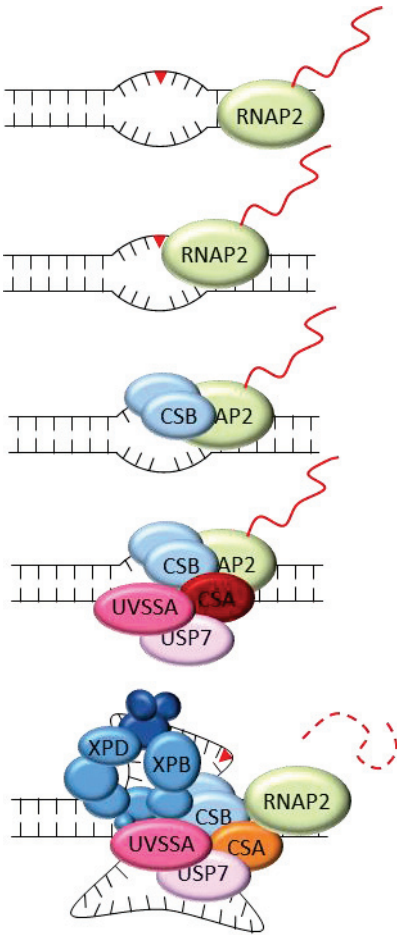

Figure 6. TCR recognition of UV lesions

TFIIS-mediated. Indeed TFIIS has been found to facilitate the transcript cleavage activity of RNAP2, which is necessary for resumption of elongation (45-47). Furthermore, Chiou at al. demonstrated that RNAP2 dissociates from the template during transcription-coupled repair (48).

After RNAP2 arrests, it recruits the CSB homodimer, a transcription elongation factor that translocates along the DNA template with RNAP2. CSB tightly binds the stalled RNAP2 and alters the RNAP2/DNA interface by wrapping the DNA around itself (49). CSB is a SWI/SNF-like DNA-dependent ATPase; its C-terminal region is required for RNAP2 interaction and CSA translocation to the nucleus and undergoes SUMOylation (50, 51). CSB colocalizes with other types of DNA lesions, such as oxidative damage, double-strand breaks and interstrand crosslink (52).

Subsequently, CSB, together with the stalled RNAP2, recruits the CSA protein. CSA is a WD40 motif-containing protein that interacts with Cullin4A (Cul4A) and ROC1/Rbx1 ubiquitin E3 ligase and is initially inhibited after UV irradiation *via* its association with the COP9 signalosome and later becomes activated to ubiquitinate and degrade CSB (53). Actually, CSA-dependent degradation of CSB is required for recovery of RNA synthesis after UV damage (54). CSA is also responsible for the recruitment of the UVSSA/USP7 complex (55).

The UVSSA protein and its partner USP7 are associated with elongating RNAP2. After the block of transcription, UVSSA and USP7 strongly bind to RNAP2. These factors facilitate CSA and CSB-dependent ubiquitination of the phosphorylated form of RNAP2, which deubiquitylates CSB to stabilize it and facilitate RNAP2 recycling for transcription restart after repair (56-58). Similar to TFIIH recruitment by XPC in GGR, UVSSA binds to the p62 PH domain and recruits TFIIH to the site of damage (59).

1.3.2. Opening, Excision and Synthesis

After the lesion recognition step, both GGR and TCR converge into the same pathway with the recruitment of the TFIIH complex in 5' to the damage. TFIIH is a basal transcription/repair complex of 10 subunits divided between the core and the CAK. Two of the core proteins, the

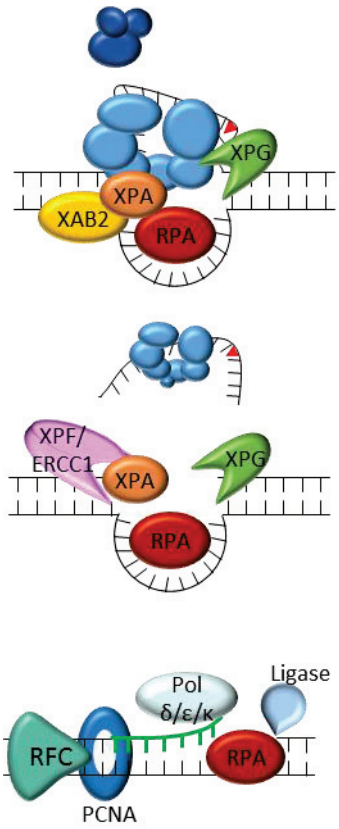

Figure 7. NER common pathway

ATPase/helicases XPB and XPD, are responsible for unwinding the DNA to create a 30 nucleotide repair bubble. Concerning the XPB protein, only its ATPase activity is essential for NER, while XPD must be active as both ATPase and helicase. Another TFIIH subunit, the small p8 protein (TTD-A) has a NER specific role by acting as a stabilizer of TFIIH and facilitating the formation of the DNA repair bubble (60, 61).

Once the pre-excision complexes are assembled, XPA, RPA and XPG are sequentially recruited. The XPA protein binds the DNA close to the 5' side of the bubble and is a central NER factor: it promotes the dissociation of the CAK complex from the TFIIH core; it interacts with TFIIH, RPA and PCNA and it recruits the XPF/ERCC1 endonuclease (62). RPA is a three subunit protein that binds the ssDNA opposite the lesion in order to protect it from other ssDNA binding proteins and from degradation (63). Interestingly, a novel protein has been found interacting with XPA, named XPA-Binding protein 2 (XAB2) (64), and its role in NER will be described in more details in the Results section.

The dual incision event is accomplished by the two endonuclease XPF/ERCC1 and XPG. XPG is the first recruited by TFIIH to the 3' side of the bubble, but this incision is only triggered later, following the 5' incision by XPF/ERCC1, which is recruited by XPA. There is a defined order for the incision step and, since XPF/ERCC1 generates a free 3' hydroxyl group, the replication machinery can initiate the synthesis of the new strand even before the second incision has taken place (65, 66).

The DNA replication machinery necessary for the synthesis of the new DNA strand is recruited to the repair bubble by the sliding clamp Proliferating Cell Nuclear Antigen (PCNA) and the Replication factor C (RFC) (67). The DNA polymerase ε is responsible for DNA synthesis in replicative cells, while DNA polymerase δ and κ synthetize the new strand in non-dividing cells (68). The proliferative status of the cell also defines the DNA ligase used for the sealing of the new strand with the contiguous filament. In proliferating and non-proliferating cells the nick is sealed by LIG3/XRCC1 and LIG1 respectively (63).

1.3.3. Transcription restart

After that repair of UV lesions on actively transcribed genes is completed, transcription by the RNAP2 and RNA synthesis need to restart. Multiple factors have been shown to be required for transcription resumption. One of these factors is the RNA polymerase 2 elongation factor Eleven-Nineteen Lysine-Rich Leukemia protein (ELL) that interacts with TFIIH via the Cyclin dependent kinase 7 (Cdk7) and has been shown to serve as a docking site and to promote resumption of transcription (69). It has also been shown that knockdown of TFIIS results in high levels of hyperphosphorylated RNAP2 and impaired transcription recovery, suggesting a post-repair function (70). Furthermore, some chromatin remodelling factors, such as DOT1L (71), HIRA and FACT, have been proposed to cooperatively work together to promote recovery of RNA synthesis (72).

1.3.4. Associated diseases

Mutations in different NER proteins can lead to several rare recessive photosensitive syndromes such as: Xeroderma Pigmentosum, Cockayne syndrome, Trichothiodystrophy and UV-sensitive syndrome. Despite these diseases have been extensively studied, there still are clinical outcomes that are not totally understood, such as the sun-sensitive skin associated with skin cancer predisposition occurring only in the case of XP patients.

1.3.4.1. Xeroderma Pigmentosum (XP)

Xeroderma pigmentosum is a rare and inherited disease caused by mutations in one of the seven complementation groups encoding for proteins XP-A to XP-G. An additional complementation group, XPV, is NER proficient and the disease is due to mutation in DNA polymerase η, a translesional polymerase responsible for replication of DNA containing unrepaired UV-lesions.

XP patients present parchment skin and freckles on skin regions exposed to the sun and they have marked skin sun sensitivity with a >1000-fold increased risk to develop skin cancers. The mean age of onset of these symptoms is 2 years and the mean age of onset of skin cancer is 8 years old. In addition to skin abnormalities, a fraction of XP patients (≈ 30%) displays progressive neurologic degeneration. Although there is no treatment for the disease at the time, some precautionary measures can be adopted, as special UV-filters which are applied on windows or to avoid skin exposure to the sun without a sunscreen (73, 74).

1.3.4.2. Cockayne Syndrome (CS)

Cockayne Syndrome is caused by mutations on the CSA and CSB complementation group proteins, so CS patients have a defective TCR repair pathway. The symptoms of the disease are mostly neurological, such as neurodemyelinnation, mental retardation, hearing loss, growth failure and microcephaly. Unlike the other NER diseases, CS also include immature sexual development. Surprisingly, CS patients are apparently not predisposed to develop skin cancer. Many of the clinical symptoms of CS patients are difficult to explain just in light of a partial defective NER, but they could be due to the CSA and CSB transcriptional engagement. Approximately 10% of CS cases present rare mutations in XPB, XPD, XPG or ERCC1 leading to a XP/CS combined phenotype. This includes XP skin phenotype, including cancer predisposition, in addition to neurological abnormality of CS (54, 73).

1.3.4.3. Trichothiodistrophy (TTD)

Trichothiodistrophy is caused by certain mutations on the XPB and XPD genes and on the TTDA gene. The hallmark of TTD is the presence of sulphur-deficient brittle hair. Depending on the severity of the case, other symptoms can include ichthyosis, microcephaly, neurological defects, premature aging feature and intellectual disability. Some TTD patients may also present photosensitivity, but without skin cancer predisposition (73).

1.3.4.4. UV-sensitive Syndrome ($UV^{S}S$)

UV-sensitive syndrome is a rare autosomal recessive disease that can be caused by mutations on CSA, CSB or UVSSA genes. Unlike other NER syndromes, it presents a relatively mild phenotype with sun sensitivity, freckles, skin dryness and abnormal pigmentation. $UV^{S}S$ patients develop normally and they do not have skin cancer predisposition (40).

1.3.5. Chromatin context

The damaged DNA present in the nucleus exists in the form of chromatin, coiled and compacted in nucleosome, and is therefore not always easily accessible to be repaired. Therefore, repair systems also have to deal with the chromatin environment. Indeed, it has been proposed a model of chromatin rearrangement for the NER mechanism, called “Access, Repair, Restore”(75, 76), which has been recently improved by the “Access/Prime and Repair/Restore” model in which chromatin and chromatin-associated proteins are not only impeding access to repair machineries but are also actively promoting repair (77). In order to access the lesion for repair, histone proteins have to be mobilized. Several chromatin-associated factors have been proposed for this step, such

as BRG1 and INO80 (78, 79). A recent study demonstrated that also factors involved in chromatin compaction are recruited to UV-damaged chromatin, such as the Heterochromatin Protein 1 (HP1), underlying the concept that chromatin organization has not to be simply considered as a barrier, but that chromatin-associated proteins can play an active role in repair (80). At the Repair/Restore step of chromatin rearrangement around a UV lesion, factors responsible for *de novo* incorporation of histones have been found: new H3.1 histones are deposited by CAF-1 and deposition of new H3.3 at UV sites is stimulated by HIRA (81, 82).

One of the fundamental mechanisms for the life of all organisms consists in the translation of the genetic information, contained in the DNA, into the proteins or to various classes of functional RNAs, in order to accomplish specific cellular roles. This mechanism is said transcription and is performed by multiple enzymatic complexes, the DNA-dependent RNA Polymerases.

There are three RNA polymerases operating in mammalian cells: RNA polymerase 1 transcribes the pre-ribosomal rRNA 47S; RNA polymerase 2 synthetizes precursors of mRNAs and most snRNAs and microRNAs; RNA polymerase 3 is in charge of tRNAs, rRNA 5S and other small RNAs transcription. In order to provide a background for the results presented, in this section and in the next one, RNAP2 and RNAP1 transcription cycles will be detailed.

2. RNA Polymerase 2 transcription

RNA polymerase 2's complete structure has been identified thanks to X-ray crystallography in 2003 and it has allowed for a better understanding of its organization and function (83, 84). We can distinguish a core composed of 10 subunits (RPB1, RPB2, RPB3, RPB5, RPB6, RPB8, RPB9, RPB10, RPB11 and RPB12) and a stalk formed by the heterodimer RPB4 and RPB7, which is required for initiation of transcription but not for the elongation step. Within the core, 5 subunits are commonly shared between RNAP1, RNAP2 and RNAP3. The two main RNAP2 subunits RPB1 and RPB2 form a deep positively charged cleft in which the open ssDNA can enter and be transcribed by the active site. The other core subunits are necessary for maintain this structure.

An important functional characteristic of the RPB1 subunit is the presence of a C-Terminal Domain (CTD). The CTD, which is specific to RNAP2, contains tandem repeats of a heptad sequence: Tyr-Ser-Pro-Thr-Ser-Pro-Ser. Modifications of phosphorylated and dephosphorylated states of Ser 2, 5 and 7 regulate all the steps of the transcription cycle, and even mRNA processing (85, 86).

2.1. Initiation

RNAP2 transcription cycle is depicted in Figure 8. The first step of RNAP2 transcription is the recognition of the promoter by the transcription machinery. Promoters of RNAP2 transcribed genes present a great variability and there are not universal core promoter (87). Sequences found in core promoters include the TATA box, the initiator element (Inr), the TFIIB recognition element (BRE) and the Downstream Promoter Element (DPE) (88). The core promoter elements represent binding site for subunits of the transcription machinery and serve to orient the pre-initiation complex (PIC) at the transcription start site (TSS) (89).

The PIC assembly starts with the binding of the TFIID subunit TBP to the TATA element; TAF1/2 components of TFIID have been implicated in Inr recognition, in order to strengthen interaction with the promoter. Then TFIIA and TFIIB are recruited to stabilise promoter bound-TFIID. Next, RNAP2, in association with TFIIF, adds to the growing PIC. This drives the association of TFIIE and lastly of TFIIH (90). An alternative PIC assembly pathway proposes a preassembled complex of RNAP2, the Mediator complex and the General Transcription Factors (except TFIID and TFIIA) binding directly to the promoter (91).

After PIC formation, the DNA double helix has to be separated around the TSS in order to form an open complex suitable for transcription. This opening occurs thanks to the ATP-dependent helicase activity of the TFIIH subunit XPB. RNAP2 is the only polymerase that requires this kind of activity for DNA melting (92, 93). The DNA template is then placed in the active site of RNAP2 and, after a series of abortive transcripts, a RNA product of more than 10 nucleotides is produced and this allows RNAP2 to leave the promoter (94). The required step for this switch to a stable elongation form is the phosphorylation of the CTD Ser5 by the TFIIH subunit Cdk7 (95). This CTD phosphorylation is also important for the process of RNA transcript because it is recognized by the capping enzymes that catalyse the addition of the 7-methylguanosin cap to the 5’ end of the nascent transcript (96). While RNAP2 clears the promoter, most of the PIC complex stays bound at the promoter forming a re-initiation scaffold complex, with TFIIF being the only factor staying with RNAP2 after this step (97).

2.2. Proximal pausing and Elongation

Once cleared the promoter, RNAP2 transcribes few nucleotides, by addition of some Nucleosides Triphosphate (NTPs) to the nascent RNA transcript, before pausing. This arrest is mediated and stabilised by several pausing factors, such as the Negative Elongation Factor (NELF) and DRB Sensitivity Inducing Factor (DSIF) (98). The release of RNAP2 into a productive elongation requires the activity of the Positive-Transcription Elongation Factor (P-TEFb) (99). The kinase subunit of P-TEFb, Cdk9, drives phosphorylation of RNAP2 CTD Ser2 and of pausing factors NELF and DSIF (100). NELF dissociates from chromatin upon its phosphorylation, whereas DSIF switches from being a negative factor to being a positive elongation element (101, 102). The exact role of this pausing event in transcription has not been clarified yet, but it has been proposed a relationship between RNAP2 pausing and the regulation of chromatin structure and gene expression (103). When RNAP2 progress toward the 3’ end of the gene, Ser5P levels appear to decrease, leaving polymerases phosphorylated at Ser2 to terminate transcription (104).

Elongating RNAP2 is supported by a series of Elongating Factors (EF) such as TFIIF, TFIIS, ELL, Elongin and histone-modifying elements (105-107).

2.3. Termination

Termination is the last step of the transcription cycle, which guarantees RNAP2 dissociation from the transcribed gene and release of the transcript. Despite its significance, transcription termination remains one of the least understood processes in gene expression (108). This step can be achieved through two pathways, depending on the RNA 3'-end processing signals and termination factors that are present at the end of the gene (109). Most of the protein-coding transcribed genes contain a poly(A) signal, 5'-AAUAAA-3', followed by a GU-rich region. A key scaffold for the recruitment of terminator factors is again the CTD tail of RNAP2, which is recognized and bound by the Cleavage Stimulatory Factor (CstF). The Cleavage and Polyadenylation Specificity Factor (CPSF) binds to the poly(A) signal and when it is transcribed, CPSF reduces RNAP2 transcriptional rate. Then, CstF binds to the downstream GU-rich sequence, CPSF binds to CstF and this interaction mediates the cleavage between the poly(A) site and the GU-rich sequence (110-112). Termination also requires the activity of the 5'-3' Exoribonuclease 2 (XRN2) that is recruited *via* interaction with CTD and is responsible for degradation of the downstream cleavage product. The physical collision between XRN2 and RNAP2 promotes RNAP2 release. The cleaved transcript undergoes polyadenylation and splicing (113).

Termination of non-polyadenylated sequences transcribed by RNAP2, including small nucleolar and small nuclear RNAs, has been described based on evidences from the yeast. It involves the activity of the Senatoxin 1 helicase, which is responsible for unwinding the RNA-DNA hybrid in RNAP2 active site and the subsequent termination (114, 115).

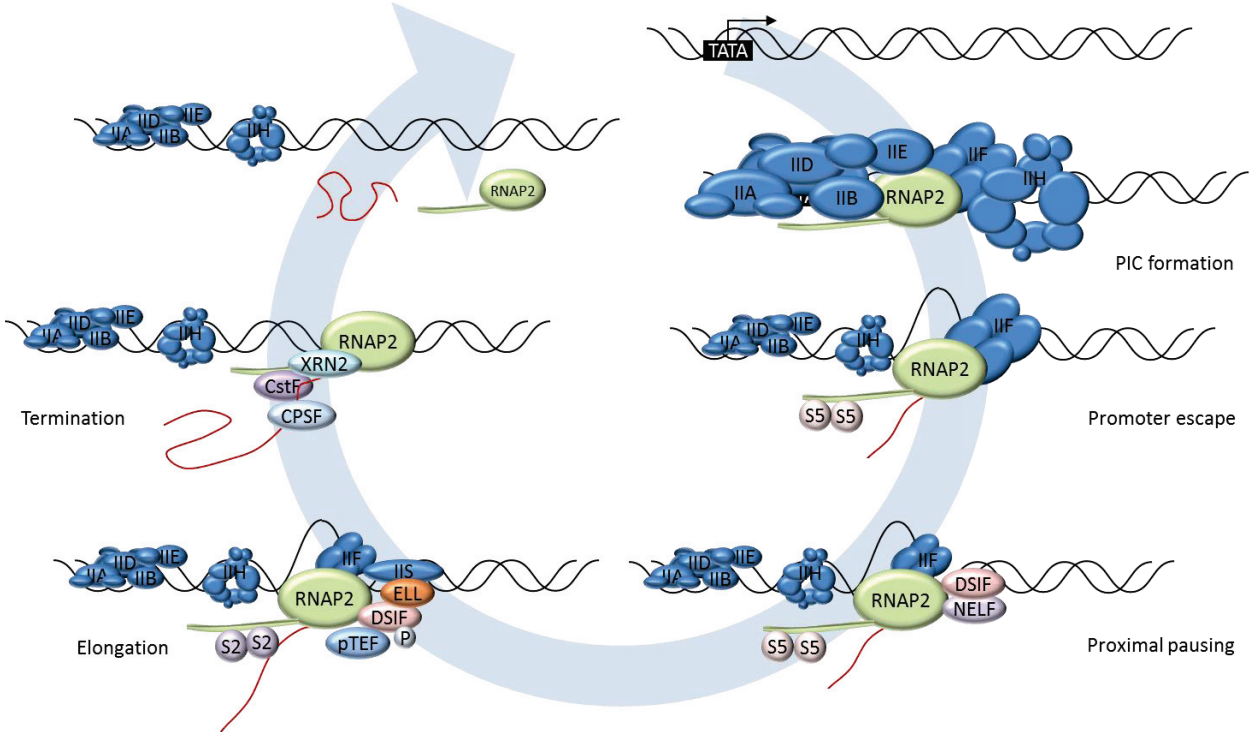

Figure 8. RNA Polymerase 2 transcription cycle

2.4. Splicing

There are about 25,000 protein-coding genes transcribed by RNAP2, but the number of different proteins is more than 90,000 (116). This discrepancy is due to the splicing mechanism, which processes the pre-mRNA transcript removing introns and/or combining different exons, resulting in various forms of mature mRNA (117). More than 95% of human genes undergoes splicing, thus explaining the great number of proteins compared to the amount of protein-coding genes (118). Splicing reactions take place at the boundary between exons and introns, which then provides important landmarks for signals alignment. Furthermore, intron structure contains specific sequences highly conserved between different organisms: the 5' and 3' intron boundaries are defined respectively by GU and AG dinucleotides, known as splice sites, and a branch-point sequence (BPS) locates 15-40 nucleotides upstream the 3' splice site (119, 120). The machinery responsible for the splicing reaction contains ≈ 175 proteins in human and is known as the spliceosome (121). The basal elements that the spliceosome is composed of are five U-rich small nuclear ribonucleoproteins (snRNPs), which contain five different small nuclear RNAs (snRNAs): U1, U2, U4, U5, U6. In addition, other non-snRNP protein complexes participate in spliceosome function, such as the Nineteen Complex (NTC, also known as PRP19 complex), Nineteen-Related (NTR) and Retention and Splicing complex (RES) (122). The different stages of the splicing reaction can be summarized as identification of the 5' and 3' end of the intron and spliceosome assembly,

spliceosome maturation, spliceosome activation and splicing catalysis. The actual splicing reaction involves two transesterification steps: the first one links the 5' end of the intron to the conserved adenine of the BPS, leading to an exon with a free 3'OH and the intron in a lariat shape; the second step ligates the two consecutive exons, causing excision of the intron lariat. After this step, the spliced mRNA is released, the spliceosome is disassembled and recycled and the intron lariat is degraded (120, 123).

The first observation of co-transcriptional spliceosome assembly came from a study on *Drosophila* conducted by Bayer et al (124). Since then, increasing evidences support the idea that transcription and splicing are physically and functionally coupled (125). The best characterized link between RNAP2 transcription and splicing involves the CTD tail of the larger subunit of RNAP2. Two models of CTD involvement have been proposed. The first one, termed "recruitment model" proposed that posttranslational modifications (PTMs) of CTD may create a binding platform for the recruitment of splicing factors, through direct binding to CTD or indirectly with CTD associated proteins (126). This model is supported, among others, by the direct interaction of the splicing protein U2AF65 with the phosphorylated CTD and by evidences that truncated or mutated CTD leads to changes in splicing (127, 128). The second model proposed is called "kinetic model" and suggests that PTMs of the CTD, along with other factors affecting RNAP2 elongation rate, influence splicing patterns (129, 130). Actually, it has been shown that changes in RNAP2 elongation rate can influence the choice of splicing sites in alternatively spliced genes (131, 132). Furthermore, a recent study adopted splicing inhibition to show that RNAP2 signal increases on intron, suggesting the activation of an elongation checkpoint to allow spliceosome assembly (133). Since these two mechanisms are not mutually exclusive, they both likely play critical roles in regulation of pre-mRNA splicing (129).

2.5. Chromatin context

A description of the RNAP2 transcription mechanism has to involve an overview on all the chromatin modifications necessary for access to the gene that has to be transcribed and the co-transcriptional chromatin changes that allow polymerase to move forward trough the 3'-end of the gene. Promoters of actively transcribed genes present high levels of H3K4me3 and multiple acetylated Lys residues of histones H3 and H4. Furthermore, gene bodies are enriched with mono-ubiquitylated H2B (H2Bub), H3K36me3, H3K79me2 and H3K79me3 (103). Besides histones modifications, elongating RNAP2 needs a dynamic turnover of nucleosomes and their subsequent reassembly. Actually, the histone octamer of a nucleosome is formed by a H3-H4 tetramer and two H2A-H2B dimers. One H2A-H2B dimer is removed from the nucleosome during RNAP2

transcription and this process is driven by the Facilitates Chromatin Transcription (FACT), which is also responsible for nucleosomes reassembly (134, 135). FACT's activity can be further facilitated by other histone chaperones, as well as SPT6, the Chromodomain-Helicase-DNA-binding protein 1 (CHD1) and Imitation SWI (ISWI) (136). In addition, the Pol II-Associated Factor 1 complex (PAF1C), which has also been implicated in pausing regulation, travels with the elongating RNAP2 and acts as a platform for the recruitment of a variety of nucleosome remodellers, such as COMPASS, E3 ubiquitin protein-ligase BRE1 and DOT1L, specific for methylation of H3K79 (103).

3. RNA Polymerase 1 transcription

3.1. The Nucleolus

Felice Fontana first described the nucleolus in 1781 (137) and, since then, a lot of work has been done in order to understand its organization and its function. The nucleolus has been described as “an organelle formed by the act of building a ribosome”, a definition proposed in 1995 (138). Indeed, the nucleolus is a membrane-less nuclear organelle and is the ribosome factory of the cell (139). It is composed of ribosomal DNA (rDNA), ribosomal RNA (rRNA), proteins involved in ribosome biogenesis, but also of snRNA and modifying enzymes responsible for pre-mRNA metabolism and translation (140, 141).

Electron microscopy studies have provided evidences that, during interphase, the nucleolus presents a tripartite structure which is divided into: the Fibrillar Center (FC), a clear area ranging from 0.1 to 1 µm; the Dense Fibrillar Component (DFC), a more dense area partially surrounding the FC; and the Granular Component (GC), mainly formed of granules with a diameter of 15-20 µm loosely distributed (142). There has been several hypothesis proposed for the location of rDNA

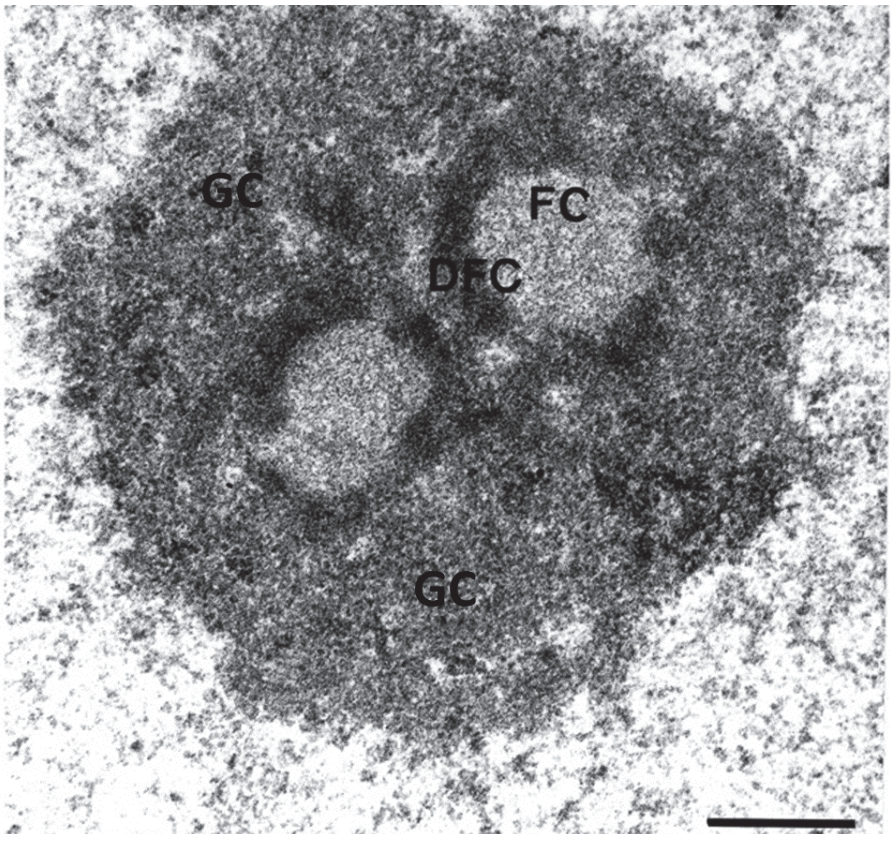

Figure 9. Organization of the nucleolus in human cells
Image of the nucleolus obtained by electron microscopy. Fiblillar Centers (FCs) are partially surrounded by the Dense Fibrillar Component (DFC) and embedded in the Granular Component (GC). Scale bar represents 0.5 µm. Adapted from *Sirri et al., 2002*

transcription by RNA polymerase 1 (RNAP1) inside the nucleolus, but the broadly accepted scenario is that it takes place at the boundary between the FC and the DFC (143). Actually, the FC contains inactive rDNA, which can be directly activated, and proteins of the transcription machinery, such as RNAP1 and the Upstream Binding Factor (UBF). On the other hand, the DFC contains pre-rRNA and early processing factors, while in the GC reside late processing factors and ribosomal proteins (142, 144).

The nucleolus presents the above-mentioned tripartite structure only during the interphase step of the cell cycle. When the cell enters mitosis, the nucleolus disassembles and its mitosis counterpart is represented by the Nucleolar Organizer Regions (NORs). NORs represent the chromosomal location of rDNA and are located on the short arm of the five acrocentric chromosomes 13, 14, 15, 21 and 22, which means there are 10 NORs per human somatic cells (145). At the beginning of mitosis, RNAP1 transcription is repressed and the transcription machinery, e.g. the UBF protein, remains associated to rDNAs within the NORs that were transcriptionally active during the previous interphase (146, 147). Furthermore, at the onset of mitosis, pre-rRNA processing events are repressed before the arrest of pre-rRNA synthesis, which leads to the presence of 45S localised around NOR during mitosis (148, 149). At the end of mitosis, RNAP1 transcription restarts and active NORs are directly involved in nucleolar reassembly. Contrarily, inactive NORs are not associated with RNAP1 transcription machinery and do not take part in nucleolar reassembly (150).

In order to rebuild the nucleolar structure after mitosis, active NORs assemble with the pre-rRNA processing complex and nucleolar proteins, such as Fibrillarin and Nucleolin, to form foci called PeriNucleolar Bodies (PNBs), that will fuse together to give rise to the interphasic nucleolus (151, 152). The number of nucleoli can vary between cells; the nucleolus can organize around a single NOR or alternatively several active NORs can associate in a single nucleolus when rRNA synthesis restarts after cell division (152).

3.2. Ribosomal DNA

The ribosomal DNA transcription unit is comprised of three genes, which code for the ribosomal RNAs 18S, 5.8S and 28S. It exists a fourth rRNA named 5S, which is transcribed outside the nucleolus by the RNA polymerase 3. The transcription unit also includes a 5’ External Transcribed Spacer (5’ETS), two Internal Transcribed Spacers (ITS) flanking the 5.8 rRNA and a 3’ ETS (153, 154). The transcription unit is present as ≈ 40 tandem repeats, separated by Non-Transcribed Intergenic Spacer regions (NTIS), forming the previously described NORs during mitosis (155). It means that in each human somatic cell the ribosomal DNA is present in ≈ 400

copies. This high number of copies represents the way the cell has adopted to cope with the high demand of ribosomes; the structural and catalytic subunit of ribosomes is composed of rRNA that cannot be amplified by translation, unlike proteins (143). This tandemly repeated array of rDNA forming the NOR is flanked by two additional regions: an upstream Proximal Junction (PJ) and a downstream Distal Junction (DJ). Floutsakou et al. have demonstrated that DJ is located at the periphery of the nucleolus and they conclude that this region is responsible for the location of rDNA within the nucleolus (156).

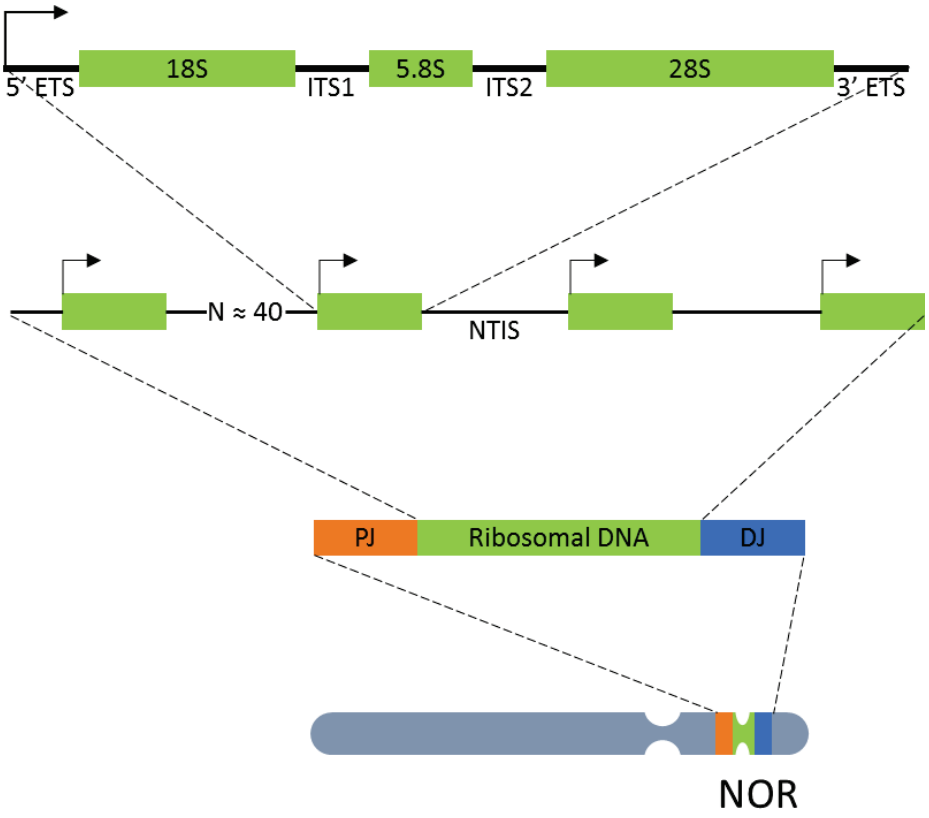

Figure 10. Transcription unit of ribosomal DNA
Ribosomal DNA transcription unit is composed of three genes: 18S, 5.8S and 28S along with External/Internal Transcribed Spacers. Each transcription unit is surrounded by Non-Transcribed Intergenic Spacers. About 40 transcription units are located per acrocentric chromosome and they are flanked by Proximal Junction and Distal Junction. During mitosis, Ribosomal DNA, PJ and DJ are organized in the Nucleolar Organizer Regions.

3.3. Transcription cycle

RNAP1 drives the synthesis of ribosomal RNAs 18S, 5.8S, 28S. Actually, the first transcript produced is the pre-rRNA 47S, which is processed and cleaved in order to obtain the three final rRNA, which are the structural and functional components of ribosomes (157). RNAP1 transcription represents 60% of the total transcriptional activity in eukaryotic cells, even if only

the 50% of rDNA genes are transcribed (158). In order to sustain adequate levels of ribosome biogenesis, approximately 100 RNAP1 proteins transcribe each active gene with a rate of 95 nucleotides per second (159).

RNAP1 is composed of 14 subunits that have been well characterized in yeast; 13 subunits homologues in humans has been identified, except for the A14 yeast subunit, which does not have a human homologue yet (160). The core enzyme is formed by 10 of these subunits and five of them (yeast Rpb5, 6, 8, 10 and 12), are shared between RNAP2 and RNAP3, forming the clamp of the enzyme together with yeast AC40 and A19. Part of the core is also the yeast AC12.2 subunit that shares functional and structural homology with TFIIS and presents RNA cleavage activity (161). The biggest RNAP1-specific yeast subunits A135 and A190 hold the DNA binding cleft and are also part of the core (162). The stalk of RNAP1 is represented by the heterodimer formed by the yeast subunits A43 and A14 and is RNAP1-specific (162). The last two RNAP1 subunits, yeast A34.5, A49 and human PAF49, PAF53, form a heterodimer that can dissociate from RNAP1 and presents structural and functional analogies to TFIIE and TFIIF. This is also essential for polymerase recruitment, promoter escape and elongation (163, 164).

3.3.1. Initiation

In eukaryotic cells, the gene promoter of rDNA contains two important elements for direct and assured efficient transcription: the Core promoter, essential for basal transcription, and the Upstream Control Element (UCE), lying from -156 to -107 nucleotides upstream of the TSS and is responsible for stimulate transcription (165). As for other polymerases, the first step of RNAP1 transcription is the formation of a PIC at the promoter and the requirement of a TBP-containing factor. In RNAP1 transcription mechanism, the Selectivity Factor 1 (SL1) is a complex of TBP and four TBP-Associated Factors (TAFs): TAF_I110, TAF_I63, TAF_I48 and TAF_I41 (166). SL1 is essential for RNAP1 recruitment to the promoter and it promotes a stable interaction between UBF and rDNA promoter (167). It has also been proposed that SL1 has a role in maintaining the promoters of rDNA genes in a hypomethylated state through an additional subunit, TAF12 (168). Another important factor that is, in part, responsible for RNAP1 PIC incorporation is the RNAP1-specific transcription initiation factor RRN3, which directly binds the A43 subunit of the initiating form of RNAP1 (RNAP1β) (169, 170). Furthermore, RRN3 association with RNAP1 requires the presence of the PAF53/PAF49 subcomplex (163). RRN3 also binds SL1 through its TAF subunits, thus facilitating polymerase recruitment to the PIC (170). Other proteins have been found specifically associated with RNAP1β, such as the serine/threonine kinase CK2. CK2 targets the TAF_I110 SL1 subunit and UBF, thus regulating PIC formation, but its main role is the phosphorylation of the TIF1A factor

(the mouse homologue for RRN3) and this modification seems to be involved in RNAP1 clearance of the promoter and thus elongation (171-173). Even if SL1 and RNAP1β are sufficient for starting basal transcription *in vitro*, UBF must be incorporated into the PIC for achieving activated transcription. Actually, UBS dimer binds throughout the actively transcribed rDNA in the cell *via* its High Mobility Group (HMG) domains (174). UBF induces topological changes in DNA, maintaining euchromatic rDNA state and is important for the nucleolar architecture. During PIC formation, UBF interacts with SL1 and with the RNAP1 PAF53/PAF49 subcomplex (175).

3.3.2. Promoter escape and Elongation

Transcription initiation by RNAP1 is defined by incorporation of the first ribonucleotides to the rRNA sequence. However, for productive transcription, RNAP1 has to dissociate from the promoter and from the PIC complex (176). This promoter escape event is concomitant with RRN3 release from the polymerase (177). After promoter escape, RNAP1β is converted into its elongation form, RNAP1α, and has been shown that effective elongation requires the presence of TFIIH on the rDNA. Actually, TFIIH is recruited at the promoter, but only its location along the transcription unit is necessary for transcription (178). When RNAP1 clears the promoter, SL1 and UBF remain promoter-bound in order to allow rapid reassemble of the PIC and re-initiation of a new transcription cycle (179).

3.3.3. Termination

Transcription termination involves several proteins and the specific rDNA sequence of the terminator element, comprising several termination sites (T_1-T_{10}), which is located downstream from the rDNA gene. The Transcription Termination Factor (TTF-1) binds the termination site, causing polymerase pausing (165). Then, actual transcription termination and RNAP1α dissociation from the rDNA is mediated by TTF-1 and the “Pol 1 and Transcript Release Factor” (PTRF), thus facilitating re-initiation of transcription (180). Recent studies in yeast have proposed a more complex mechanism for RNAP1 termination, similar to the “torpedo” process known for RNAP2, and involving the progressive digestion of the downstream RNA cleavage product associated with RNAP1 by a 5’-3’ exonuclease (181).

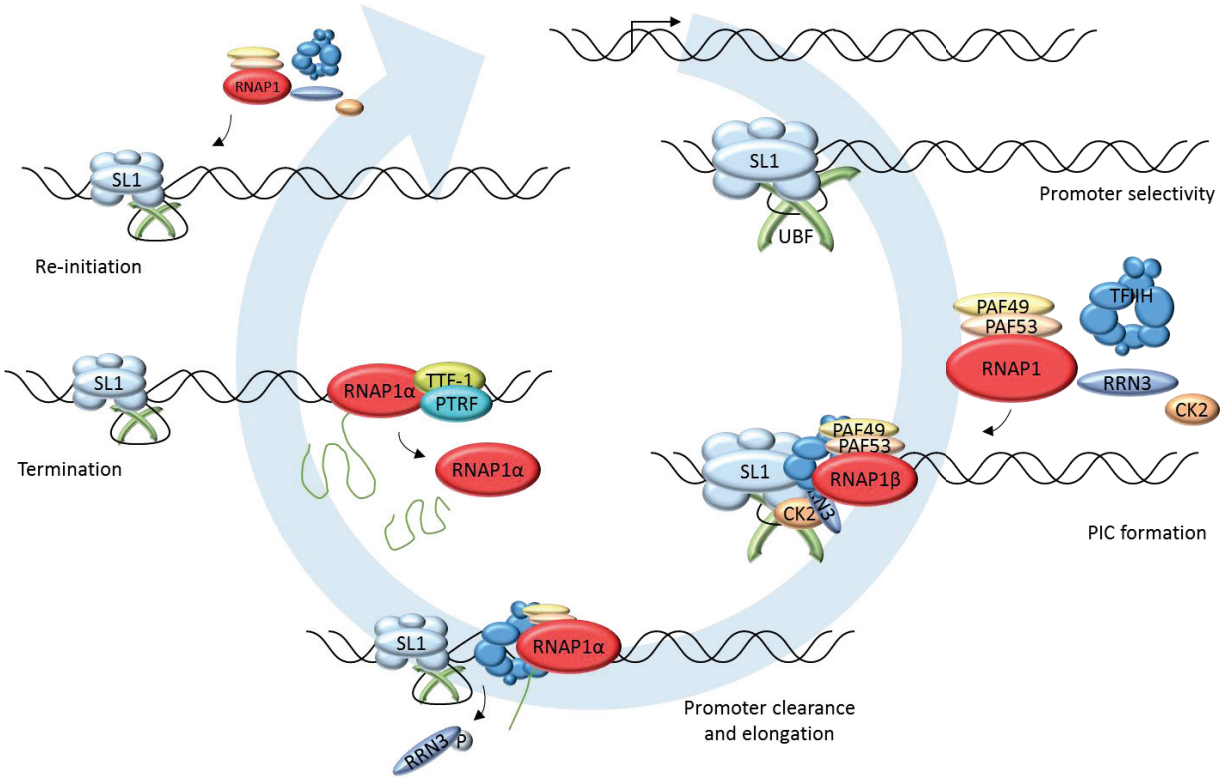

Figure 11. RNA Polymerase 1 transcription cycle

3.4. Chromatin context

Ribosomal DNA transcription can be directly regulated by its own chromatin state and this epigenetic regulation determines the number of active and inactive rDNA genes. Actually, rDNA exists in an active, silent or stable silent chromatin state. Active rDNA genes reside at the boundary between the FC and the DFC and they do not present neither CpG-methylation nor nucleosome association. rDNA that needs to be transiently silenced, resides at the centre of the FC, is non-methylated and is organized in nucleosomes with repressive marks. Stable silent rDNA is characterized by both histone repressive marks and DNA CpG methylation and is located at the nucleolar periphery (143, 182). One important factor responsible for establishment of epigenetic state of rDNA is TTF-1 (183). It mediates gene silencing by recruitment of the Nucleolar Remodelling Complex (NoRC) to the promoter. NoRC in turn recruits methyltransferases DNMT1 and DNMT3 and a histone deacetylase complex, which mediates transcriptional repression (184, 185). Another essential factor for rDNA transcription is the UBF protein, which occupies and stabilizes a Nucleosomal-Free Region (NFR) for the actively transcribed genes (186).

RESULTS

Mechanistic Insights in Transcription-Coupled Nucleotide Excision Repair of Ribosomal DNA

Laurianne DANIEL[a,*], Elena CERUTTI[a,*], Lise-Marie DONNIO[a], Julie NONNEKENS[b], Christophe CARRAT[b], Simona ZAHOVA[a], Pierre-Olivier MARI[a], Giuseppina GIGLIA-MARI[a]

[a] Institut NeuroMyoGène, CNRS UMR 5310, INSERM U1217, Université de Lyon, Université Claude Bernard Lyon 1, 69622 Villeurbanne CEDEX, France

[b] Institut de Pharmacologie et de Biologie Structurale, CNRS UMR 5089, Université Paul Sabatier, BP64182, F-31077 Toulouse, France

* Co-first authors

Mechanistic insights in transcription-coupled nucleotide excision repair of ribosomal DNA

Laurianne Daniel[a,1], Elena Cerutti[a,1], Lise-Marie Donnio[a], Julie Nonnekens[b], Christophe Carrat[b], Simona Zahova[a], Pierre-Olivier Mari[a], and Giuseppina Giglia-Mari[a,2]

[a]Institut NeuroMyoGène, CNRS UMR 5310, INSERM U1217, Université de Lyon, Université Claude Bernard Lyon 1, 69622 Villeurbanne CEDEX, France; and [b]Institut de Pharmacologie et de Biologie Structurale, CNRS UMR 5089, Université Paul Sabatier, BP64182, F-31077 Toulouse, France

Edited by Philip C. Hanawalt, Stanford University, Stanford, CA, and approved June 12, 2018 (received for review September 21, 2017)

Nucleotide excision repair (NER) guarantees genome integrity against UV light-induced DNA damage. After UV irradiation, cells have to cope with a general transcriptional block. To ensure UV lesions repair specifically on transcribed genes, NER is coupled with transcription in an extremely organized pathway known as transcription-coupled repair. In highly metabolic cells, more than 60% of total cellular transcription results from RNA polymerase I activity. Repair of the mammalian transcribed ribosomal DNA has been scarcely studied. UV lesions severely block RNA polymerase I activity and the full transcription-coupled repair machinery corrects damage on actively transcribed ribosomal DNAs. After UV irradiation, RNA polymerase I is more bound to the ribosomal DNA and both are displaced to the nucleolar periphery. Importantly, the reentry of RNA polymerase I and the ribosomal DNA is dependent on the presence of UV lesions on DNA and independent of transcription restart.

human ribosomal DNA | nucleotide excision repair | RNAP1 transcription | UV lesions | nucleolar organization

DNA integrity is continuously challenged by a large variety of DNA-damaging agents. To ensure genome stability, cells have developed different mechanisms, such as the nucleotide excision repair (NER) pathway that removes UV-induced lesions (1). NER is composed of two subpathways that are distinguished only by the lesion recognition step: the global genome repair (GG-NER) that occurs on the whole genome and the transcription-coupled repair (TC-NER) that has been associated with the RNA polymerase II (RNAP2) actively transcribed genes (2). Damaging agents randomly harm the genome and block many cellular functions. As mRNA production is impaired due to RNAP2 stalling, transcription of ribosomal genes (rDNA) should also be blocked when RNA polymerase I (RNAP1) stalls on a lesion.

rDNA transcription by RNAP1 represents 60% of the total cellular transcription activity in dividing cells and is the first and rate-limiting step of ribosome biogenesis (3). Ribosomes are responsible for the production of the proteins required for all cellular functions. Therefore, it is of fundamental importance for the cell to maintain a functional RNAP1 transcription by repairing DNA lesions on the rDNAs active copies.

While the mechanism of RNAP1 transcription has been elucidated to a large extent (4), the repair of bulky lesions on rDNA has hardly been studied. Few studies performed more than 20 y ago in mammals (5, 6) and lately several studies conducted in yeast (7–9) have shown opposite conclusions on the implication of the TC-NER–like mechanism in rDNA repair. Moreover, the mammalian studies put forward the idea that rDNAs, being located within the nucleolus, are not accessible to repair proteins (6). However, it is common knowledge nowadays that some repair proteins are part of the nucleolus (10, 11) and that mutations in repair proteins can affect ribosome biogenesis (12). This new evidence prompted us to investigate a possible role of these repair proteins in the removal of helix-distorting lesions on rDNAs in human cells. We made use of an approach by measuring specifically RNAP1 transcription reduction and recovery after UV exposure, which is generally used for the measurement of TC-NER on RNAP2 transcribed regions (13).

Our results show that transcription of the rRNA genes is blocked shortly after irradiation and recovers over time. We show here that in mammalian cells, the TC-NER machinery repairs UV lesions in the rDNAs and that this process is CSA, CSB, and UVSSA dependent, but XPC independent. We also show that RNAP1 is not released from the rDNAs sequences and not degraded. Finally, we show that the repair reaction takes place at the periphery of the nucleolus, where all the repair proteins can access the damaged rDNAs. Importantly, we demonstrated that UV lesions present on the rDNAs specifically trigger the displacement of the rDNAs at the periphery of the nucleolus.

Results

RNAP1 Retention on the rDNAs After UV Irradiation. Recent studies in yeast (14) have described the dissociation of the RNAP1 from ribosomal DNA after UV irradiation. To investigate whether the mammalian RNAP1 behaves in the same manner as yeast RNAP1 in response to UV-induced damage, we performed chromatin immunoprecipitation coupled with quantitative PCR (ChIP-qPCR) assays against RNAP1, in absence of UV lesions, 3 and 16 h after UV irradiation. ChIP-qPCR experiments were performed using 14 couples of primers; their location is indicated in Fig. 1*A*. Our results described the binding of the RPA194 subunit of RNAP1 along rDNA in both untreated and irradiated cells. In untreated cells, the binding profile did not differ from the previously published results (12). Indeed, Nonnekens et al. have shown that RNAP1 only binds to the rDNA coding sequence (12). Remarkably, the RPA194

Significance

RNAP1 transcription, dedicated to ribosomal DNAs (rDNAs), is the first and rate-limiting step of ribosome biogenesis. rDNAs are grouped into several copies. This redundancy is important to guarantee that at low damage levels one rDNA gene can be temporarily silenced without affecting overall ribosome biogenesis. Nevertheless, when DNA repair is defective or overloaded, several rDNAs could be damaged, disturbing the whole RNAP1 transcription process and later on modifying the ribosome content of cells. Therefore, it is of fundamental importance for the cell to maintain a functional RNAP1 transcription by repairing DNA lesions on rDNAs. In this work we identified, in mammals, the repair mechanism of rDNAs along with a specific behavior for RNAP1 after UV irradiation.

Author contributions: P.-O.M. and G.G.-M. designed research; L.D., E.C., L.-M.D., J.N., C.C., and S.Z. performed research; L.D., P.-O.M., and G.G.-M. analyzed data; and L.D., P.-O.M., and G.G.-M. wrote the paper.

The authors declare no conflict of interest.

This article is a PNAS Direct Submission.

[1]L.D. and E.C. contributed equally to this work.

[2]To whom correspondence should be addressed. Email: ambra.mari@univ-lyon1.fr.

This article contains supporting information online at www.pnas.org/lookup/suppl/doi:10.1073/pnas.1716581115/-/DCSupplemental.

Published online July 2, 2018.

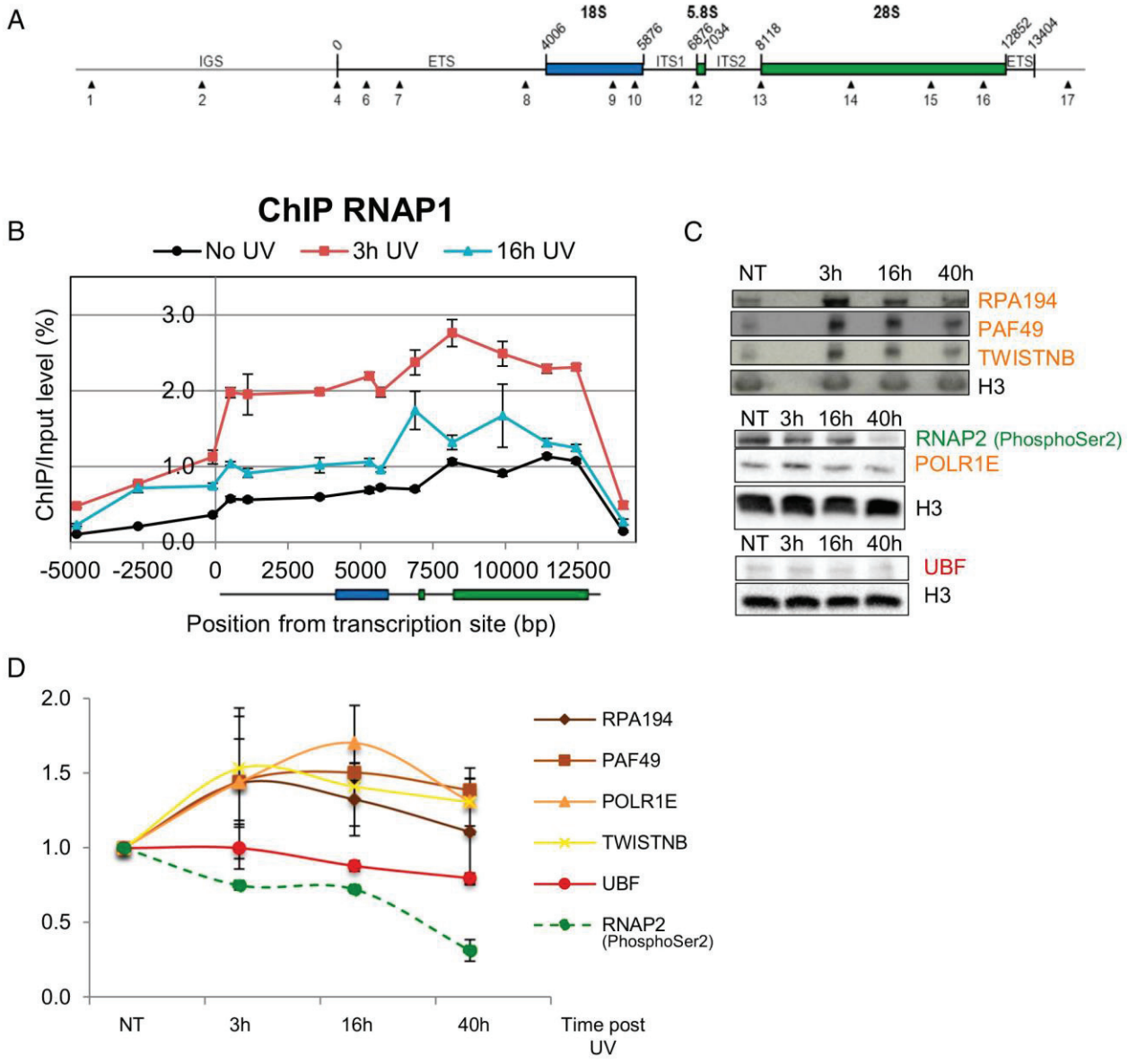

Fig. 1. After UV irradiation, RNAP1 is retained on rDNAs without being degraded. (*A*) Scheme of the murine ribosomal DNA unit. Positions of the primers used for ChIP-qPCR assay are indicated with arrowheads and numbers. ETS, external transcribed spacer; IGS, intergenic spacer; ITS, internal transcribed spacer. (*B*) ChIP-qPCR results showing the binding profile of RNAP1 on ribosomal DNA in murine embryonic stem cells, not treated (no UV), 3 or 16 h after UV exposure. The *y* axis depicts the ChIP/input ratio minus background (mock/input ratio) and error bars represent the SEM. (*C*) Western blot against RNAP1 subunits (orange), RNAP2 PhosphoSer2 (green), and UBF (red) on chromatin extracts from WT human fibroblasts at different times after UV exposure. The proteins H3 and RNAP2 were respectively used as loading and positive control. (*D*) Quantification of Western blots against RNAP1 subunits, UBF and RNAP2 PhosphoSer2 on chromatin extracts from WT cells. Error bars show the SEM of three biological replicates. UV dose: 16 J/m^2.

binding profile on rDNA was drastically modified 3 h after the UV exposure, showing that more of this subunit binds the ribosomal DNA in response to UV irradiation (Fig. 1*B*). Interestingly, 16 h after UV irradiation, a time point at which most of the repair reaction is completed, the binding profile of RPA194 on rDNA is close to the unchallenged profile, showing that the increased binding of RNAP1 to the substrate is reversible and specific to the DNA repair reaction. This result was in contrast to what has been described for yeast RNAP1 (15) and for mammalian RNAP2 (16, 17) after UV irradiation. To verify whether the whole RNAP1 complex is more bound to chromatin after UV irradiation, we prepared chromatin extracts at different times after UV exposure and we carried out Western blots against several RNAP1 subunits (RPA194, PAF49, TWISTNB, and POLR1E), the upstream binding factor (UBF) and RNAP2 (Fig. 1*C*). Quantification of the Western blots clearly showed that RNAP1 subunits accumulated on chromatin 3 h after UV irradiation, then partially detached from the chromatin upon repair 40 h post-UV. Interestingly, at this time point the binding of RNAP1 was still higher than the one measured in untreated cells, suggesting that it would take more time for RNAP1 to restore its binding dynamics after UV damage. Under our conditions and as expected, RNAP2 unbound the chromatin after UV exposure (Fig. 1*D*). Differently from the RNAP1 binding behavior, the

binding of the RNAP1-associated transcription factor UBF on the chromatin did not change upon UV irradiation. Furthermore, we showed, by quantifying Western blots against RPA194 (RNAP1's biggest subunit) on nuclear extracts after UV irradiation, that RNAP1 total protein level is unchanged (*SI Appendix*, Fig. S1), supporting our results on chromatin extracts.

Together, these data describe a surprising and specific outcome for RNAP1 after UV-induced damage: RNAP1 is not degraded and is more bound to rDNA when it encounters a UV lesion.

RNAP1 Transcription Arrest After UV Irradiation. We showed that UV irradiation induced a modification of RNAP1 binding on rDNA and we wondered whether this modification could affect RNAP1 transcriptional activity. To follow rDNA repair, we used RNA fluorescence in situ hybridization (RNA FISH) experiments to measure rDNA transcription restart in the same way as RNAP2 transcription recovery is used to follow RNAP2 transcribed gene repair (13). RNA FISH used a probe that specifically recognized the first transcript of the RNAP1: the 47S prerRNA (Fig. 2*A*), which is rapidly processed during rRNA processing, an action not fully determined as to whether it occurs co- or posttranscriptionally (18, 19). For this reason, RNA FISH performed with this specific probe is a reliable indicator of the ribosomal transcription level and speed (18). To quantify transcriptional activity after UV damage induction, cells were UV irradiated at different doses (5, 10, or 16 J/m^2) and fixation was performed at different times after UV (1, 3, or 16 h).

Our results showed that UV irradiation induced a decrease of the 47S prerRNA level, indicating that RNAP1 transcription was rapidly hindered (Fig. 2*B*) and reached a minimum level between 1 and 3 h depending on the UV dose. Namely, a higher UV dose (16 J/m^2) blocked the transcriptional activity faster than a lower UV dose (5 J/m^2) (Fig. 2*C*).

Our results also demonstrated that no matter the dose used, RNAP1 transcription progressively restarted 16 h post-UV. To determine when the RNAP1 transcription levels were completely restored, we measured by Northern blot the 47S prerRNA level up to 48 h post-UV. Quantification of the Northern blots revealed a total resumption of the ribosomal transcription between 36 and 48 h after UV exposure (Fig. 2*D*).

TC-NER–Dependent UV Lesion Repair of rDNA. We showed that RNAP1 transcription is fully restored 36–48 h after UV irradiation, meaning that UV lesions, hindering RNAP1 activity, have been removed. Because in mammalian cells NER pathway repairs UV damage, we decided to further investigate the implication of NER factors into UV lesion removal on rDNA and RNAP1 transcription restart.

Therefore, we studied RNAP1 transcription activity after UV irradiation in NER-deficient cell lines and to distinguish between TC-NER and GG-NER we specifically used cell lines that are deficient for these subpathways. Hence, we performed RNA FISH and Northern blot experiments on wild type (WT), TC-NER–deficient (CSA, CSB, and UVSSA), and GG-NER–deficient (XPC) cells at different times post-UV (Fig. 3).

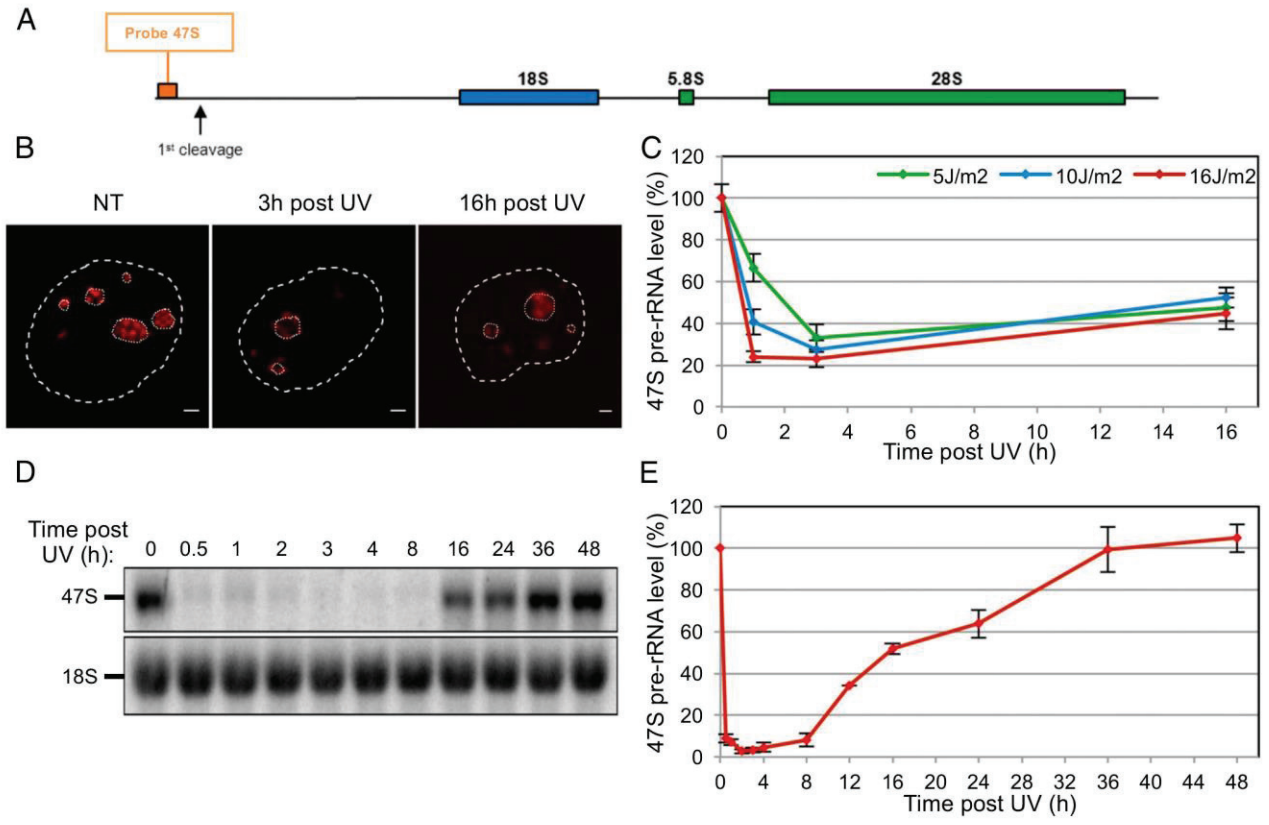

Fig. 2. UV irradiation blocks RNAP1 transcription. (*A*) Schematic representation of rDNA unit and localization of the 47S prerRNA probe. (*B*) Confocal images from RNA FISH experiment showing the 47S prerRNA level in WT cell. Cells were UV irradiated or not (NT) and fixation was performed 3 or 16 h after UV exposure (16 J/m^2). (Scale bar: 2 μm.) (*C*) Quantification of the 47S prerRNA level over time after different UV doses (5, 10, and 16 J/m^2). (*D*) Northern blot showing over time the 47S prerRNA level after UV irradiation (16 J/m^2). The amount of 18S rRNA is used as control. (*E*) Northern blot quantification of the 47S prerRNA level overtime after UV exposure (16 J/m^2). Error bars show the SEM of three independent experiments.

Both Northern blot assays (Fig. 3*A* and *SI Appendix*, Fig. S2) and RNA FISH labeling (Fig. 3 *B–D*) showed that 47S prerRNA level decreased 3 h after irradiation in all cell types. However, while in WT cells and GG-NER–deficient cells (XPC) RNAP1 transcription slowly resumed over time, in TC-NER–deficient cells (CSA, CSB, and UVSSA) no resumption of RNAP1 activity could be

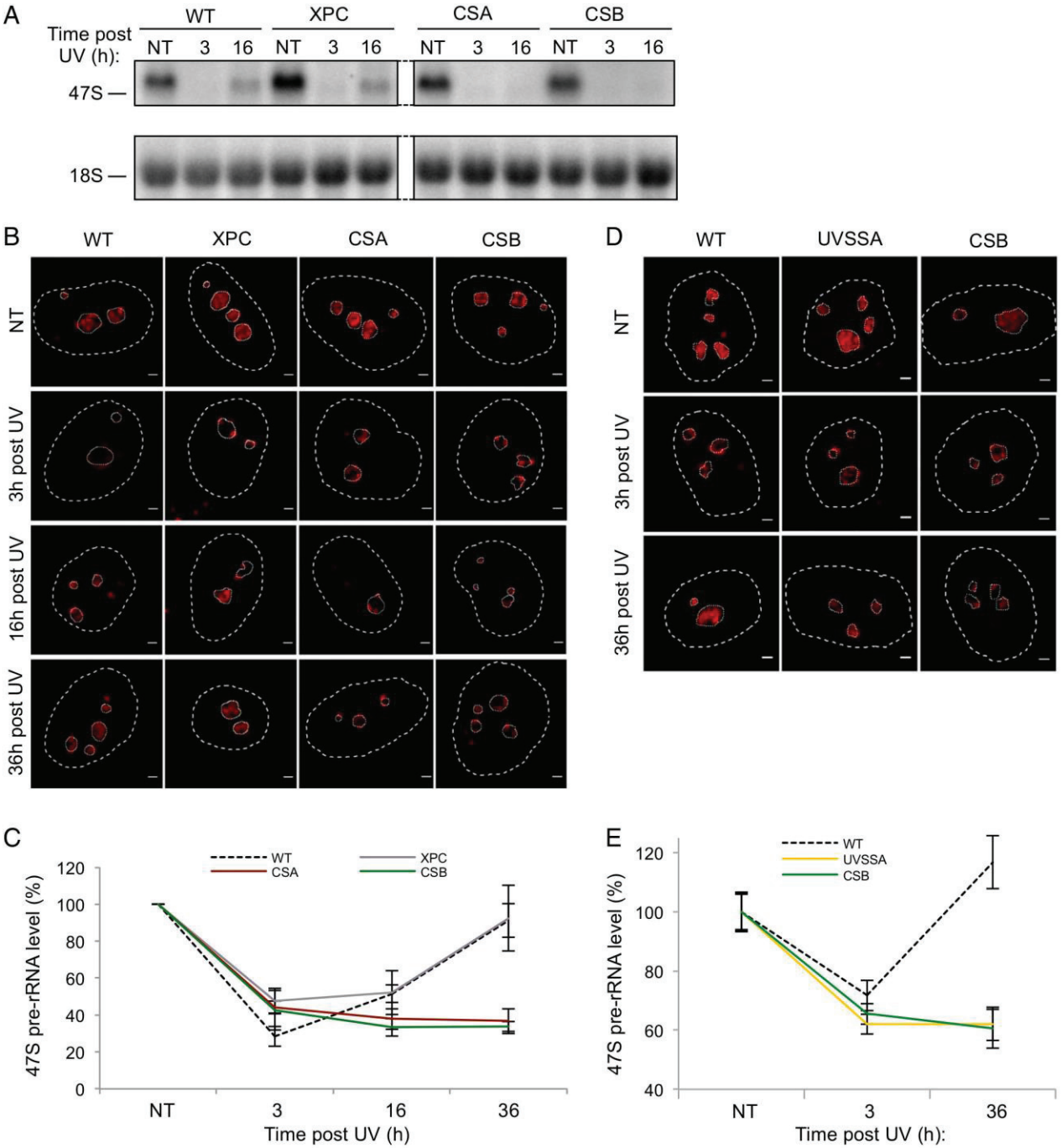

Fig. 3. Repair of the transcribed rDNA is performed by TC-NER. (*A*) Northern blot against the 47S prerRNA was performed at different times after UV irradiation in WT, XPC, CSA, and CSB cells. 18S was used as control. (*B*) Confocal images from RNA FISH labeling the 47S prerRNA level performed on WT, XPC (GG-NER deficient), CSA, and CSB (TC-NER deficient) cells. Cells were irradiated or not (NT) and fixed 3, 16, or 36 h after UV exposure. Nuclei and nucleoli are delimited by dashed and dotted lines, respectively. (Scale bar: 2 μm.) (*C*) Quantification of RNA FISH assay showing the 47S prerRNA level in WT, XPC, CSA, and CSB cells. Error bars represent the SEM of three independent experiments. UV dose: 16 J/m^2. (*D*) Confocal images from RNA FISH labeling the 47S prerRNA level performed on WT, UVSSA, and CSB (TC-NER deficient) primary cells. Cells were irradiated or not (NT) and fixed 3 or 36 h after UV exposure. Nuclei and nucleoli are delimited by dashed and dotted lines, respectively. (Scale bar: 2 μm.) (*E*) Quantification of RNA FISH assay showing the 47S prerRNA level in WT, UVSSA, and CSB primary cells. Error bars represent the SEM of three independent experiments. UV dose: 16 J/m^2.

detected (Fig. 3 *C*–*E*). Concomitantly, after UV irradiation, we could detect the presence of UV lesions (both 64PP and CPD) on the rDNA sequences by DNA immunoprecipitation and specific qPCR (*SI Appendix*, Fig. S3) using a technique published by Zavala et al. (15). We could also show that already 3 h after UV irradiation, UV lesions are repaired from rDNA sequences (*SI Appendix*, Fig. S3). These combined results suggest that RNAP1 transcription inhibition is most likely due to the presence of UV lesions on the rDNAs and that resumption of transcriptional activity is the consequence of the DNA repair of UV lesions on rDNAs but also that the timing of repair is faster than the restart of transcription. Finally, these results indubitably involved TC-NER factors CSA, CSB, and UVSSA, but not the GG-NER factor XPC in repair of the actively transcribed rDNAs.

We showed that the specific TC-NER factors CSA, CSB, and UVSSA were required for rDNA UV lesion repair and we wondered whether other known NER factors could be involved in this repair mechanism. We, therefore, conducted RNA FISH assays in different NER mutant cell lines (XPA, XPB^{XPCS}, XPB^{TTD}, XPD^{XPCS}, XPD^{XP}, and TTDA) (*SI Appendix*, Fig. S6*A*). As seen previously for the WT, GG-NER (XPC) and TC-NER (CSA and CSB), the NER-deficient cells (XPA, XPB, XPD, and TTDA) showed a decrease of the 47S prerRNA production 3 h post-UV. Similarly to CSA and CSB cells (TC-NER deficient), but unlike the WT and XPC cells (GG-NER deficient), no resumption of 47S prerRNA production was observed in these cells lines (*SI Appendix*, Fig. S6*B*). After UV irradiation, RNAP1 transcription did not recover in these NER mutants evidently implying that the whole TC-NER machinery was required for the UV-induced lesion repair on rDNA.

Displacement of RNAP1 and rDNA During TC-NER. We showed that NER factors were implicated in rDNA repair of UV lesions. Nevertheless, some basic NER factors were excluded from the nucleolus (XPC, XPA, and ERCC1-XPF) (20) and it remains unrevealed if and how these repair proteins reach the rDNA within the nucleolus to repair it.

To determine the location of the rDNA during repair, we used a LacO-GFP-LacR reporter system to visualize the rDNA by microscopy in cells. Several LacO sequences were inserted downstream from the ribosomal transcription unit. These cells (HT80) were subsequently transfected with a plasmid carrying the GFP-LacR reporting system. The GFP-LacR, when expressed, targeted the LacO sequences downstream from the ribosomal genes allowing one to visualize the rDNA (Fig. 4*A*). To detect both the rDNA and the RNAP1, we performed an immunofluorescence (IF) assay against the biggest subunit of RNAP1 (RPA194) in these cells. We observed that in the untreated cells, rDNA and RNAP1 were located within the nucleolus (the method used to delimit nucleolus borders is depicted in *SI Appendix*, Fig. S4). However, 3 h after the irradiation rDNA, together with RNAP1, relocated to the periphery of the nucleoli and after the repair reaction is completed, both rDNA and RNAP1 returned within the nucleolus (Fig. 4*B*). The fact that not only rDNA was displaced but also RNAP1 confirms our results from ChIP-qPCR experiments (Fig. 1*B*) showing that after UV damage, RNAP1 did not dissociate from the rDNA.

To investigate whether this relocation is due to the DNA repair reaction, in the first place we performed a UV dose assay in WT cells untreated (NT) or 3 h post-UV at different UV doses. Our results showed that RNAP1 was displaced to the nucleolar periphery in a UV dose-dependent manner (*SI Appendix*, Fig. S5). Namely, UV doses from 1 to 10 J/m^2 did not affect RNAP1 position within the nucleolus. However, at 12 J/m^2, RNAP1 gathered in few foci within the nucleolus but closer to the nucleolar periphery, whereas at 16 J/m^2 the RNAP1 foci were clearly located at the nucleolar periphery. Because of these results, we decided to use 16 J/m^2 as the standard UV dose. At this dose in WT cells, in which

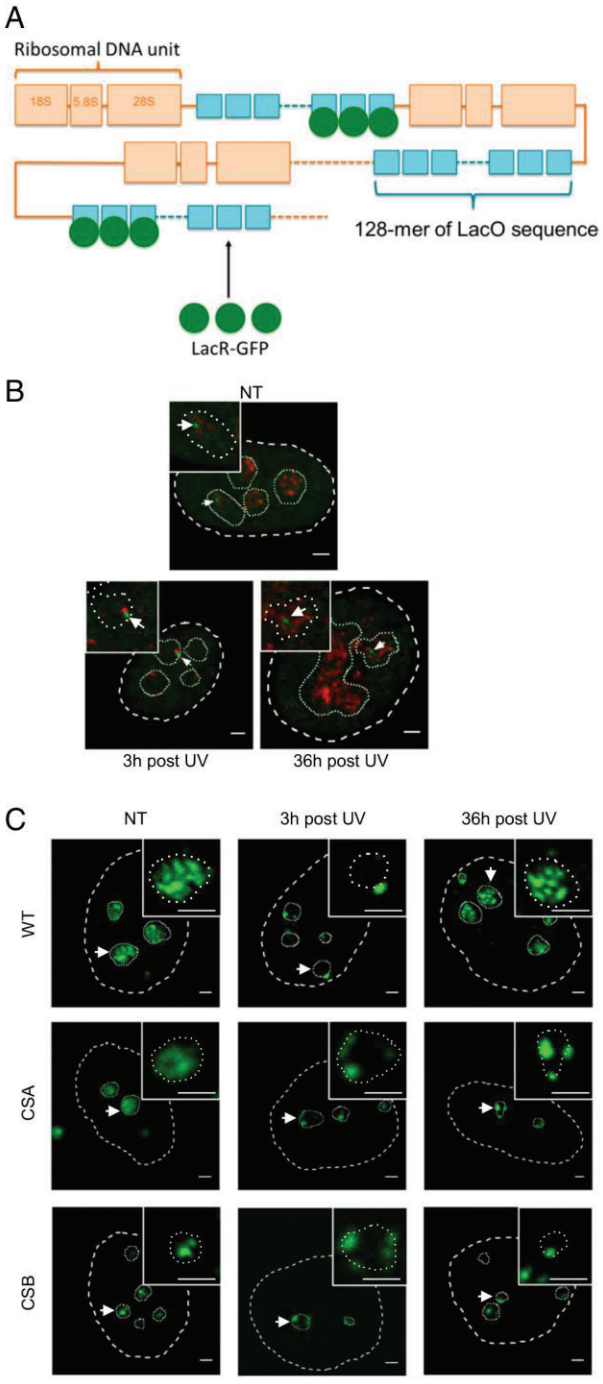

Fig. 4. Displacement of RNAP1 and rDNA during TC-NER. (*A*) Schematic representation of the LacO/LacR system used to visualize the ribosomal DNA. Several Lac operon sequences have been inserted, as a 128-mer array, downstream of the rDNA repeats in the cells, which were also transfected with a plasmid carrying the Lac repressor sequence tagged with the GFP coding sequence. (*B*) Confocal images of immunofluorescence assay against RNAP1 (red) in GFP-LacR (green) expressing cells. Cells were exposed or not (NT) to 16 J/m^2 of UV and fixed 3 or 36 h after UV exposure. (*C*) Confocal images of immunofluorescence staining against RNAP1 (green) performed on WT, CSA, and CSB cells. Cells were treated and fixed as mentioned above. Nuclei and nucleoli are indicated by dashed and dotted lines, respectively. *Insets* zoom into the nucleoli indicated with arrows. (Scale bars: 2 μm.)

NER is functional, RNAP1 was displaced at the nucleolar periphery 3 h post-UV and returned within the nucleolus at later time points (36 h post-UV), when repair was achieved (Fig. 4*C*). In CSA and CSB cells, which are TC-NER deficient, at 3 h post-UV a displacement of RNAP1 at the nucleolar periphery was observed as in WT cells. However, no return of the RNAP1 within the nucleolus was described at later time points (Fig. 4*C*). Furthermore, NER-deficient cells (XPA, XPB, XPD, and TTDA) showed a similar RNAP1 behavior after UV damage induction (*SI Appendix*, Fig. S7).

UV Lesions on rDNA Induce RNAP1 Retention at the Nucleolar Periphery. To investigate whether the reentry of RNAP1 within the nucleoli depends on transcription blockage (Fig. 3 and *SI Appendix*, Fig. S7), we performed an IF assay in a GG-NER–deficient cell line (XPC). In XPC cells, UV lesions located on nontranscribed strands of DNA are not repaired. However, in these cells, UV lesions located on active rDNA genes were repaired and RNAP1 transcription restarted (Fig. 3 and *SI Appendix*, Fig. S7). This situation was different from CSB cells, in which UV lesions located in active rDNA were not repaired and their presence inhibited transcription (Fig. 3). Within these GG-NER–deficient (XPC) and TC-NER–deficient (CSB) cells, we performed IF against RPA194. As previously described, RNAP1 relocated to the nucleolar periphery 3 h after irradiation in all cell types (Fig. 5*A*). In WT cells, RNAP1 returned within the nucleolus 36 h post-UV (Figs. 4*C* and 5*A*), and transcription restarted (Fig. 3 *B* and *C*). In contrast, in CSB cells RNAP1 remained at the nucleolar periphery (Fig. 5*A*) concomitantly with a transcription blockage (Fig. 3). Surprisingly RNAP1 remained at the nucleolar periphery in XPC cells (Fig. 5*A*) despite ribosomal transcription resumption (Fig. 3 *B* and *C*). We were able to verify these results in living cells by expressing a GFP-tagged version of the subunit RPA43 in WT, XPC, and CSB cells (Fig. 5*B*). Namely, in XPC cells, RPA43-GFP did not return in the nucleolus after DNA damage induction and repair of the transcribed rDNA.

We further investigated the dynamic behavior of RNAP1 in living cells by performing fluorescent recovery after photobleaching (FRAP) on RNAP1-GFP foci in wild type, CSB, and XPC cells at different times after UV irradiation (3, 16, and 40 h). Our FRAP data (Fig. 5 *C*–*E*) showed a recovery of fluorescence of individually bleached foci, in about 6 min, indicating an almost complete turnover of rDNA-bound RNAP1-GFP in that time interval. In WT cells, our FRAP data showed that 3 h post-UV RNAP1-GFP turnover was incomplete compared with untreated cells (Fig. 5*C*). Forty hours after UV, although a small change in the FRAP profile was seen in the first part of the curve, RNAP1-GFP turnover remained incomplete compared with non-irradiated WT cells. This partial recovery of fluorescence indicates

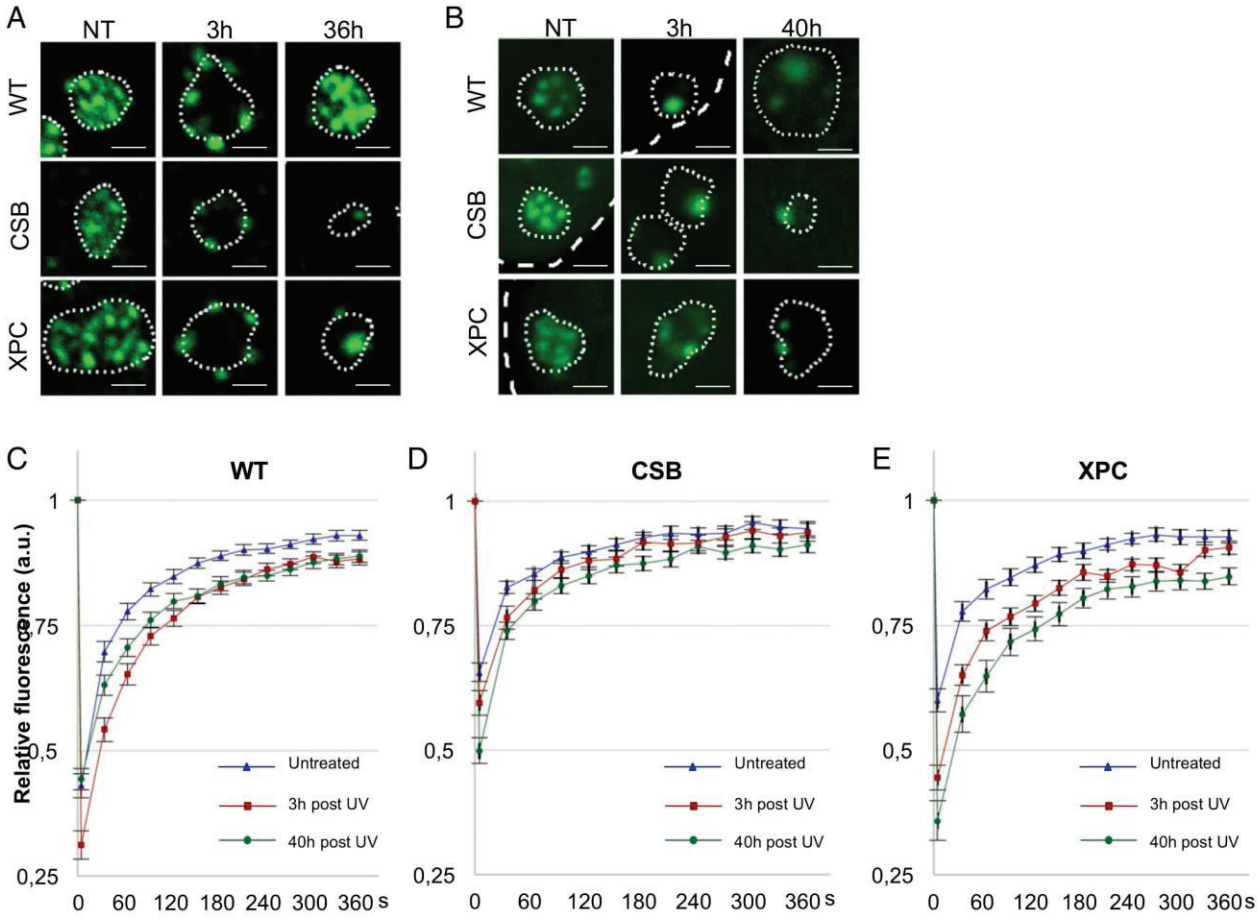

Fig. 5. Unrepaired UV lesions keep the RNAP1 at the nucleolar periphery despite transcription restart. Changes in the localization of endogenous (*A*) and GFP-tagged RNAP1 (*B*) in the nucleoli of WT, CBS, and XPC cells, untreated or at 3 and 36 h post-UV exposure. (*C*–*E*) FRAP curves of RNA Pol I-GFP protein stably expressed in WT, CSB, and XPC cells, respectively, untreated (blue) or UV irradiated 3 h before (red) or 40 h before (green) photobleaching. Error bars represent the SEM of three independent experiments. Nuclei and nulceoli are delimited by dashed and dotted lines, respectively. (Scale bar: 2 μm.) UV dose: 16 J/m^2.

that, in live cells, RNAP1-GFP is more bound within the nucleolar foci, 3 and 40 h post-UV, consistent with the Western blot observations in Fig. 1*C*. In CSB cells, UV irradiation did not significantly impact RNAP1-GFP fluorescence recovery (Fig. 5*D*), i.e., the bound fraction of RNAP1 was not modified by UV in these TC-NER–deficient cells. The same FRAP on foci procedure performed on GG-NER–deficient XPC cells, showed that 3 h post-UV, RNAP1-GFP turnover was incomplete (Fig. 5*E*). The effect observed 40 h after UV was even stronger, indicating that RNAP1 appeared progressively more bound.

Discussion

Nucleotide excision repair has been extensively studied in correlation with RNAP2-transcribed genes (2, 21–24). However, the repair mechanism of UV-damaged rDNA has been scarcely investigated in mammals and the few studies carried out have shown contradictory results (5, 7, 14, 25). Our research has focused on human rDNA repair after UV irradiation.

In this study, we have reported a decrease of RNAP1 transcription shortly after UV irradiation, followed by a slow recovery of rDNA transcription between 36 and 48 h post-UV (Fig. 2). RNAP1 transcription resumption is slower than RNAP2 transcription recovery, which occurs within 16–24 h (26). It is our opinion that the slow resumption of RNAP1 transcription could be due to the structure in which the transcription takes place: the nucleolus.

Although some studies have identified some NER factors interacting with RNAP1 in the nucleolus (10, 11, 27, 28), most of the repair proteins have not yet been found to localize in this nuclear region (20). For this reason, it is plausible that the transcription machinery needs to be relocated at the nucleolar periphery to be repaired, as in other cellular processes such as replication (29) and chromatin remodeling (30).

Indeed, rDNA and/or RNAP1 were located at the nucleolar periphery during rDNA replication and DSB repair of ribosomal genes (29–31). To confirm this hypothesis, we have investigated RNAP1 location during repair of UV lesions. Our data have demonstrated that RNAP1 shifts to the nucleolar periphery after UV exposure and returns into the nucleolus, when repair is completed 36 h post-UV in WT cells (Fig. 4*C*). Moreover, we have reported that, while not degraded, RNAP1 binds more to the rDNA after UV irradiation (Fig. 1 and *SI Appendix*, Fig. S1). Consistent with these findings, we have observed that rDNA is also displaced to the nucleolar periphery after UV irradiation and returns into the nucleoli after repair (Fig. 5*B*). Our results support the hypothesis that the rDNA/RNAP1 complex is transferred to the nucleolar periphery to access specific repair factors.

More than three decades ago, Cohn and Lieberman (5) showed that rDNA was repaired through NER in humans. Conversely, later on, several studies have established that rDNA was not repaired through the TC-NER mechanism in mammalian cells (25, 32, 33). However, these studies have worked on total rDNA, making no difference between active and inactive regions of the rDNA. Indeed, 50% of the rDNA is silent (34). To circumvent this bias, different studies performed in yeast have separated the inactive rDNA from the active one and have described the implication of TC-NER in repair of UV lesions on active rDNA (7, 35), even though the NER factor CSB did not seem to be involved (8).

Despite the apparent absence of TC-NER of rDNA in mammals (25, 32, 33) but in view of the fact that many similarities have been previously described between yeast and human processes, we investigated the implication of TC-NER factors during repair of UV-damaged rDNA in human cells. In this study, we have reported that UV lesions are quickly removed from the rDNA sequences (*SI Appendix*, Fig. S3) and that a complete TC-NER mechanism is required to repair the UV lesions present on active rDNA (Fig. 3 and *SI Appendix*, Fig. S6). Notably, both Cockayne syndrome proteins (CSA and CSB) are implicated in the repair reaction of ribosomal genes, and remarkably also the protein UV-stimulated scaffold protein A (UVSSA) (36), a newly discovered TC-NER–specific protein, plays a role in this particular repair, most likely because UVSSA is required for the stabilization of CSB specifically after UV irradiation (37). Because patients with UV-sensitive syndrome (UVSS) and patients with CSB have in common dermatological symptoms such as sun sensitivity but not the neurological abnormalities, we could suggest that the faulty repair of rDNAs is just responsible for the dermatological manifestations of both patients with UVSS and CSB.

During TC-NER of active rDNA, RNAP1 binds more to its substrate, as demonstrated by the FRAP experiments conducted in WT and XPC cells (GG-NER deficient but TC-NER proficient). Indeed, in WT and XPC cells, the turnover between the RNAP1 bound to rDNA and its free pool in the nucleolus is slower after UV irradiation, meaning that either more RNAP1 is bound to rDNA or the dissociation of RNAP1 from rDNA occurs less often (Fig. 5 *C*–*E*). This result was concomitantly confirmed by ChIP-qPCR experiments (Fig. 1*B*) and Western blot (Fig. 1 *C* and *D*), showing an increased binding of RNAP1 on chromatin after UV exposure in WT cells. In CSB cells (TC-NER deficient), no difference is observed in FRAP experiments before and after UV exposure (Fig. 5*D*), meaning that in CSB cells RNAP1 is not retained on rDNA after UV exposure, most probably because TC-NER is not functional in these cells. These results all together led us to conclude that TC-NER was required for rDNA repair of UV-induced lesions.

Interestingly, these results are different from those previously found in mammals showing that TC-NER is not involved in rDNAs repair (25, 32, 33). Moreover, differently from yeast (14), mammalian RNAP1 does not dissociate from its substrate during rDNA repair. Furthermore, in contrast with what has been shown for RNAP2, i.e., backtracking or unbinding of DNA followed by its degradation during repair (2, 38, 39), RNAP1 is not degraded during DNA repair but accumulates on rDNA and relocates at the nucleolar periphery as described in this study. In addition, Lisica et al. (40) have shown that RNAP1 was able to backtrack on rDNA, up to 20 nt, and then resume its transcription activity. This result confirms our hypothesis concerning the access of the repair machinery to the lesion on rDNA. A 20-nt backtrack seems sufficient to repair the lesion and allows the RNAP1 transcription resumption.

Intriguingly, RNAP1 remains bound to rDNA up to 40 h post-UV even though rDNA repair was completed (*SI Appendix*, Fig. S3) and transcription has restarted (Figs. 1 *C* and *D*, 2*E*, and 5*C*). This result indicates that RNAP1 requires a certain time to recover its binding dynamic after UV irradiation. In fact, although UV lesions might be repaired quickly and within 3 h (*SI Appendix*, Fig. S3), RNAP1 might take some time to be remobilized and of course transcription restart would also take a certain time to properly restart. Additionally, in the case of RNAP1, another layer of complexity is added because of RNAP1 displacement at the periphery of the nucleolus and its return within the nucleolus in wild-type cells while restoring transcription. All these steps do not need to happen within the same time frame, but of course, UV lesion repair has to be the first one to happen (*SI Appendix*, Fig. S3). On the contrary, UBF, which is a RNAP1 transcription partner, does not change its binding profile after UV irradiation, meaning that UBF is not more recruited to, or excluded from, rDNA during repair. This result can be explained by the fact that UBF is structurally needed to give the rDNA a conformation suitable for transcription, but it does not participate enzymatically in the transcription reaction per se. Indeed, in mammals, in addition to its implication in RNAP1 initiation (41), UBF induces the formation of the enhancesome by modifying structurally the rDNA to allow RNAP1 elongation through the rDNA (42).

Interestingly, in this study we have described the relocation of the RNAP1/rDNA complex at the nucleolar periphery after UV irradiation (Fig. 4 *A* and *C*). Several research groups have shown the formation of nucleolar caps (containing rDNA) at the nucleolar periphery after actinomycin D treatment and DSB induction inhibiting RNAP1 transcription (30, 43, 44). Another study has clearly demonstrated that DSBs inhibited RNAP1 transcription through the ATM pathway and has indicated RNAP1 relocation at the nucleolar periphery (45). However, Moore et al. (46) have shown opposite conclusions, i.e., nucleolar caps were formed after UV irradiation (36 J/m^2), but not following ionizing radiation (IR). These contradicting results could be explained by the diversity of DSB-inducing methods. Indeed, Moore et al. used IR, whereas in the other studies, laser microirradiation, the CRISPR/Cas9 technique, or the endonuclease I-PpoI were used (30, 44, 45). Despite these differences, the converging idea in the field is that the stall of transcription induced RNAP1 displacement at the nucleolar periphery. Our study challenges this accepted view.

We have investigated RNAP1/rDNA relocation at the nucleolar periphery during DNA repair in various NER-deficient cell lines. We have shown that while in WT cells, 36 h post-UV, ribosomal transcription restarts and RNAP1 returns into the nucleolus, in TC-NER–deficient cells (CSB and CSA), transcription is permanently inhibited and RNAP1 remains at the nucleolar periphery (Figs. 3 and 5). Remarkably, in XPC cells that are TC-NER proficient but GG-NER deficient, even though rDNA transcription restarts, RNAP1 remains at the nucleolar periphery. In fact, in these cells, while UV lesions on the active rDNAs are repaired (proficient TC-NER), UV lesions on the inactive genome in proximity of rDNA (active or inactive) are not repaired and are still present on the DNA. These results support two main ideas: (*i*) Firstly, RNAP1 position at the nucleolar periphery is not always associated with transcription inhibition, and transcription recovery is not enough to induce RNAP1 reentry; and (*ii*) secondly, and most importantly, unrepaired UV lesions on silent area nearby active rDNA or in inactive rDNA are sufficient to maintain RNAP1 to the nucleolar periphery, despite transcription restart. The presence of unrepaired UV lesions could be a signal for the transport of RNAP1/rDNA to, and/or the signal for its retention at the nucleolar periphery. But also, unrepaired UV lesions could induce specific chromatin modification and/or remodeling around the lesion, as seen with the spread of γH2AX signal through the chromatin to enhance DSB repair (47), that would imply rDNA relocation for the recruitment of repair proteins near the lesion.

Ribosomal DNA repair of UV-induced lesions has hardly been studied in human cells and the few studies were performed more than 20 y ago. However, rDNA transcription represents a crucial and limiting step of ribosome biogenesis, an essential cellular process that has been involved in several diseases called ribosomopathies (48). In this study, we demonstrated in human cells that rDNA repair after UV irradiation involves the complete TC-NER mechanism. We also determined that RNAP1/rDNA relocation, at the nucleolar periphery during repair, and reentry, within the nucleolus, are strictly dependent on the repair of all UV lesions (in transcribed/untranscribed DNA) rather than subordinate to transcription resumption.

Many questions remain to be elucidated. In the next years, it will be important to investigate the mechanistic aspects of RNAP1/rDNA eviction and reentry. Further studies should be set up to identify the partners involved in this RNAP1/rDNA nucleolar motion, detect chromatin modifications during this displacement, as well as decipher its impact on RNAP1 transcription in the long term and on ribosome biogenesis.

Materials and Methods

RPA43-GFP Fusion Protein Production and Expression in Transformed Human Fibroblasts. The full-length RNAP1 subunit (RPA43) was cloned in frame into the pEGFP-N1 vector (Clontech). The construct was sequenced before transfection. Transfection in MRC5, CSA, CSB, and XPC SV40-transformed human fibroblasts was performed using Fugene transfection reagent (Roche). Stably expressing cells were isolated after selection with G418 (Gibco) and single cell sorting was carried out using FACS (FACScalibur; Beckton Dickinson).

Cell Culture and Treatments. The cells used in this study were: (*i*) wild-type SV40-immortalized human fibroblasts (MRC5); (*ii*) GG-NER–deficient SV40-immortalized human fibroblast: XPC (XP4PA); (*iii*) TC-NER–deficient SV40-immortalized human fibroblast: CSA (CS3BE) and CSB (CS1AN); (*iv*) NER (GG-NER and TC-NER)-deficient SV40-immortalized human fibroblast: XPA (XP12RO), XPB (TTD6VI), XPB (XPCS2BA), XPD (XP6BE), XPD (XPCS2), and TTDA (TTD1BR); (*v*) MRC5, CSB, and XPC stably expressing RPA43-GFP (RNAP1 subunit; G418 selected 0.2 mg/mL); (*vi*) WT and TC-NER–deficient primary fibroblasts: WT (C5RO), UVSSA (KPS3), and CSB (CS1AN). Wild-type murine embryonic stem (ES) cells were derived from the XPB-YFP mouse model (49). HT-1080 cells stably expressing an adapted Lac operator/Lac repressor (LacO/LacR) system (selected using Blasticidin S and hygromycin, 5 μg/mL and 100 μg/mL, respectively) were used to detect the rDNA as previously described (50, 51).

Transformed human fibroblasts were cultured in a 1:1 mixture of Ham's F-10 and DMEM (Lonza) supplemented with 1% antibiotics (penicillin and streptomycin; Lonza) and 10% FBS (Gibco). Transformed human fibroblasts were incubated at 37 °C with 20% O_2 and 5% CO_2.

Primary human fibroblasts were cultured in Ham's F-10 (Lonza) supplemented with 1% antibiotics (penicillin and streptomycin; Lonza) and 10% FBS (Gibco). Primary human fibroblasts were incubated at 37 °C with 3% O_2 and 5% CO_2.

Murine ES cells were cultured in a 1:1 mixture of DMEM (Lonza) and BRL conditioned medium, supplemented with antibiotics (penicillin and streptomycin; Lonza), 10% FBS (Gibco), nonessential amino acids (Gibco), β-mercaptoethanol (Sigma), and ESGRO leukemia inhibitory factor (Merck Millipore). HT-1080 cells with LacO/GFP-LacR were cultured in DMEM (Lonza), supplemented with 1% antibiotics (penicillin and streptomycin; Lonza) and 10% FBS (Gibco). ES cells were incubated at 37 °C with 3% O_2 and 5% CO_2.

DNA damage was inflicted by UV-C light (254 nm, 6-W lamp). Cells were globally irradiated with different doses of UV-C (1 J/m^2, 2 J/m^2, 4 J/m^2, 5 J/m^2, 6 J/m^2, 8 J/m^2, 10 J/m^2, 12 J/m^2, and 16 J/m^2). Experiments were performed at different time points after UV exposure (0.5, 1, 3, 16, 24, 36, and 40 h post-UV). Mock-irradiated cells (untreated) were used as control. UV irradiation at 16 J/m^2 induces statistically two lesions per 10 kb (52).

RNA FISH. Cells were grown on 12-mm coverslips, washed with warm PBS, and fixed with 4% paraformaldehyde for 15 min at 37 °C. Coverslips were washed twice with PBS. Cells were permeabilized by washing with PBS 0.4% Triton X-100 for 7 min at 4 °C. Cells were washed rapidly with PBS before incubating them with prehybridization buffer (2× SSPE and 15% formamide) [20× SSPE, (pH 8.0): 3 M NaCl, 157 mM $NaH_2PO_4.H_2O$, and 25 mM EDTA] for at least 30 min. A total of 1.5 μL of probe (10 ng/mL) was diluted in 30 μL of hybridization mix (2× SSPE, 15% formamide, 10% dextran sulfate, 0.5 mg/mL tRNA) and heated to 90 °C for 1 min. Hybridization of the probe was conducted overnight at 37 °C in a humid environment. Subsequently, cells were washed twice for 20 min with prehybridization buffer, then once for 20 min with 1× SSPE, and finally mounted with Vectashield (Vector Laboratories) and kept at −20 °C. The designed probe, including a cyanin5 fluorochrome, was conceived to recognize the 5′ part of the 47S prerRNA, upstream from the first cleavage site, rapidly processed during rRNA processing. The probe sequence (5′–3′) is: Cy5-AGACGAGAACGCCTG ACACGCACGGCAC. At least three biological replicates were obtained and at least 30 cells were imaged for each condition of each cell line.

Northern Blot. Extractions of total RNAs from cells were performed using TRI reagent (Sigma-Aldrich). Briefly, subconfluent growing cells were trypsinized and washed in PBS. The pellet was suspended in 1 mL TRI reagent and processed as recommended by the manufacturer. An additional step of phenol/chloroform extraction was performed on the RNA-containing soluble fraction before isopropanol precipitation.

Four micrograms of total RNAs was separated on a 1.2% agarose gel as described in ref. 53. RNAs were transferred to Amersham Hybond N+ membranes (GE Healthcare), which were hybridized with ^{32}P-labeled oligonucleotides

using Rapid-Hyb buffer (GE Healthcare). The membranes were exposed to Phosphor Screens developed in a Phospho Imager apparatus and quantified with ImageQuant software. The oligonucleotide sequences used as probes were: 47S, AGACGAGAAC GCCTGACACGCACGGCAC (targets the same area of the 47S prerRNA as described in the RNA FISH section) and 18S, ATGTGGTAGCCGTTTCTCAG.

ChIP on ES Nuclear Extract. ChIP was performed as described previously (12). Briefly, ES cells were grown under optimal growth conditions, UV irradiated with 16 J/m^2 UV-C, and after 3 and 16 h cells were fixed and harvested by scraping in PBS. Cell lysis was performed with lysis buffer and nuclei washed with wash buffer. Afterward, nuclei were suspended in IP buffer and sonicated in a Bioruptor UDC-200 (set up high for 30 min, with cycles of 30 s on/1 min off; Diagenode) to yield DNA fragments with an average size of 300 bp. Samples were centrifuged at 14,000 × *g* for 5 min to remove insoluble material and measured with a nanodrop at 260 nm. Optimal amounts of ES extracts to maximize the ChIP ratio were incubated in 150 μL total volume with antibody (RPA194 C-1, sc-48385; Santa Cruz) (ChIP) or no antibody (mock), overnight. IP was performed for 1 h with 40 μL of washed magnetic Bio-Adembeads Protein G (Ademtech). After IP, the beads were washed and DNA and proteins eluted with elution buffer. DNA from ChIP, mock, and input preparations were decross-linked and purified by phenol-chloroform extraction. Samples were amplified by real-time PCR (qPCR) using the Power SYBR Green PVR master mix (Applied Biosystems) on a 7300 real-time PCR system (Applied Biosystems). ChIP data were normalized to the input (to take copy number into account) and subtracted with the background (mock). Biological replicates were generated for each experiment. Primer sequences for qPCR can be found in ref. 12.

Chromatin Extracts. MRC5s were grown in a 14.5-cm plate. Cells were irradiated as described above and washed once with PBS. In vivo cross-linking was performed as described (54, 55) with few modifications. All procedures were carried out at 4 °C unless otherwise stated. Briefly, control or irradiated cells were cross-linked with 12 mL of 1% formaldehyde (in PBS) prepared from an 11% stock [0.05 M Hepes (pH 7.8), 0.1 M NaCl, 1 mM EDTA, 0.5 mM EGTA, 11% formaldehyde] for 16 min. Cross-linking was neutralized with 12 mL of glycin solution [PBS, glycin 0.125M, (pH 6.8)] for 7 min, followed by two washes with cold PBS. The cells were collected by scraping in cold PBS (PBS, 1 mM EDTA) and spun down 10 min at 1,200–1,500 rpm at 4 °C.

All buffers used for cell extraction contained, among others, 1 mM EDTA, 0.5 mM EGTA, and 1 mM PMSF, and a mixture of proteinase and phosphatase inhibitors (EDTA-free protease inhibitor tablets; Roche). Just before use, Napy-sodium pyrophosphate (0.33 M stock) was added.

Cell pellet was washed twice with cold PBS. The cell pellet was suspended in Chro-lysis buffer [1 mL per 12.5 × 10^6 cells; 50 mM Hepes-KOH (pH 7.8), 0.14 M NaCl, 1 mM EDTA (pH 8.0), 0.5 mM EGTA (pH 8.0), 0.5% Nonidet P-40, 0.25% Triton, 10% glycerol] and rotated for 10 min. The suspension was spun down (1,200–1,400 rpm, 10 min, 4 °C). Cell pellet was washed with wash buffer [1 mL per 12.5 × 10^6 cells; 0.01 M Tris·HCl (pH 8.0), 0.2 M NaCl, 1 mM EDTA (pH 8.0), 0.5 mM EGTA (pH 8.0)] rotated for 10 min, spun down (1,200–1,400 rpm, 10 min, 4 °C), suspended in RIPA buffer [1 mL RIPA buffer per 25–35 × 10^6 cells; 0.01 M Tris·HCl (pH 8.0), 0.14 M NaCl, 1 mM EDTA (pH 8.0), 0.5 mM EGTA (pH 8.0), 1% Triton, 0.1% Na-deoxycholate, 0.1% SDS] and incubated for 30 min.

The nuclear suspension was sonicated on ice-cooled water using a Bioruptor UDC-200 for 45 min (power setting on high; 30 s on/1 min off; Diagenode) to yield DNA fragments with an average size of 300 bp. After the sonication, samples were spun down (10,000 rpm, 10 min, 4 °C) and the supernatant that contained the cross-linked chromatin was aliquoted, frozen with liquid nitrogen, and stored at −80 °C.

Nuclear Extracts. Nuclear extracts were performed using the Nuclear Extract kit for mammalian cells (NXTRACT-1KT CellLytic NuCLEAR Extraction Kit; Sigma-Aldrich) according to the manufacturer.

Western Blot. Protein concentration was determined by using the Bradford method. Samples were diluted with 2× Laemmli buffer, heated at 95 °C (1× 30 min, spin down, 1× 25 min, spin down) and loaded on a SDS/PAGE gel. Proteins were separated on 8% and 14% SDS/PAGE, transferred onto a polyvinylidene difluoride membrane (PVDF) (0.45 μm; Millipore). The membrane was blocked in 5% milk PBS 0.1% Tween (PBS-T) and incubated for 1.5 h with the primary antibodies (see *Primary Antibodies*) in milk PBS-T. The loading was controlled with the anti-Histon3 antibody. Subsequently, membrane was washed with PBS-T (3× 10 min) and incubated with the secondary antibody in milk PBS-T. After the same washing procedure, protein bands were visualized via chemiluminescence (ECL Enhanced Chemo Luminescence; Pierce ECL Western Blotting Substrate) using the ChemiDoc MP system (BioRad).

Western Blot Antibodies.

Primary antibodies. The primary antibodies are as follows: mouse anti-RPA194(C1) (sc-48385) 1/500; mouse anti-UBF(F-9) (sc-13125) 1/500; rabbit anti-TWISTNB (ab99305) 1/2,000; rabbit anti-hPAF49 (GTX102175) 1/250; mouse anti-POLR1E (sc-398270) 1/500; rabbit anti-Pol II CTD repeat YSPTSPS Phospho Ser2 (ab5095) 1/250; and rabbit anti-Histone H3 (ab1791) 1/10,000.

Secondary antibodies. The secondard antibodies are as follows: goat anti-mouse HRP conjugate (170-6516; Biorad) 1/5,000; and goat anti-rabbit HRP conjugate (170-6515; Biorad) 1/5,000.

Immunofluorescence Assay. Cells were grown on 24-mm coverslips, washed with warm PBS, and fixed with 2% paraformaldehyde for 15 min at 37 °C. Cells were permeabilized with PBS 0.1% Triton X-100 (3× short + 2× 10 min). Blocking of nonspecific signal was performed with PBS$^+$ (0.5% BSA; 0.15% glycin) for at least 30 min. Then, coverslips were incubated with 100 μL of primary antibody mix (mouse anti-RPA194; 1/500 in PBS$^+$; sc-48385) for 2 h at room temperature in a moist chamber, washed with PBS (3× short; 2× 10 min), and quickly washed with PBS$^+$ before incubating with 100 μL of secondary antibody mix (goat anti-mouse Alexa Fluor 488 and goat anti-mouse Alexa Fluor 594; 1/400 in PBS$^+$; A-11001 and A-11005; Invitrogen, respectively) for 1 h at room temperature in a moist chamber. After the same washing procedure, coverslips were finally mounted using Vectashield with DAPI (Vector Laboratories) and kept at −20 °C. At least three biological replicates were performed and at least 30 cells were imaged for each condition of each cell line.

FRAP. FRAP experiments were performed on a Zeiss LSM 710 NLO confocal laser scanning microscope, using a 40×/1.3 oil objective, under a controlled environment (37 °C, 5% CO_2). Briefly, RNAP1-GFP foci were selected in the nucleolus and photobleached at 100% laser intensity of the 488 line of a 25-mW argon laser. Then, recovery of fluorescence was monitored at 1% laser intensity, every 30 s directly after the bleach and up to 6 min after bleaching. All FRAP data were normalized to the average prebleached fluorescence after background removal. The loss of fluorescence induced by the measure every 30 s was also taken into account. Every plotted FRAP curve is an average of at least 30 measured cells.

Fluorescent Imaging and Analysis. Imaging was performed on a Zeiss LSM 780 NLO confocal laser-scanning microscope, using a 60×/1.4 oil objective. Images were analyzed with ImageJ software. For all images of this study, nuclei and nucleoli were delimited with dashed and dotted line, respectively, using DAPI staining or transmitted light.

Statistical Analysis. Error bars represent the SEM of the biological replicates. Student's *t* test was used to assess whether the mean values of the replicates were statistically significant, assuming equal variance. A *P* value of 0.05 or less was considered as significant (*$P < 0.05$; **$P < 0.01$; ***$P < 0.001$).

ACKNOWLEDGMENTS. We thank Elizabeth Kerr and Jonathan Chubb (Wendy Bickmore's research team, Medical Research Council Institute of Genetics & Molecular Medicine, Edinburgh, UK) for kindly providing the HT80 cells carrying the LacO/LacR system, as well as all the information related to this cell line; and Dr. Tomoo Ogi for providing us with the UVSSA cell line Kps3. This work was supported by grants from La Ligue Nationale Contre le Cancer (L.D. and E.C.), l'Agence Nationale de la Recherche (ANR FreTNET: Grant ANR10-BLAN-1231-01; ANR DyReCT: Grant ANR-14-CE10-0009), and the Association pour la Recherche sur le Cancer (projet Fondation Award ARC PJA 20131200188).

1. Iyama T, Wilson DM, 3rd (2013) DNA repair mechanisms in dividing and non-dividing cells. *DNA Repair (Amst)* 12:620–636.
2. Marteijn JA, Lans H, Vermeulen W, Hoeijmakers JHJ (2014) Understanding nucleotide excision repair and its roles in cancer and ageing. *Nat Rev Mol Cell Biol* 15:465–481.
3. Grummt I (2003) Life on a planet of its own: Regulation of RNA polymerase I transcription in the nucleolus. *Genes Dev* 17:1691–1702.
4. Russell J, Zomerdijk JCBM (2005) RNA-polymerase-I-directed rDNA transcription, life and works. *Trends Biochem Sci* 30:87–96.
5. Cohn SM, Lieberman MW (1984) The use of antibodies to 5-bromo-2′-deoxyuridine for the isolation of DNA sequences containing excision-repair sites. *J Biol Chem* 259:12456–12462.
6. Christians FC, Hanawalt PC (1993) Lack of transcription-coupled repair in mammalian ribosomal RNA genes. *Biochemistry* 32:10512–10518.

7. Conconi A, Bespalov VA, Smerdon MJ (2002) Transcription-coupled repair in RNA polymerase I-transcribed genes of yeast. *Proc Natl Acad Sci USA* 99:649–654.
8. Verhage RA, Van de Putte P, Brouwer J (1996) Repair of rDNA in Saccharomyces cerevisiae: RAD4-independent strand-specific nucleotide excision repair of RNA polymerase I transcribed genes. *Nucleic Acids Res* 24:1020–1025.
9. Tremblay M, Teng Y, Paquette M, Waters R, Conconi A (2008) Complementary roles of yeast Rad4p and Rad34p in nucleotide excision repair of active and inactive rRNA gene chromatin. *Mol Cell Biol* 28:7504–7513.
10. Bradsher J, et al. (2002) CSB is a component of RNA pol I transcription. *Mol Cell* 10: 819–829.
11. Iben S, et al. (2002) TFIIH plays an essential role in RNA polymerase I transcription. *Cell* 109:297–306.
12. Nonnekens J, et al. (2013) Mutations in TFIIH causing trichothiodystrophy are responsible for defects in ribosomal RNA production and processing. *Hum Mol Genet* 22:2881–2893.
13. Andrade-Lima LC, Veloso A, Paulsen MT, Menck CFM, Ljungman M (2015) DNA repair and recovery of RNA synthesis following exposure to ultraviolet light are delayed in long genes. *Nucleic Acids Res* 43:2744–2756.
14. Tremblay M, et al. (2014) UV light-induced DNA lesions cause dissociation of yeast RNA polymerases-I and establishment of a specialized chromatin structure at rRNA genes. *Nucleic Acids Res* 42:380–395.
15. Zavala AG, Morris RT, Wyrick JJ, Smerdon MJ (2014) High-resolution characterization of CPD hotspot formation in human fibroblasts. *Nucleic Acids Res* 42:893–905.
16. Bregman DB, et al. (1996) UV-induced ubiquitination of RNA polymerase II: A novel modification deficient in Cockayne syndrome cells. *Proc Natl Acad Sci USA* 93: 11586–11590.
17. Ratner JN, Balasubramanian B, Corden J, Warren SL, Bregman DB (1998) Ultraviolet radiation-induced ubiquitination and proteasomal degradation of the large subunit of RNA polymerase II. Implications for transcription-coupled DNA repair. *J Biol Chem* 273:5184–5189.
18. Cui C, Tseng H (2004) Estimation of ribosomal RNA transcription rate in situ. *Biotechniques* 36:134–138.
19. Tomecki R, Sikorski PJ, Zakrzewska-Placzek M (2017) Comparison of preribosomal RNA processing pathways in yeast, plant and human cells–Focus on coordinated action of endo- and exoribonucleases. *FEBS Lett* 591:1801–1850.
20. Andersen JS, et al. (2005) Nucleolar proteome dynamics. *Nature* 433:77–83.
21. Chitale S, Richly H (2017) Timing of DNA lesion recognition: Ubiquitin signaling in the NER pathway. *Cell Cycle* 16:163–171.
22. Coin F, et al. (2008) Nucleotide excision repair driven by the dissociation of CAK from TFIIH. *Mol Cell* 31:9–20.
23. Hanawalt PC (1994) Transcription-coupled repair and human disease. *Science* 266: 1957–1958.
24. Spivak G (2015) Nucleotide excision repair in humans. *DNA Repair (Amst)* 36:13–18.
25. Christians FC, Hanawalt PC (1994) Repair in ribosomal RNA genes is deficient in xeroderma pigmentosum group C and in Cockayne's syndrome cells. *Mutat Res* 323: 179–187.
26. Bohr VA, Smith CA, Okumoto DS, Hanawalt PC (1985) DNA repair in an active gene: Removal of pyrimidine dimers from the DHFR gene of CHO cells is much more efficient than in the genome overall. *Cell* 40:359–369.
27. Assfalg R, et al. (2012) TFIIH is an elongation factor of RNA polymerase I. *Nucleic Acids Res* 40:650–659.
28. Koch S, et al. (2014) Cockayne syndrome protein A is a transcription factor of RNA polymerase I and stimulates ribosomal biogenesis and growth. *Cell Cycle* 13: 2029–2037.
29. Dimitrova DS (2011) DNA replication initiation patterns and spatial dynamics of the human ribosomal RNA gene loci. *J Cell Sci* 124:2743–2752.
30. Franek M, Kovaříková A, Bártová E, Kozubek S (2016) Nucleolar reorganization upon site-specific double-strand break induction. *J Histochem Cytochem* 64:669–686.
31. Larsen DH, Stucki M (2016) Nucleolar responses to DNA double-strand breaks. *Nucleic Acids Res* 44:538–544.
32. Balajee AS, May A, Bohr VA (1999) DNA repair of pyrimidine dimers and 6-4 photoproducts in the ribosomal DNA. *Nucleic Acids Res* 27:2511–2520.
33. Vreeswijk MP, et al. (1994) Analysis of repair of cyclobutane pyrimidine dimers and pyrimidine 6-4 pyrimidone photoproducts in transcriptionally active and inactive genes in Chinese hamster cells. *J Biol Chem* 269:31858–31863.
34. Conconi A, Widmer RM, Koller T, Sogo JM (1989) Two different chromatin structures coexist in ribosomal RNA genes throughout the cell cycle. *Cell* 57:753–761.
35. Charton R, Guintini L, Peyresaubes F, Conconi A (2015) Repair of UV induced DNA lesions in ribosomal gene chromatin and the role of "odd" RNA polymerases (I and III). *DNA Repair (Amst)* 36:49–58.
36. Nakazawa Y, et al. (2012) Mutations in UVSSA cause UV-sensitive syndrome and impair RNA polymerase IIo processing in transcription-coupled nucleotide-excision repair. *Nat Genet* 44:586–592.
37. Higa M, Zhang X, Tanaka K, Saijo M (2016) Stabilization of ultraviolet (UV)-stimulated scaffold protein A by interaction with ubiquitin-specific peptidase 7 is essential for transcription-coupled nucleotide excision repair. *J Biol Chem* 291:13771–13779.
38. Cheung ACM, Cramer P (2011) Structural basis of RNA polymerase II backtracking, arrest and reactivation. *Nature* 471:249–253.
39. Wilson MD, Harreman M, Svejstrup JQ (2013) Ubiquitylation and degradation of elongating RNA polymerase II: The last resort. *Biochim Biophys Acta* 1829:151–157.
40. Lisica A, et al. (2016) Mechanisms of backtrack recovery by RNA polymerases I and II. *Proc Natl Acad Sci USA* 113:2946–2951.
41. Jantzen HM, Admon A, Bell SP, Tjian R (1990) Nucleolar transcription factor hUBF contains a DNA-binding motif with homology to HMG proteins. *Nature* 344:830–836.
42. Stefanovsky VY, Moss T (2008) The splice variants of UBF differentially regulate RNA polymerase I transcription elongation in response to ERK phosphorylation. *Nucleic Acids Res* 36:5093–5101.
43. Reynolds RC, Montgomery PO, Hughes B (1964) Nucleolar "caps" produced by actinomycin D. *Cancer Res* 24:1269–1277.
44. van Sluis M, McStay B (2015) A localized nucleolar DNA damage response facilitates recruitment of the homology-directed repair machinery independent of cell cycle stage. *Genes Dev* 29:1151–1163.
45. Kruhlak M, et al. (2007) The ATM repair pathway inhibits RNA polymerase I transcription in response to chromosome breaks. *Nature* 447:730–734.
46. Moore HM, et al. (2011) Quantitative proteomics and dynamic imaging of the nucleolus reveal distinct responses to UV and ionizing radiation. *Mol Cell Proteomics* 10: M111.009241.
47. Price BD, D'Andrea AD (2013) Chromatin remodeling at DNA double-strand breaks. *Cell* 152:1344–1354.
48. Danilova N, Gazda HT (2015) Ribosomopathies: How a common root can cause a tree of pathologies. *Dis Model Mech* 8:1013–1026.
49. Giglia-Mari G, et al. (2009) Differentiation driven changes in the dynamic organization of Basal transcription initiation. *PLoS Biol* 7:e1000220.
50. Chubb JR, Boyle S, Perry P, Bickmore WA (2002) Chromatin motion is constrained by association with nuclear compartments in human cells. *Curr Biol* 12:439–445.
51. Robinett CC, et al. (1996) In vivo localization of DNA sequences and visualization of large-scale chromatin organization using lac operator/repressor recognition. *J Cell Biol* 135:1685–1700.
52. Mayne LV, Lehmann AR (1982) Failure of RNA synthesis to recover after UV irradiation: An early defect in cells from individuals with Cockayne's syndrome and xeroderma pigmentosum. *Cancer Res* 42:1473–1478.
53. Sambrook JF, Russell DW, eds (2001) *Molecular Cloning: A Laboratory Manual* (Cold Spring Harbor Lab Press, Woodbury, NY), 3rd Ed.
54. Orlando V, Strutt H, Paro R (1997) Analysis of chromatin structure by in vivo formaldehyde cross-linking. *Methods* 11:205–214.
55. Parekh BS, Maniatis T (1999) Virus infection leads to localized hyperacetylation of histones H3 and H4 at the IFN-β promoter. *Mol Cell* 3:125–129.

Supplementary Information

Supplementary Information Text

Material and Method

DNA IP of 6-4PP and CPD lesions

MRC5SV cells were grown in 14.5 cm plate. Cells were irradiated as described in the M&M section and washed once with PBS. 20 µl of washed magnetic Bio-Adembeads Protein G (Ademtech) were incubated for 8 hours with mock antibody (Anti-Human IgM Sigma I6385), 6-4PP antibody (Anti-6-4PP CosmoBio Clone 64M-2) or CPD antibody (Anti-CPD CosmoBio Clone TDM-2). Cells were collected by scraping and genomic DNA was extracted using the GenElute Mammalian Genomic kit (Sigma) according to the manufacturer. Subsequently, samples ware sonicated in a Bioruptor UDC-200 (set up high for 20 min, with cycles of 30 sec ON/30 min OFF; Diagenode)) to yield DNA fragments with an average size of 300bp. 10 µg of DNA were diluted in PBS + Triton X100 0.025% + tRNA 25 µg/ml, kept at 95°C for 5 min and then on ice.
Previously incubated beads were washed twice with PBS + Triton X100 0.025% + tRNA 25 µg/ml and then incubated with DNA O/N at 4°C. After IP, the beads were washed and DNA eluted with elution buffer. DNA from IP, Mock and input preparations were purified by phenol-chloroform extraction. Samples were amplified by real-time PCR (qPCR) using the Power SYBR Green PVR master mix (Applied Biosystems) on a 7300 real-time PCR system (Applied Biosystems). IP and Mock data were normalized to the input and then IP data subtracted with the background (Mock). Data from all conditions were normalized to the 0h condition.

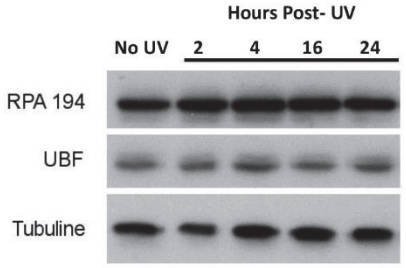

Fig. S1. Total protein level of RNAP1 and its transcription factor UBF after UV exposure

Western blot against RNAP1 biggest subunit (RPA194) and UBF (RNAP1 transcription factor) performed on nuclear extracts of wild type cells at different times after a 16J/m2 of UV-C irradiation. Tubulin was used as loading control.

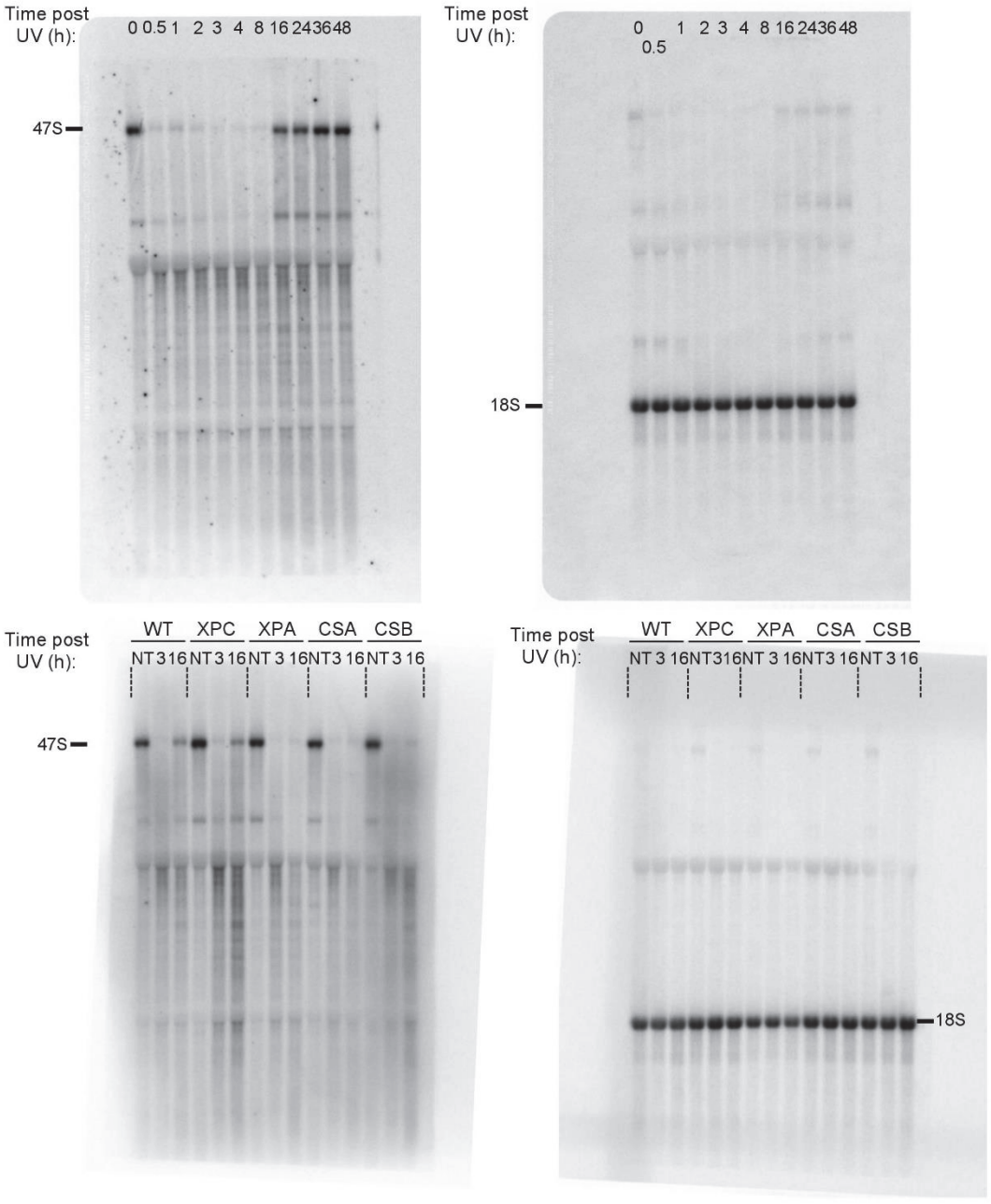

Figure S2. Northern blot analysis, uncropped blots corresponding to Figure 2D and 3A

Uncropped Northern blot showing over time the 47S pre-rRNA level after UV irradiation (16J/m2). The amount of 18S rRNA is used as control.

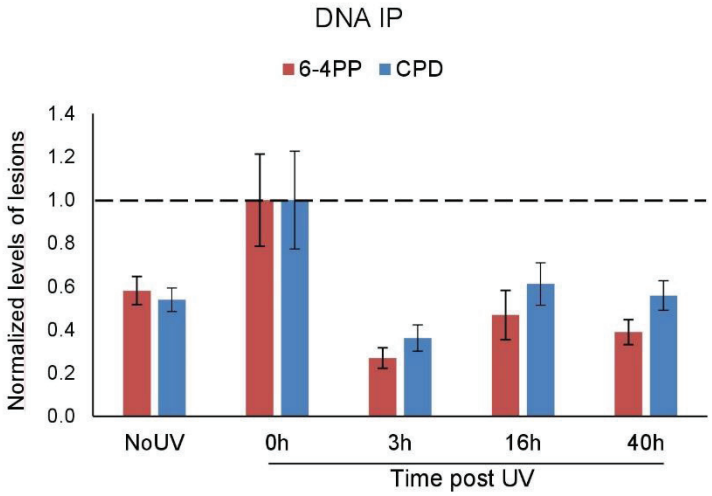

Figure S3. DNA lesions on rDNAs

Quantification of DNA IP of 64PP and CPD and qPCR of rDNAs sequences before and after UV irradiation. Error bars represent SEM.

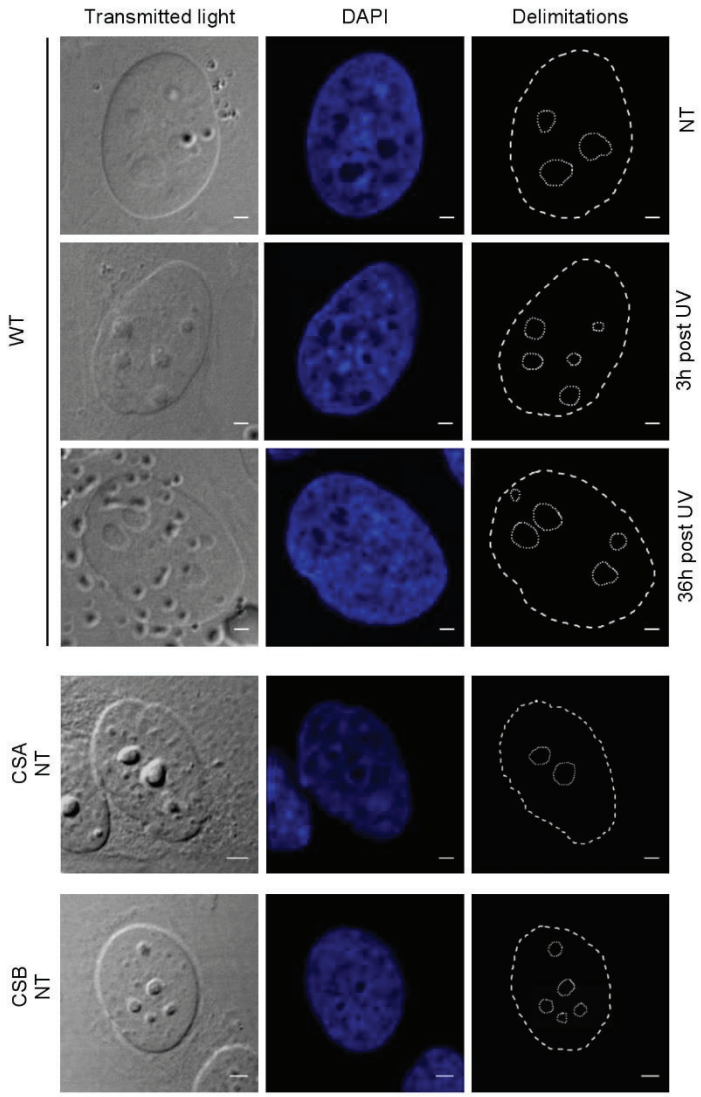

Figure S4. Method used to delimit the nuclei and nucleoli

Delimitations of nuclei and nucleoli (indicated by dashed or dotted lines respectively) were drawn by combining transmitted light and/or DAPI staining images. Examples shown for wild type (WT) cells non treated (NT), 3h post UV and 36h post UV, as well as for TC-NER deficient (CSA & CSB) non treated cells. Scale bars: 2µm.

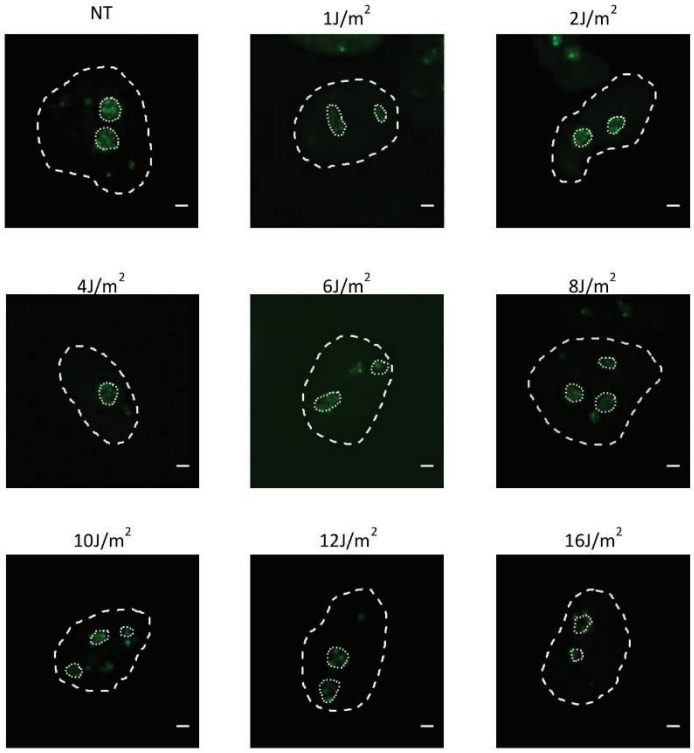

Figure S5. RNAP1 relocation at the nucelolar periphery is UV dose-dependant

Confocal images of human fribroblast stably expressing RNAP1-GFP. Cells were exposed or not (NT) to different doses of UV (1; 2; 4; 6; 8; 10; 12 and 16J/m2) and fixed 3 hours after irradiation. Nuclei and nucleoli are indicated by dashed and dotted lines respectively. Scale bar: 2µm.

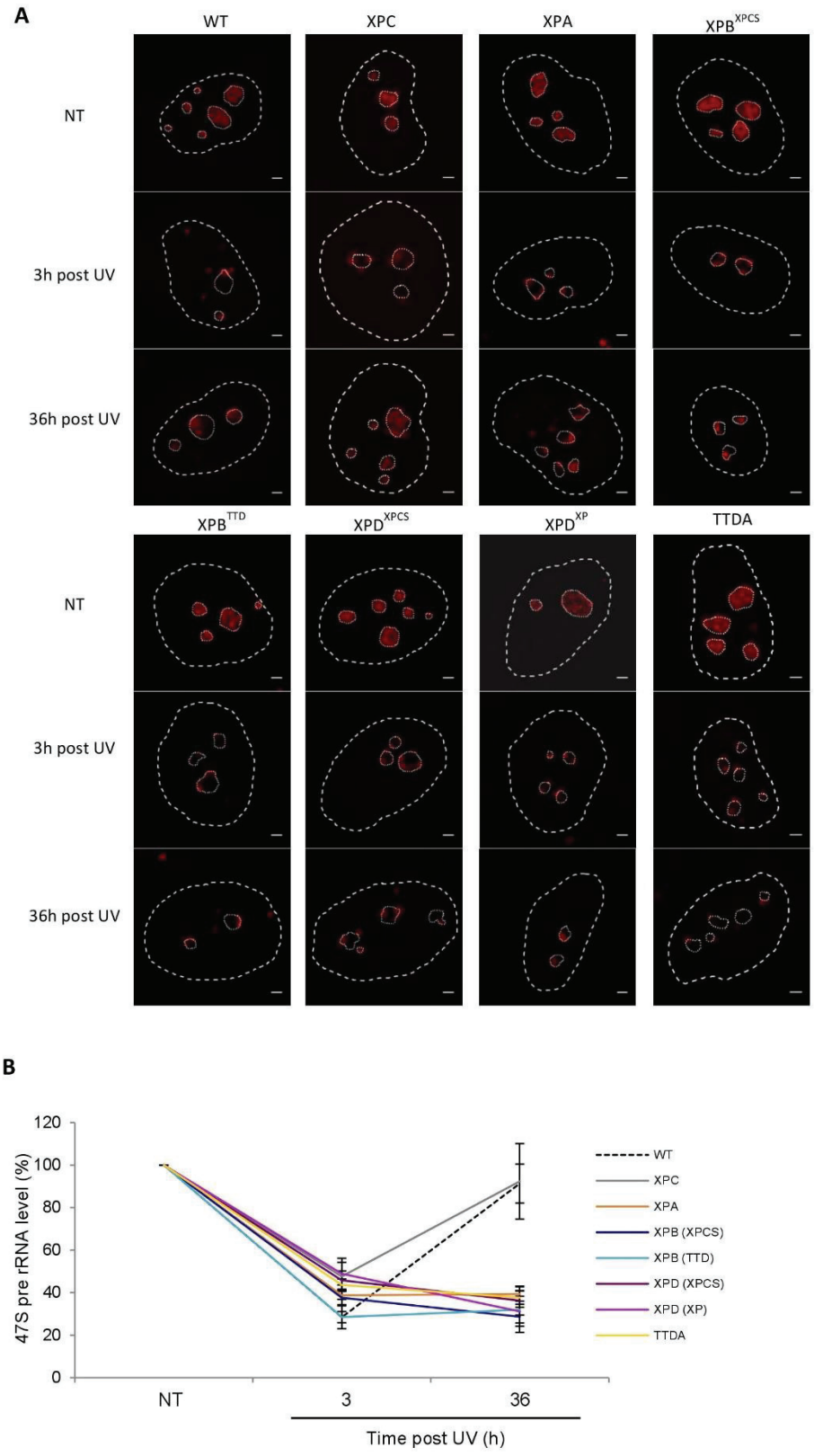

Figure S6. The complete TC-NER machinery is involved in the repair of rDNAs

A) Confocal images from RNA FISH experiment, showing the 47S pre-rRNA level, performed on WT, XPC (GG-NER deficient), XPA, XPB^{XPCS}, XPB^{TTD}, XPD^{XPCS}, XPD^{XP} and TTDA (GG-NER and TC-NER deficient) cells. Cells were irradiated or not (NT) and fixed 3 or 36 hours after UV exposure. Nuclei and nucleoli are delimited by dashed and dotted lines respectively. Scale bars: 2 µm. **B**) Quantification of the 47S pre-rRNA level from RNA FISH assays performed in the same cells as mentioned above. Error bars represent the SEM of 3 independent experiments. UV dose: $16J/m^2$.

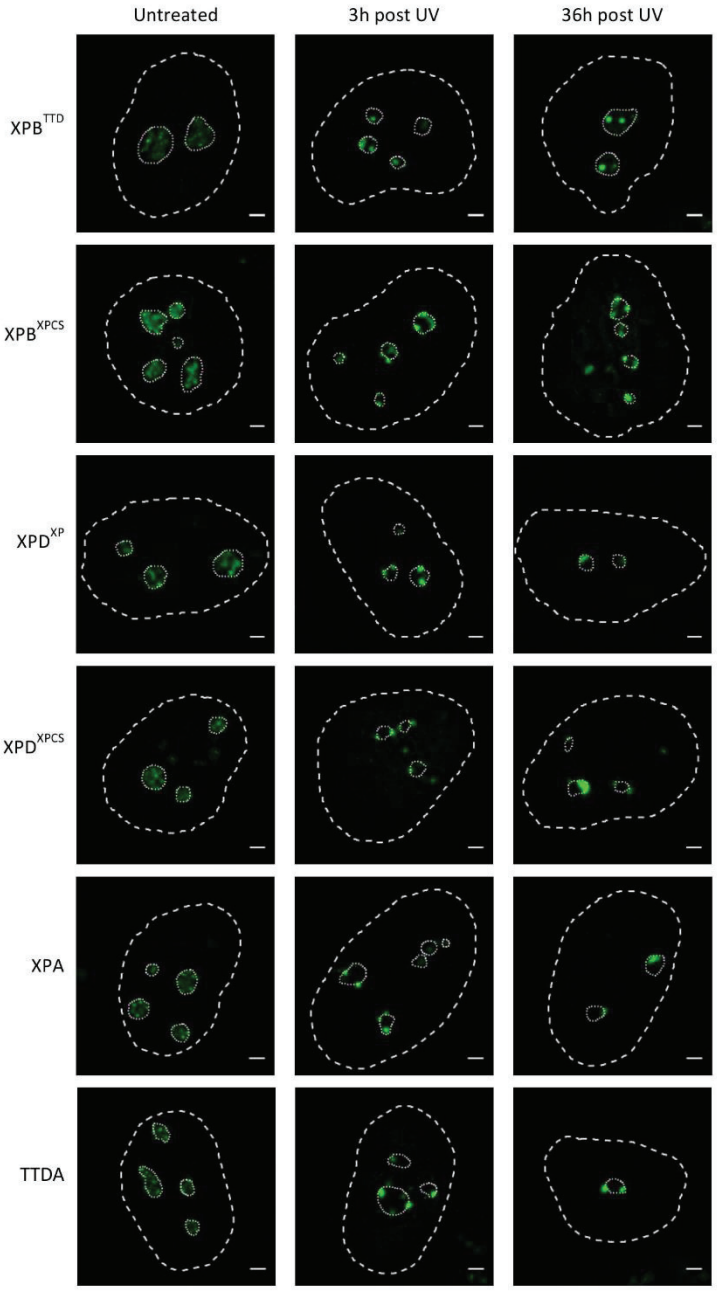

Figure S7. RNAP1 location in NER deficient cells upon UV

Confocal images of immunofluorescence staining against RNAP1 (green) performed on NER deficient cells. Cells were UV-irradiated (16J/m2) or not (NT) and fixed 3 or 36 hours after UV exposure. Nuclei and nucleoli are indicated by dashed and dotted lines respectively. Scale bar: 2µm.

10

Submitted as a Letter to Nature

β-Actin and Nuclear Myosin I are implicated in rDNA/RNAP1 repositioning after rDNA repair

Elena Cerutti[1], Laurianne Daniel[1], Lise-Marie-Donnio[1], Damien Neuillet[1], Charlene Magnani[1], Pierre-Olivier Mari[1] and Giuseppina Giglia-Mari[1]

1: Institut NeuroMyoGène (INMG), CNRS UMR 5310, INSERM U1217, Université de Lyon, Université Claude Bernard Lyon1, 16 rue Dubois, 69622 Villeurbanne CEDEX France

Keywords:

Beta-Actin; Nuclear Myosin I; RNAP1 relocation, rDNA Transcription, UV lesions, Nucleolus, Nucleotide Excision Repair

Abstract

During DNA Repair, ribosomal DNA and RNA polymerase I (rDNA/RNAP1) are reorganized within the nucleolus and undergo relatively long-distance movements.

In fact, UV lesions trigger the DNA repair reaction, blocking RNAP1 transcription and displacing the rDNA/RNAP1 complex at the periphery of the nucleolus. Because most repair proteins are present outside the nucleolus, this movement is believed to be important for the repair reaction to take place properly. Only when the repair reaction is fully completed, the rDNA/RNAP1 complex returns within the nucleolus.

The proteins and the molecular mechanism governing this movement remain unknown.

Here we show that Nuclear Myosin I (NMI) and Nuclear Beta Actin (ACTβ) are essential for the proper re-entry of the rDNA/RNAP1 within the nucleolus, after completion of the DNA Repair reaction.

We found that, in NMI and ACTβ depleted cells, the rDNA/RNAP1 complex can be displaced at the periphery of the nucleolus after DNA damage induction but cannot re-enter within the nucleolus after completion of the DNA Repair reaction. In these cells, repair is proficient and rDNA transcription normally restarts after the lesions-induced blockage. Both proteins act concertedly in this process. NMI binds the damaged rDNA that is displaced at the periphery of the nucleolus during repair reactions, *via* the phosphorylation of γH2AX, while ACTβ brings the rDNA back within the nucleolus after DNA repair completion.

Our results reveal a previously unidentified function for NMI and ACTβ within the nucleolus and disclose how these two proteins work in coordination to re-establish the proper rDNA position after DNA repair.

We consider our findings to be the first mechanistic step of a still fully unexplored process, the reorganization of nucleolar DNA. It is conceivable to think that a complex network of proteins will govern DNA long-distance movements within the nucleolus during DNA repair or other stress reactions.

Results and Discussion

Ribosome biogenesis is one of the most complex and energetically costly activities of the cell. The first and limiting step of ribosome biogenesis is the production of ribosomal RNA (rRNAs), specifically transcribed from ribosomal genes (rDNA) by the RNA polymerase I (RNAP1) within a specialized nuclear domain: the nucleolus. Despite nucleoli do not have membranes to isolate them from the nucleoplasm, they are impermeable to different nuclear proteins and their DNA content is kept inside during the majority of the cell cycle. Because of this apparent hermetical nature, some cellular functions, such as DNA repair of ribosomal genes imply that the DNA confined in the nucleolus would be externalised to allow repair proteins, and more generally, nuclear proteins, to access rDNA. Indeed, rDNA displacement at the periphery of the nucleolus happens during DNA replication (1) and DNA repair (2-5). Particularly, during DNA repair of UV lesion (5), rDNA and RNAP1 are displaced at the periphery of the nucleolus after UV-irradiation (displacement) and are repositioned within the nucleolus when DNA repair is completed (5) (repositioning) (Figure 1). Interestingly, these rDNA/RNAP1 movements are triggered by the presence of UV lesions on the DNA contained within the nucleolus and if UV damage is not fully repaired, the rDNA/RNAP1 complex remains at the periphery of the nucleolus (5).

The proteins involved in this displacement/repositioning cycle remain still unknown, as well as the molecular mechanism governing this movement. To disclose the foundation of this phenomenon, we explored the possibility that nuclear motors proteins could be responsible for the displacement and/or the repositioning of the rDNA/RNAP1 complex during DNA repair reactions. Two of the major nuclear motor proteins are nuclear β-actin (ACTβ) and Nuclear Myosin I (NMI). Firstly identified in the cytoplasm, ACTβ and NMI are also involved in several cellular events such as cell migration, muscle contraction or organelle movements (5) and interestingly these proteins have been implicated in long-range chromosomes movements within the nucleus (6), repositioning of active genes (7) and more recently in relocalisation of double strand breaks damaged DNA from the heterochromatin compartment to the nuclear periphery in Drosophila cells (8). Intriguingly, ACTβ and NMI are also involved in RNAP1 transcription (9-11), making them the best candidates to start exploring the rDNA/RNAP1 relocalisation during DNA repair.

We knocked down ACTβ and NMI in human fibroblasts (Figure S2) and UV irradiate them to induce the relocation of the rDNA/RNAP1 complex. RNAP1 was visualised by immunofluorescence staining while rDNA was visualised using a LacO-LacR-GFP system (kindly provided by W. Bickmore) in which Lac-O sequences were inserted in the close proximity of rDNA genes (Figure S1A). As previously observed, in siMock-treated cells rDNA and RNAP1 are displaced at the

periphery of the nucleolus after DNA damage induction and are repositioned within the nucleolus when DNA repair is completed (5). In ACTβ and NMI depleted cells while the displacement of the rDNA/RNAP1 is unaltered, the repositioning is severely affected (Figure 1). Concomitantly, we measured the RNAP1 activity by measuring the 47S production by RNA-Fish (Figure S3, panel A and B). In our experimental conditions, depletion of ACTβ and NMI does not modify RNAP1 productivity, probably because depletion is not complete and the remaining 10-20 % of proteins (Figure S2) is sufficient to maintain an efficient RNAP1 transcription. Interestingly, after DNA repair completion, RNAP1 transcription restarts in ACTβ and NMI depleted cells as in siMock-treated cells. This situation was observed also in DNA-repair deficient cells (XP-C cells), in which UV-lesions on untranscribed DNA are not repaired, while transcribed sequences are repaired (5). In XP-C cells, as in ACTβ and NMI depleted cells, rDNA/RNAP1 remains at the periphery of the nucleolus because of remaining UV lesions on untranscribed sequences, while RNAP1 transcription restarts, as transcribed rDNA sequences are specifically repaired by the transcription coupled repair pathway (5). To exclude that depletion of ACTβ and NMI would induce a DNA repair deficiency, we conducted the Unscheduled DNA synthesis (UDS) measure, a specific assay to monitor the efficiency of the Global Genome Nucleotide Excision Repair pathway (GG-NER) which corrects UV-lesions on untranscribed DNA sequences and that is deficient in XP-C cells (Figure S5) (5). We could show that depleted ACTβ and NMI cells are proficient in GG-NER and that hence, UV-lesions are efficiently repaired, indicating that ACTβ and NMI are involved in the repositioning of the rDNA/RNAP1 after DNA repair completion. We wondered whether ACTβ and NMI involvement in this relocation was specific to the DNA repair reaction or if it was a general role in relocation of the rDNA/RNAP1 throughout other cellular stress events, such as transcription inhibition. To verify this, we treated ACTβ and NMI depleted cells with cordycepin to specifically induce RNAP1 transcription inhibition, the advantage of using cordycepin is that the effect is reversible simply by chasing it with a cordycepin-free medium, reproducing the displacement/repositioning cycle observed after UV-dependent DNA repair. We could show that ACTβ and NMI depleted cells are, in this case, efficient in both displacement and repositioning of rDNA/RNAP1 (Figure S7). These results show that ACTβ and NMI are specifically involved in the repositioning of rDNA/RNAP1 within the nucleolus after completion of the DNA repair reaction.

To investigate in details the implication of ACTβ and NMI in this process, we measured the binding activity of ACTβ and NMI on rDNA sequences by ChIP-qPCR using specific set of primers that locate along the rDNA genes and on the adjacent sequences outside of the transcribed rDNAs. We could perform this assay in absence of DNA damage, after UV irradiation during repair reaction and after completion of DNA repair (Figure 2A and 2B) and we could show that in absence of DNA

damage, no detectable ACTβ and NMI are binding directly the rDNA genes or the adjacent untranscribed sequences. Remarkably, 3 hours after UV-irradiation, when RNAP1 transcription is shut down and the rDNA/RNAP1 is displaced at the periphery of the nucleolus both ACTβ and NMI bind rDNA genes and adjacent sequences, showing that the presence of DNA lesions and/or the position of rDNAs at the periphery of the nucleolus triggers the binding of ACTβ and NMI. Interestingly, when repair is completed (40 hours after UV irradiation), while NMI is released from rDNA (Figure 2A), ACTβ remains strongly bound to rDNA (Figure 2B). Intrigued, by the fact that NMI binds rDNAs at 3 hours post-irradiation but is released when DNA repair is completed and knowing that some research groups found NMI interacting with γH2AX chromatin (12), we explored the possibility that DNA damage signalling on rDNAs could be the trigger of the proper binding of NMI. In order to verify this hypothesis, we analysed rDNA/RNAP1 displacement and repositioning after UV-irradiation and DNA repair in cells treated with an ATR-inhibitor (Figure 3), which will impede UV-dependent phosphorylation of H2AX. Our results show that in absence of γH2AX phosphorylation the displacement of the rDNA/RNAP1 is unaltered while the repositioning is severely affected, exactly as in NMI depleted cells (Figure 3).

To investigate whether ACTβ and NMI, interacts with RNAP1 or with each other during this process, we performed IP with RNAP1 and NMI antibodies. We could show that, in our experimental setting, RNAP1 interacts with ACTβ, more strongly in absence of DNA damage (Figure 2C) when RNAP1 transcription is not inhibited and rDNA/RNAP1 is located within the nucleolus. Interestingly, NMI interacts with ACTβ more strongly during DNA repair reactions when RNAP1 transcription is inhibited and the rDNA/RNAP1 is at the periphery of the nucleolus (Figure 2C). In our experimental setting, we could not find a direct interaction between NMI and RNAP1. These results suggest that ACTβ and NMI could work synergistically to bind rDNA and that both are needed in the same process of repositioning rDNA/RNAP1 within the nucleolus once repair is completed.

We propose a mechanistic model from the rDNA/RNAP1 repositioning (Figure 4) in which after UV exposure, rDNA/RNAP1 is displaced to the periphery of the nucleolus in order to allow repair proteins to access the lesion. The UV-induced phosphorylation of γH2Ax induces the binding of NMI to the rDNAs at 3 h post-irradiation and probably this interaction stimulates ACTβ molecules to be recruited on the damaged rDNAs sequences. After repair completion, while NMI is released from the rDNAs, more ACTβ molecules are bound on the repaired rDNAs sequences. In absence of ACTβ or NMI (or in absence of the γH2Ax signal) the rDNA/RNAP1 repositioning cannot take place.

This work reveals ACTβ, NMI and the γH2Ax signal involvement in the rDNA/RNAP1 repositioning of rDNA/RNAP1 during repair of UV lesions. This is the starting point for further studies that will disclose the molecular mechanism of nucleolar motions. Many factors remain to be discovered, as well as the chromatin remodelling and the genomic environment of rDNA during and after this reorganization.

Acknowledgements

We acknowledge Elizabeth Kerr and Jonathan Chubb (Wendy Bickmore's research team, MRC Institute of Genetics & Molecular Medicine, Edinburgh, UK) for kindly providing the HT80 cells carrying the LacO/LacR system as well as all the information related to this cell line. This work was supported by La Ligue Nationale Contre le Cancer (LNCC), l'Agence Nationale de la Recherche (ANR FreTNET: ANR10-BLAN-1231-01; ANR DyReCT: ANR-14-CE10-0009) and the ARC foundation (Association pour la Recherche sur le Cancer).

Author contributions

GGM and EC designed the experiments. EC, LD, LMD, DN and CM performed the experiments and analysed the data. POM assisted with the microscopy imaging and analysis. GGM, EC and LD wrote the paper.

Conflicts of interest

The authors disclose no potential conflict of interest.

Bibliography

1. Dimitrova DS. DNA replication initiation patterns and spatial dynamics of the human ribosomal RNA gene loci. J Cell Sci. 2011;124(Pt 16):2743-52. doi: 10.1242/jcs.082230. PubMed PMID: 21807939.

2. van Sluis M, McStay B. A localized nucleolar DNA damage response facilitates recruitment of the homology-directed repair machinery independent of cell cycle stage. Genes Dev. 2015;29(11):1151-63. doi: 10.1101/gad.260703.115. PubMed PMID: 26019174; PubMed Central PMCID: PMCPMC4470283.

3. Larsen DH, Stucki M. Nucleolar responses to DNA double-strand breaks. Nucleic Acids Res. 2016;44(2):538-44. doi: 10.1093/nar/gkv1312. PubMed PMID: 26615196; PubMed Central PMCID: PMCPMC4737151.

4. Franek M, Kovarikova A, Bartova E, Kozubek S. Nucleolar Reorganization Upon Site-Specific Double-Strand Break Induction. J Histochem Cytochem. 2016;64(11):669-86. doi: 10.1369/0022155416668505. PubMed PMID: 27680669; PubMed Central PMCID: PMCPMC5084524.

5. Daniel L, Cerutti E, Donnio LM, Nonnekens J, Carrat C, Zahova S, et al. Mechanistic insights in transcription-coupled nucleotide excision repair of ribosomal DNA. Proc Natl Acad Sci U S A. 2018;115(29):E6770-E9. Epub 2018/07/02. doi: 10.1073/pnas.1716581115. PubMed PMID: 29967171; PubMed Central PMCID: PMCPMC6055190.

6. Chuang CH, Carpenter AE, Fuchsova B, Johnson T, de Lanerolle P, Belmont AS. Long-range directional movement of an interphase chromosome site. Curr Biol. 2006;16(8):825-31. doi: 10.1016/j.cub.2006.03.059. PubMed PMID: 16631592.

7. Dundr M, Ospina JK, Sung MH, John S, Upender M, Ried T, et al. Actin-dependent intranuclear repositioning of an active gene locus in vivo. J Cell Biol. 2007;179(6):1095-103. doi: 10.1083/jcb.200710058. PubMed PMID: 18070915; PubMed Central PMCID: PMCPMC2140015.

8. Caridi CP, D'Agostino C, Ryu T, Zapotoczny G, Delabaere L, Li X, et al. Nuclear F-actin and myosins drive relocalization of heterochromatic breaks. Nature. 2018;559(7712):54-60. doi: 10.1038/s41586-018-0242-8. PubMed PMID: 29925946; PubMed Central PMCID: PMCPMC6051730.

9. Philimonenko VV, Zhao J, Iben S, Dingová H, Kyselá K, Kahle M, et al. Nuclear actin and myosin I are required for RNA polymerase I transcription. Nat Cell Biol. 2004;6(12):1165-72. Epub 2004/11/21. doi: 10.1038/ncb1190. PubMed PMID: 15558034.

10. Sarshad A, Sadeghifar F, Louvet E, Mori R, Bohm S, Al-Muzzaini B, et al. Nuclear myosin 1c facilitates the chromatin modifications required to activate rRNA gene transcription and cell cycle progression. PLoS Genet. 2013;9(3):e1003397. doi: 10.1371/journal.pgen.1003397. PubMed PMID: 23555303; PubMed Central PMCID: PMCPMC3605103.

11. Ye J, Zhao J, Hoffmann-Rohrer U, Grummt I. Nuclear myosin I acts in concert with polymeric actin to drive RNA polymerase I transcription. Genes Dev. 2008;22(3):322-30. doi: 10.1101/gad.455908. PubMed PMID: 18230700; PubMed Central PMCID: PMCPMC2216692.

12. Kulashreshtha M, Mehta IS, Kumar P, Rao BJ. Chromosome territory relocation during DNA repair requires nuclear myosin 1 recruitment to chromatin mediated by ϒ-H2AX signaling. Nucleic Acids Res. 2016;44(17):8272-91. Epub 2016/06/30. doi: 10.1093/nar/gkw573. PubMed PMID: 27365048; PubMed Central PMCID: PMCPMC5041470.

Figures

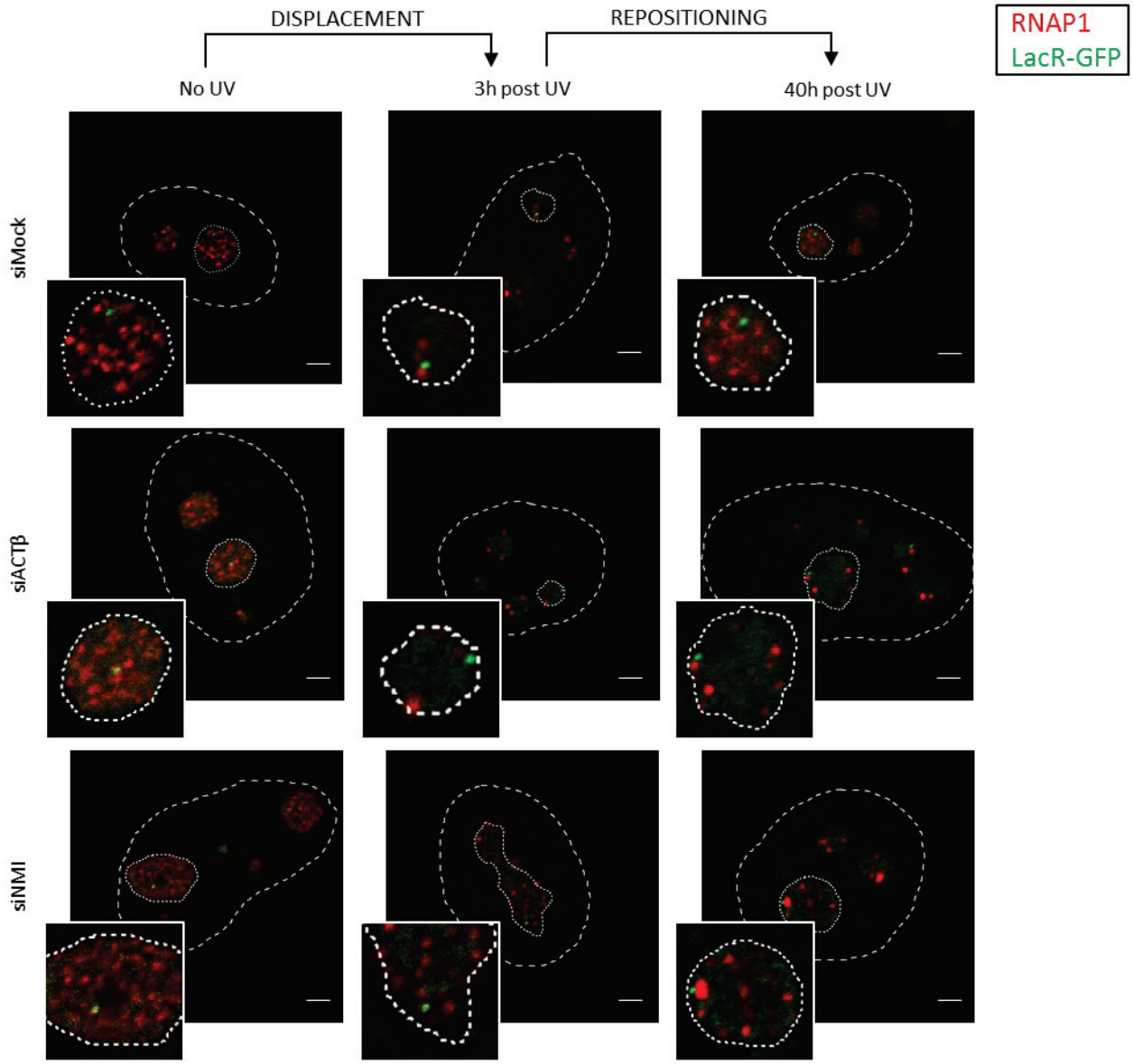

Figure 1. rDNA/RNAP1 repositioning is ACTβ and NMI-dependent
Confocal images of immunofluorescence assay against RNAP1 (red) in LacR-GFP (green) expressing cells transfected with siRNA against indicated factors and treated or not with UV-C. Nuclei and nucleoli are indicated by dashed lines and dotted lines respectively. Scale bar represents 3 µm.

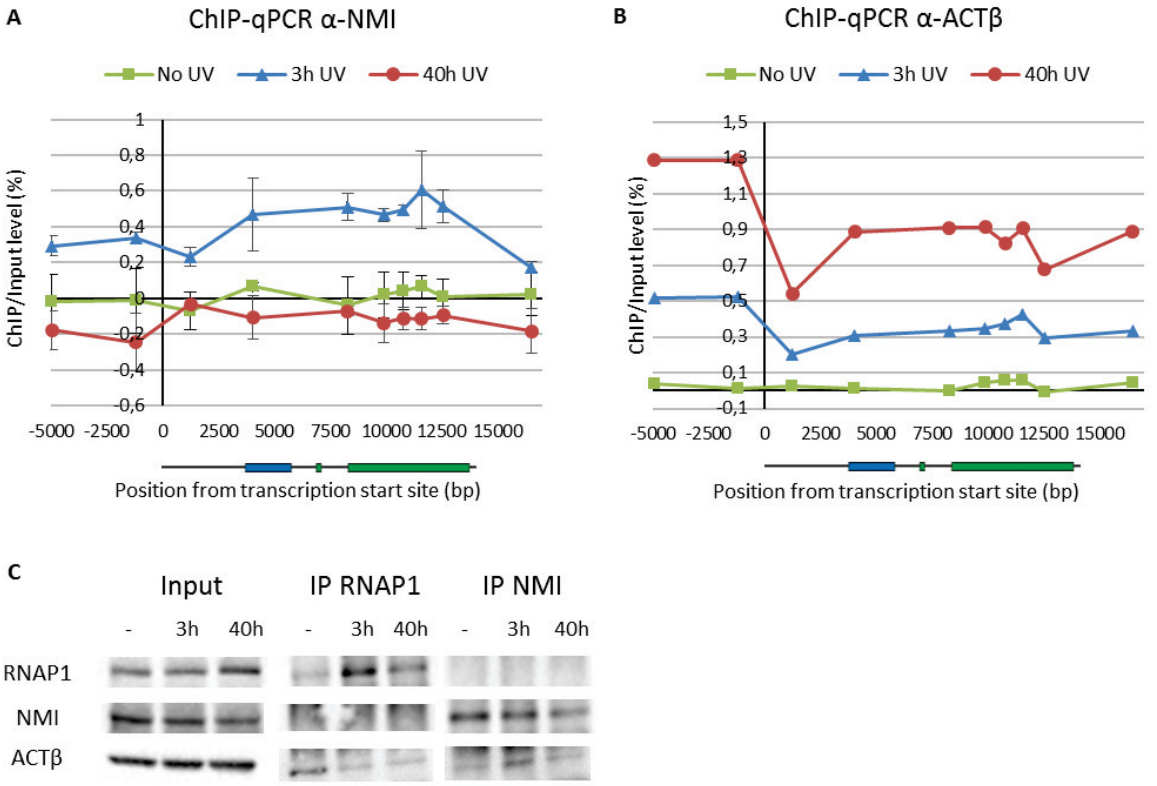

Figure 2. ACTβ and NMI binding activity on rDNA sequences and interaction with RNAP1
A) ChIP-qPCR results showing the binding profile of NMI on ribosomal DNA in MRC5 cells treated or not with UV-C. The y-axis depicts the ChIP/Input ratio minus background (Mock/Input ratio). Scqle bqr represents the SD **B)** ChIP-qPCR results showing the binding profile of ACTβ on ribosomal DNA in MRC5 cells treated or not with UV-C. The y-axis depicts the ChIP/Input ratio minus background (Mock/Input ratio). **C)** Chromatin Immunoprecipitation of RNAP1, NMI in MRC5 cells treated or not with UV-C. Bound proteins were revealed by Western Blot using antibodies against RNAP1, NMI and ACTβ. INPUT corresponds to 20% of the lysate used for IP reactions.

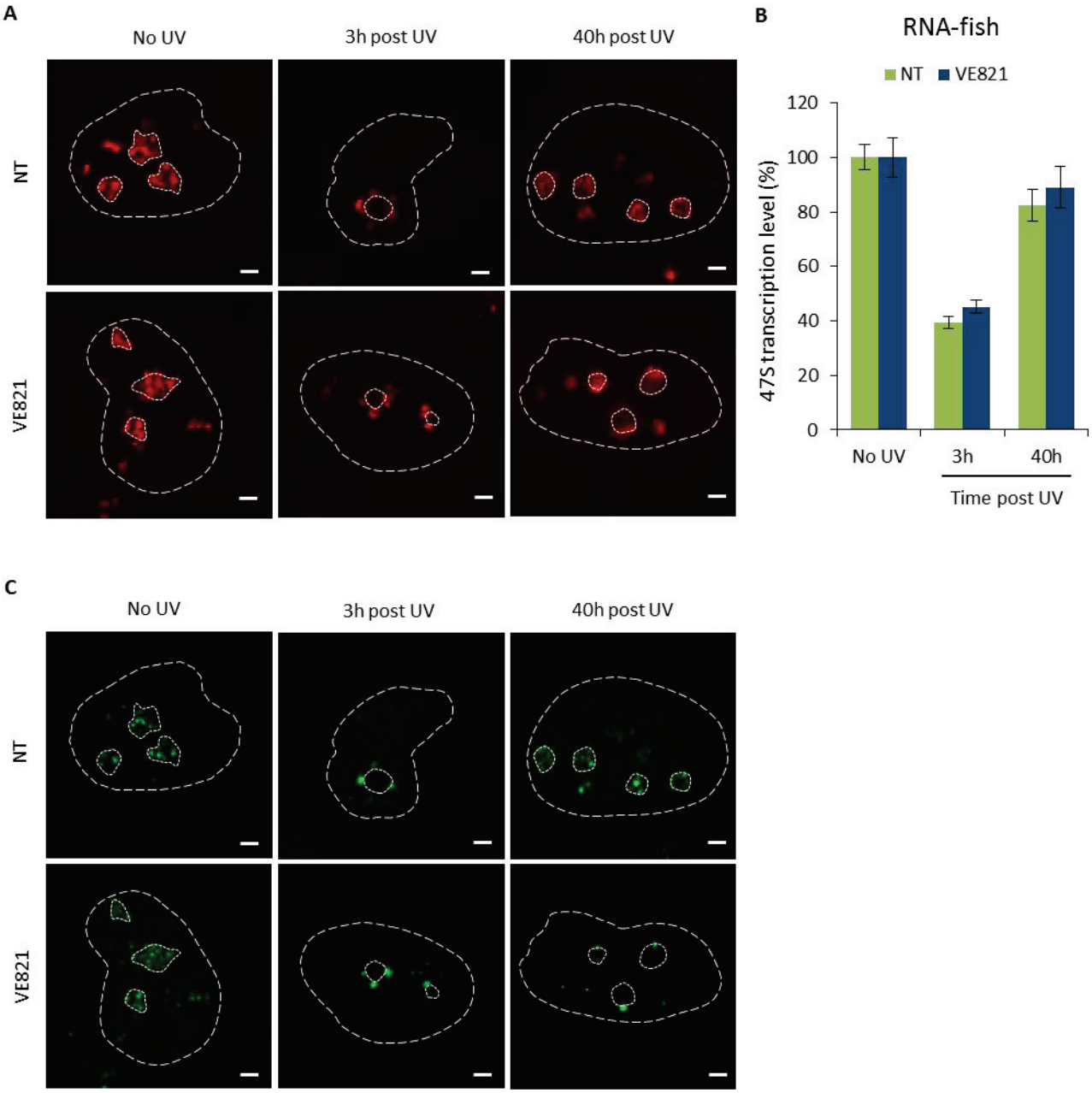

Figure 3. Impaired rDNA/RNAP1 post-UV repositioning upon ATR inhibition
A) Confocal images of RNA FISH labelling (red) performed on MRC5 cells treated or not with VE821 at 10 µM and treated or not with UV-C. Nuclei and nucleoli are indicated by dashed and dotted lines respectively. Scale bar represents 3 µm. **B)** Quantification of the RNA FISH experiments shown in A). Error bar represents the SEM. **C)** Confocal images of immunofluorescence assay against RNAP1 (green) in MRC5 cells treated or not with VE821 at 10µM and treated or not with UV-C. Nuclei and nucleoli are indicated by dashed lines and dotted lines respectively. Scale bar represents 3 µm.

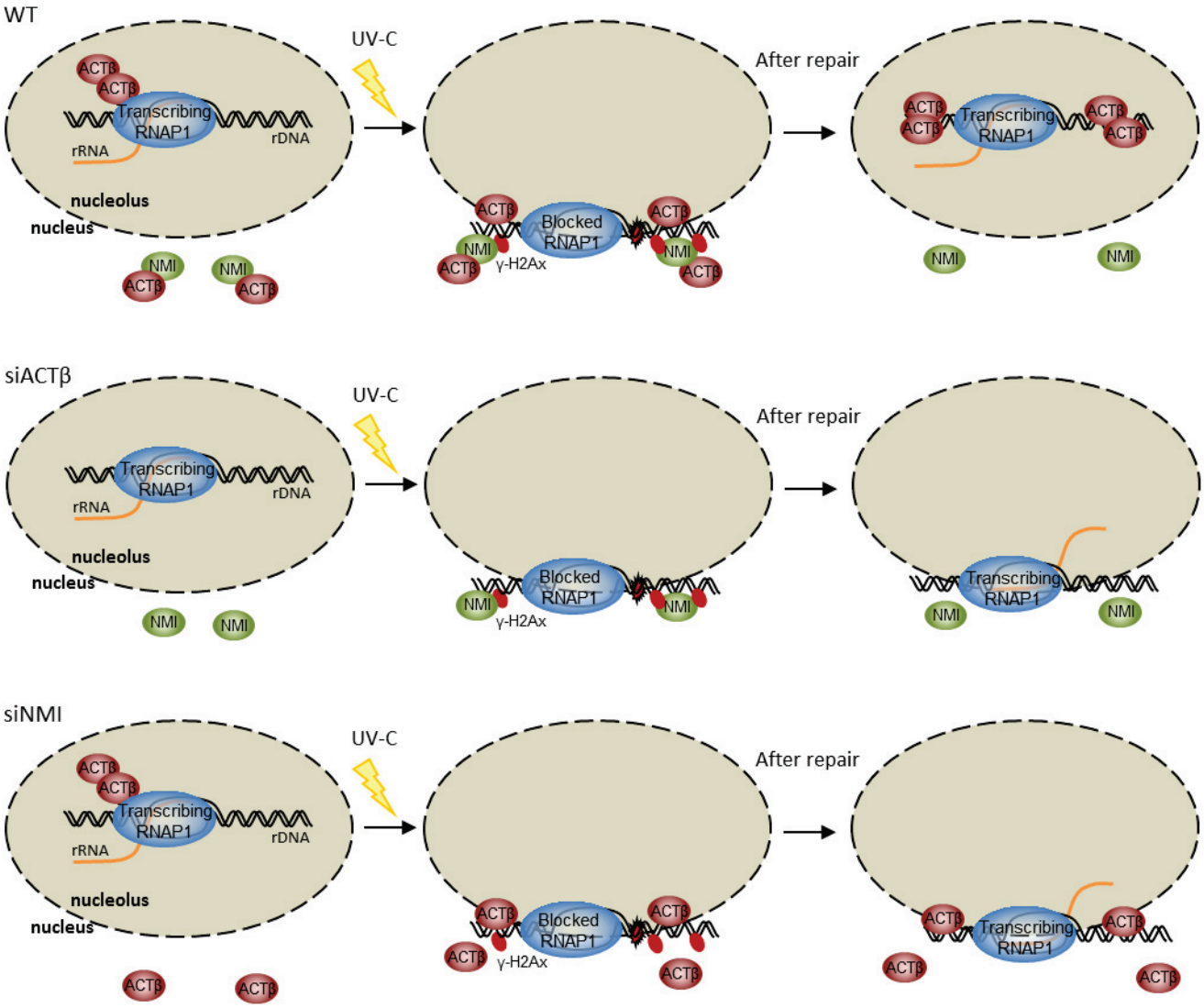

Figure 4. Model of the proposed mechanism involved in rDNA/RNAP1 repositioning
ACTβ binds RNAP1 during transcription of rDNA and NMI weakly binds ACTβ outside the nucleolus. After UV exposure, rDNA/RNAP1 is displaced to the periphery of the nucleolus in order to allow repair proteins to access the lesion. The UV-induced phosphorylation of γ-H2Ax induces the binding of NMI to the rDNAs at post-UV and probably this interaction stimulates ACTβ molecules to be recruited on the damaged rDNAs sequences. After repair completion, while NMI is released from the rDNAs, more ACTβ molecules are bound on the repaired rDNAs sequences. In absence of ACTβ or NMI (or in absence of the γ-H2Ax signal) the rDNA/RNAP1 repositioning cannot take place.

Extended data

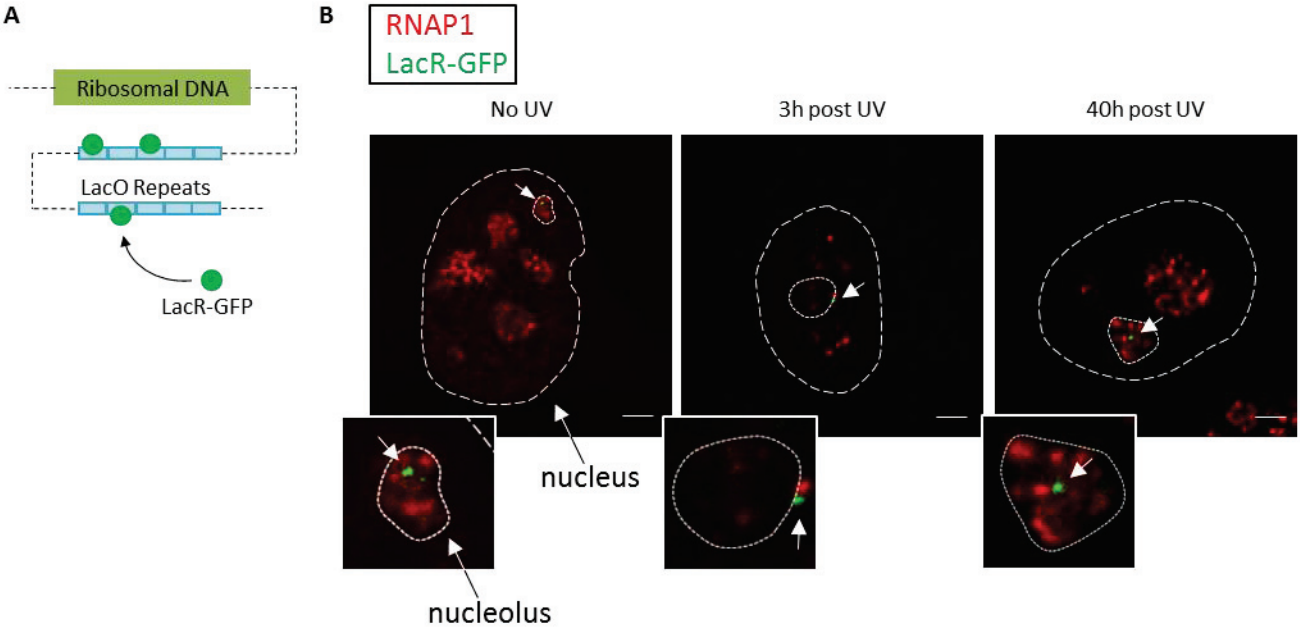

Figure S1. rDNA location during DNA repair
A) Schematic representation of the LacO/LacR system used to visualize the ribosomal DNA. Several Lac Operon genes were integrated downstream of the rDNA of the cells, which were also transfected with a plasmid carrying the Lac Repressor gene tagged with the GFP coding sequence. **B)** Confocal images of immunofluorescence assay against RNAP1 (red) in LacR-GFP (green) expressing cells treated or not with UV-C. Nuclei, nucleoli and LacO array (GFP green dot) are indicated by dashed lines, dotted lines and white arrows respectively. Scale bar represents 3 µm.

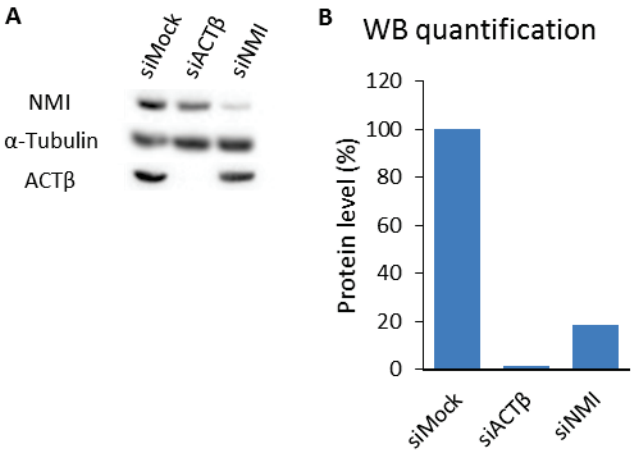

Figure S2.
A) Western Blot on whole cell extracts performed on LacO/LacR-GFP cells treated with siRNA against indicated factors and represented in Figure 1. **B)** Quantification of WB shown in A). Protein amount is normalized to α-Tubulin signal.

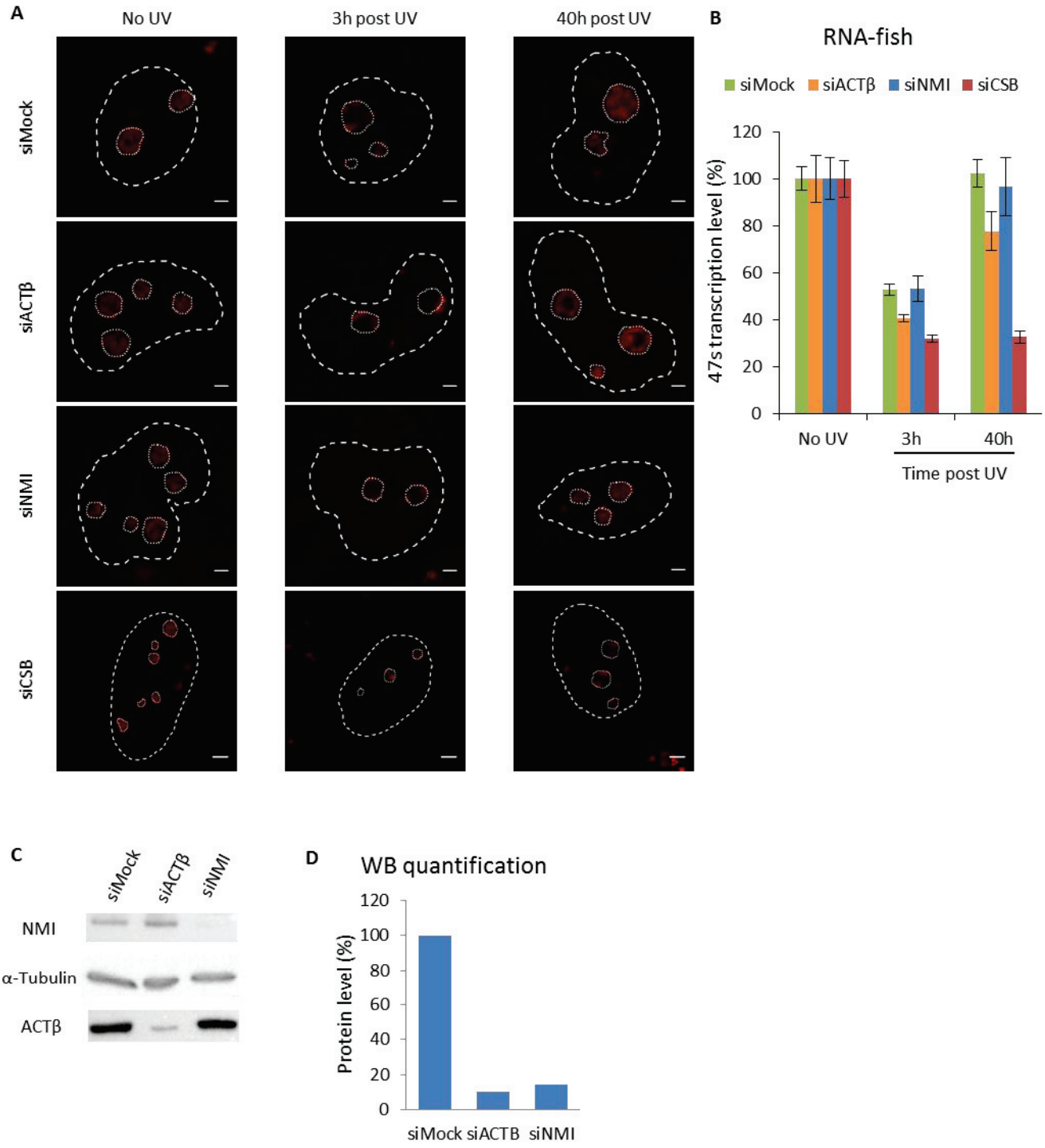

Figure S3.

A) Confocal images of RNA FISH labelling (red) performed on MRC5 cells transfected with siRNA against indicated factors and treated or not with UV-C. Nuclei and nucleoli are indicated by dashed and dotted lines respectively. Scale bar represents 3 µm. **B)** Quantification of the RNA FISH experiments shown in A). Error bar represents the SEM. **C)** Western Blot on whole cell extracts performed on MRC5 cells of RNA FISH experiment shown in A) **D)** Quantification of WB shown in C). Protein amount is normalized to α-Tubulin signal.

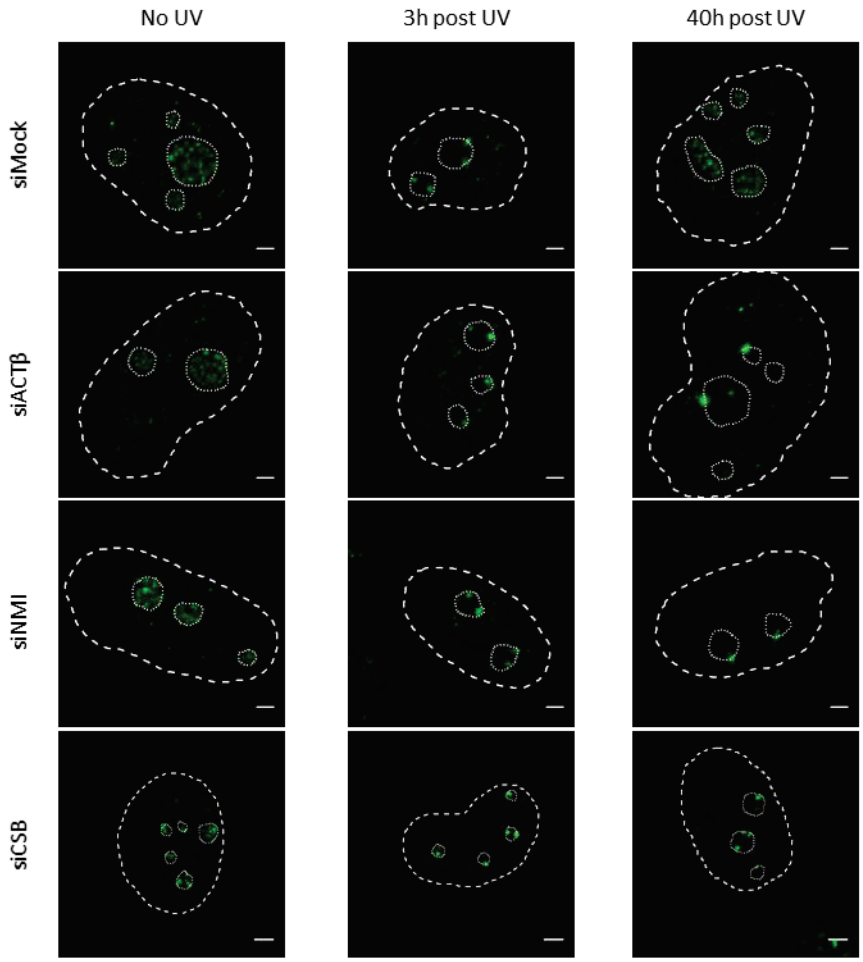

Figure S4.
Confocal images of immunofluorescence assay against RNAP1 (green) in MRC5 cells transfected with siRNA against indicated factors and treated or not with UV-C. Nuclei and nucleoli are indicated by dashed lines and dotted lines respectively. Scale bar represents 3 µm.

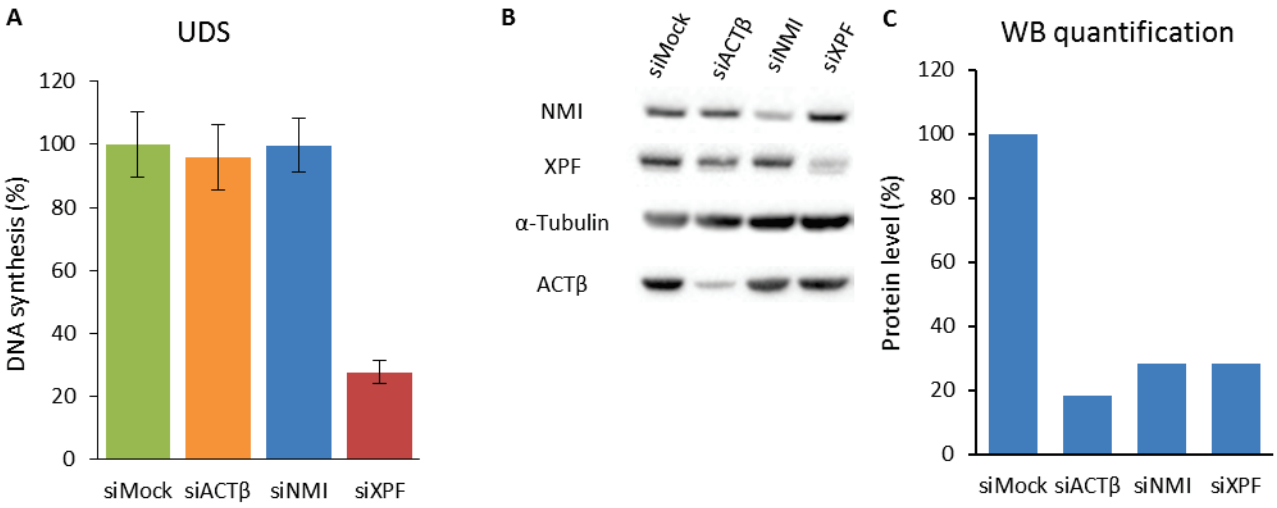

Figure S5.
A) Unscheduled DNA Synthesis determined by EdU incorporation after local damage induction with UV-C in MRC5 cells treated with siRNAs against indicated factors. **B)** Western Blot on whole cell extracts performed on MRC5 cells of UDS experiment shown in A). **C)** Quantification of WB shown in B). Protein amount is normalized to α-Tubulin signal.

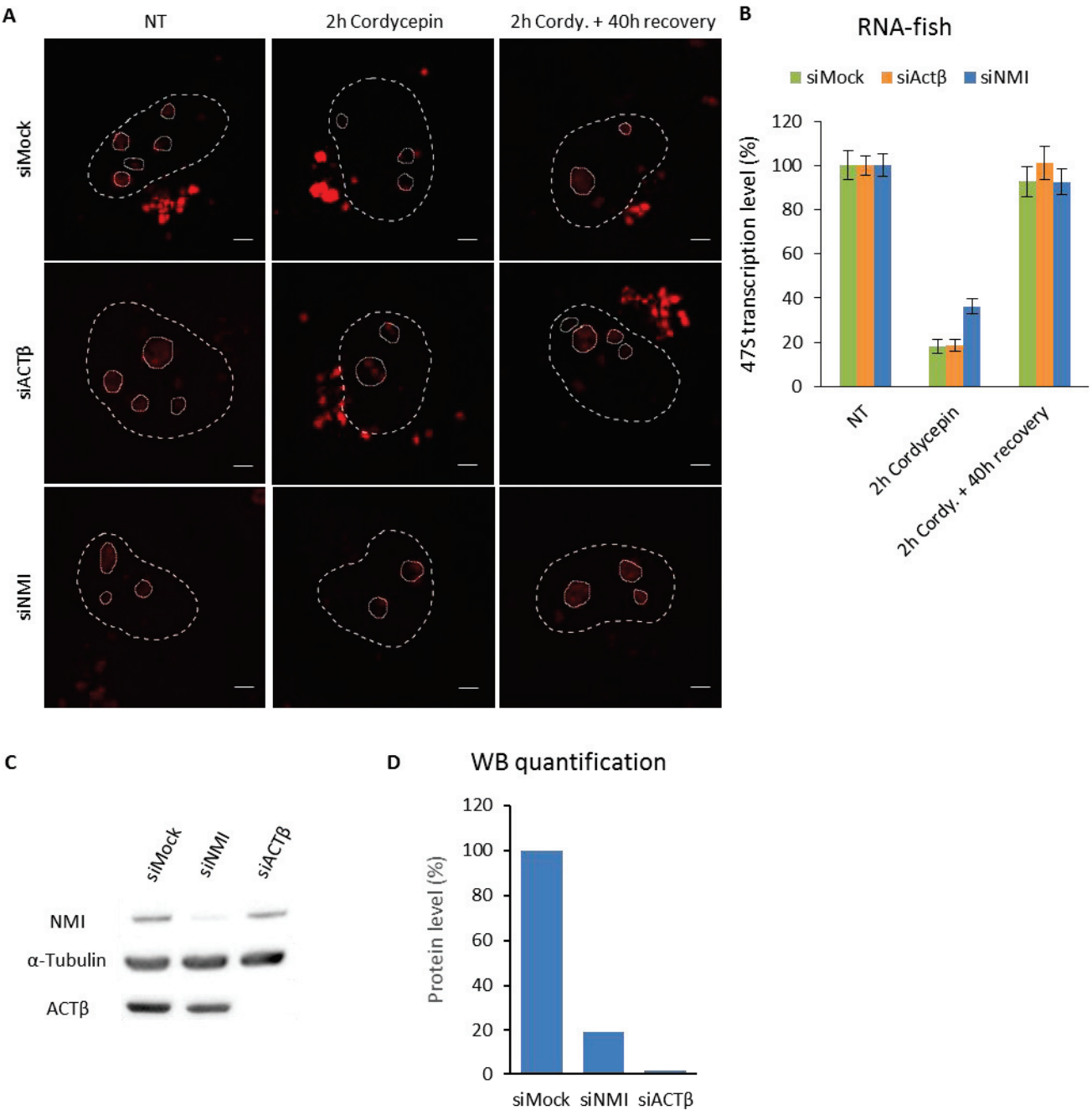

Figure S6.

A) Confocal images of RNA FISH labelling (red) performed on MRC5 cells transfected with siRNA against indicated factors and treated or not with Cordycepin at 50 µg/ml. Nuclei and nucleoli are indicated by dashed and dotted lines respectively. Scale bar represents 3 µm. **B)** Quantification of the RNA FISH experiments shown in A). Error bar represents the SEM. **C)** Western Blot on whole cell extracts performed on MRC5 cells of RNA FISH experiment shown in A) **D)** Quantification of WB shown in C). Protein amount is normalized to α-Tubulin signal.

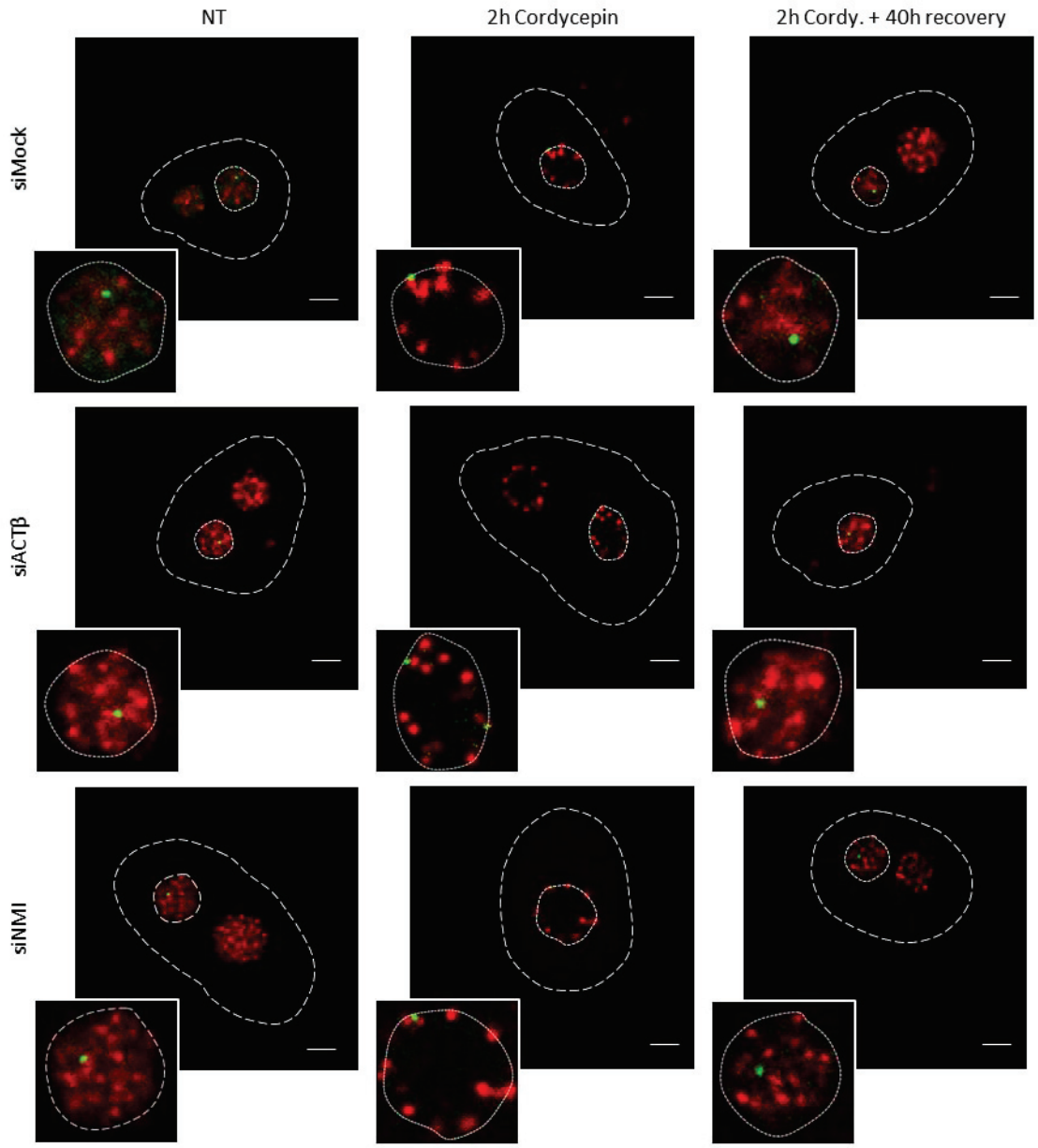

Figure S7.
Confocal images of immunofluorescence assay against RNAP1 (red) in LacR-GFP (green) expressing cells transfected with siRNA against indicated factors and treated or not with Cordycepin at 50 µg/ml. Nuclei and nucleoli are indicated by dashed lines and dotted lines respectively. Scale bar represents 3 µm.

Methods

Cell culture and treatments

Wild type SV40-immortalized human fibroblasts (MRC5) were cultured in a 1:1 mixture of Ham's F10 and DMEM (Lonza) supplemented with 1% antibiotics (penicillin and streptomycin; Lonza) and 10% fetal bovine serum (Gibco) and incubated at 37°C with 20% O_2 and 5% CO_2.

HT-1080 cells (Rasheed et al., 1974) stably expressing an adapted Lac Operator/Lac Repressor (LacO/LacR) system (selected using BlasticidinS and Hygromycin, 5 µg/ml and 100 µg/ml respectively), were used to detect the rDNA as previously described (Chubb et al., 2002; Robinett et al., 1996). These cells were cultured in DMEM (Lonza), supplemented with 1% antibiotics (penicillin and streptomycin; Lonza) and 10% fetal bovine serum (Gibco), and at 37°C with 20% O_2 and 5% CO_2.

DNA damage was inflicted by UV-C light (254 nm, 6-Watt lamp). Cells were globally irradiated with a 16 J/m^2 dose of UV-C or locally irradiated with a 100 J/m^2 dose of UV-C through a Millipore filter (holes of 5 µm of diameter). Experiments were performed at different time points after UV exposure (3h and 40h post UV). Not irradiated cells (No UV) were used as control.

RNAP1 transcription inhibition has been achieved by 2h incubation in medium containing Cordycepin at 50 µg/ml. Resumption of transcription has been obtained by replacement of Cordycepin medium with normal medium for 40h. Not treated cells (NT) were used as control.

VE821 drug was used at the concentration of 10 µM. Cells were treated in VE821 containing medium for 3h, then cells were UV-C globally irradiated with a 16 J/m^2 dose, or not irradiated as control, and left in drug containing medium for 40h or 3h before fixation.

Transfection of small interfering RNAs (siRNAs)

On day 0, 100 000 cells were seeded in a 6-wells plate and/or on 18 mm coverslips. The first and second transfections were performed on day 1 and day 2, using Lipofectamine® RNAiMAX reagent (Invitrogen; 13778150) or Gen Jet (Tebu-Bio), according to the manufactures' protocols. Experiments were performed between 24h and 72h after the second transfection. SiRNA efficiency was confirmed by western blot on whole cell extracts. SiRNAs sequences are described in Table 1.

Target	Final Concentration	Reference/Sequence
siMock	10 nM	D-001206-14
siActinβ	10 nM	L-003451-00

siNuclear Myosin I	10 nM	AACCCGUCCAGUAUUUCAACA
siXPF	10 nM	M-019946-00
siCSB	10 nM	L-004888-00

Table 1. Small interfering RNAs

Whole cell extracts

Cells were collected using trypsin and centrifuged 10 min at 1400 rpm. Firstly, cell pellet was washed with PBS supplemented with the Protease Inhibitor Cocktail (Roche) and spinned down 10 min at 1400 rpm. Secondly, cell pellet was incubated with Lysis buffer (ProteoJETTM Mammalian Cell Lysis Reagent, Fermentas) complemented with the Protease Inhibitor Cocktail (Roche), for 10 min at room temperature on a shaker (500 rpm). Finally, samples were centrifuged at 16000 g for 15 min and supernatant was freezed at - 80° C. Protein concentration was determined using the Bradford method, samples were diluted with 1X Laemmli buffer and heated 10 min at 95° C.

Chromatin extracts

All procedures were carried out on ice unless otherwise stated. Cells were grown in 14.5 cm dish. After treatments, cells were washed twice with PBS and cross-linked with a solution of 1 % formaldehyde in PBS (7.5 min at RT, shaking) prepared from a 37 % stock (Sigma-Aldrich, F1635). Cross-linking was neutralized by adding glycine for a final concentration of 0.125 M, followed by a wash with cold PBS. Cells were collected by scraping in PBS supplemented with the EDTA-free protease inhibitor tablets (Roche) and centrifuged 10 min at 2000 rpm and 4° C.

All buffers used for chromatin extraction contained, among others, the EDTA-free protease inhibitor tablets (Roche).

Cell pellet was suspended in Lysis buffer (50 mM Hepes-KOH [pH 8], 1 mM EDTA, 500 mM NaCl, 10 % glycerol, 0.5 % NP-40, 0.25 % Triton X-100) and incubated 10 min rotating at 4° C. The suspension was centrifuged 10 min at 2000 rpm and 4° C. Cell pellet was then washed with Wash buffer (10 mM Tris-HCl [pH 8], 1 mM EDTA, 500 mM NaCl), incubated 10 min rotating at 4° C and centrifuged 10 min at 2000 rpm and 4° C. Cell pellet was finally incubated for 30 min in 1 ml IP buffer (50 mM Hepes-KOH [pH 7.5], 1 mM EDTA, 500 mM NaCl, 1 % Triton X-100, 0.1 % Na-deoxycholate, 0.1 % SDS) before sonication. The nuclear suspension was sonicated using the S220 Focused-ultrasonicator (Covaris) for 8 min (Average Incident Power 14 Watt, Peak Power 140 Watt, Duty Factor 10 %, Cycle/Burst 200 count) to yield DNA fragments with an average size of 250 bp. Samples were then centrifuged (14.000 rpm, 10 min, 4° C) and the supernatant containing

the cross-linked chromatin was freezed at - 80° C. DNA concentration was quantified using the NanoDropTM 2000 Spectrophotometer (Termo Scientific).

ChIP qPCR

50 µg of MRC5 chromatin extracts were incubated overnight at 4° C in 150 µl total volume of IP buffer (see above) with antibody (ACTβ: ab8227 Abcam; NMI: M3567 Sigma) (ChIP) or no antibody (Mock). Immunoprecipitation (IP) was performed for 1 hour with 40 µl of washed magnetic Bio-Adembeads Protein G (Ademtech). After IP, the chromatin-beads interaction was washed twice with IP buffer, once with Na-deoxycholate buffer (10 mM Tris-HCl [pH 8], 1 mM EDTA, 250 mM LiCl, 0.5 % NP-40, 0.5 % Na-deoxycholate) and once with TE1 buffer (50 mM Tris-HCl [pH 8], 10 mM EDTA). Chromatin was then eluted in Elution buffer (50 mM Tris-HCl [pH 8], 10 mM EDTA, 1 % SDS) for 20 min at 37° C, 1400 rpm and diluted in TE2 buffer (10 mM Tris-HCl [pH 8], 1 mM EDTA). DNA from ChIP, Mock and Input preparations were decrosslinked and purified by phenol chloroform extraction. Samples were amplified by real-time PCR (qPCR) using the Power SYBR Green PCR master mix (Applied Biosystems) on a CFX Connect™ Real-Time PCR Detection System (BioRad). ChIP data were normalized to the Input (to consider copy number) and subtracted with the background (Mock). Primer sequences for qPCR are listed in Table 2.

Name		Position	Sequence
#1	F	-5036	ACCTAGCGGTCACTGTTACTC
	R	-4898	TCAAAGTGGCGATTTCCTAG
#2	F	-1250	TCTGTCTCTGCGTGGATTC
	R	-1169	AGGGAGGGAGAAAGAACAC
#3	F	1173	GCTCTGCCTCGGAAGGAAG
	R	1289	CTGCGGTACGAGGAAACAC
#4	F	4007	GTCTGCCCTATCAACTTTCG
	R	4098	ATGTGGTAGCCGTTTCTCAG
#5	F	8230	AAAGCGGGTGGTAAACTCC
	R	8324	ACGCCCTCTTGAACTCTC
#6	F	9849	CATCAGACCCCAGAAAAGG
	R	9932	TGATTCGGCAGGTGAGTTG
#7	F	10743	GGCATGTTGGAACAATGTAGG

	R	10798	CCTTAGAGCCAATCCTTATCC
#8	F	11504	CGCCTAGCAGCCGACTTAG
	R	11655	GTTACTCCCGCCGTTTACCC
#9	F	12519	CAGGTTCAGACATTTGGTG
	R	12582	AGGCGTTCAGTCATAATCCC
#10	F	16474	CATCCCCATTACCTGAGACTAC
	R	16540	CACATACCTACCTACGGAAAAC

Table2. Primers used for ChIP-qPCR experiment

ChIP WB

90 µg of MRC5 chromatin extracts were incubated overnight at 4° C in 150 µl total volume of IP buffer (see above) with antibody (RNAP1: anti-RPA194, sc-48385, Santa Cruz; NMI: M3567 Sigma) (ChIP) or no antibody (Mock). Immunoprecipitation was performed as for ChIP qPCR experiment (see above). Chromatin was then eluted with 2X Laemmli buffer. ChIP, Mock and Input preparations were heated at 95° C for 45 min and loaded on a SDS-PAGE gel.

Western blot

Proteins were separated on a SDS-PAGE gel at an acrylamide percentage appropriate to protein size and transferred onto a polyvinylidene difluoride membrane (PVDF, 0.45 µm Millipore). The membrane was blocked in 5 % milk in PBS 0.1 % Tween 20 (PBS-T) solution and incubated for 1.5 h RT or overnight at 4° C with the primary antibodies in milk PBS-T (RNAP1: anti-RPA194, sc-48385, Santa Cruz; ACTβ: A5316, Sigma or ab8227, Abcam; NMI: M3567, Sigma; α-Tubulin: T5168, Sigma, XPF: MS-1351-P1, NeoMarkers). Subsequently, membrane was washed repeatedly with PBS-T and incubated 1 h RT with the secondary antibody in milk PBS-T (Goat anti-mouse IgG HRP conjugate (170-6516; BioRad); Goat anti-rabbit IgG HRP conjugate (170-6515; BioRad)). After the same washing procedure, protein bands were visualized via chemiluminescence (ECL Enhanced Chemo Luminescence; Pierce ECL Western Blotting Substrate) using the ChemiDoc MP system (BioRad).

RNA Fluorescence In Situ Hybridization

Cells were grown on 18 mm coverslips, washed with warm (37°C) PBS and fixed with 4% paraformaldehyde for 15 min at 37° C. Coverslips were washed twice with PBS. Cells were permeabilized by washing with PBS 0.4 % Triton X-100 for 7 min at 4° C. Cells were washed rapidly with PBS before incubating them with pre-hybridization buffer (2X SSPE and 15 % formamide) (20X

SSPE, [pH 8.0]: 3 M NaCl, 157 mM NaH2PO4.H2O and 25 mM EDTA) for at least 30 min. 3.5 µl of probe (10 ng/ml) was diluted in 70 µl of hybridization mix (2X SSPE, 15 % formamide, 10 % dextran sulphate, 0.5 mg/ml tRNA) and heated at 90° C for 1 min. Hybridization of the probe was conducted overnight at 37° C in a humidified environment. Subsequently, cells were washed twice for 20 min with pre-hybridization buffer, then once for 20 min with 1X SSPE and finally mounted with Vectashield (Vector Laboratories) and kept at -20° C. The probe sequence (5' to 3') is: Cy5-AGACGAGAACGCCTGACACGCACGGCAC. At least 30 cells were imaged for each condition.

Immunofluorescence

Cells were grown on 18 mm coverslips, washed with warm (37° C) PBS and fixed with 2% paraformaldehyde for 15 min at 37° C. Cells were permeabilized with PBS 0.1 % Triton X-100 (3X short + 2X 10 min washes). Blocking of non-specific signal was performed with PBS+ (PBS, 0.5 % BSA, 0.15 % glycine) for at least 30 min. Then, coverslips were incubated with 70 µl of primary antibody mix (RNAP1: Mouse anti-RPA194, 1/500 in PBS+, sc-48385) for 2 h at RT in a moist chamber, washed with PBS (3X short + 2X 10 min), quickly washed with PBS+ before incubating with 70 µl of secondary antibody mix (Goat anti-mouse Alexa Fluor® 488 or Goat anti-mouse Alexa Fluor® 594 1/400 in PBS+, Invitrogen) for 1 h at RT in a moist chamber. After the same washing procedure, coverslips were finally mounted using Vectashield with DAPI (Vector Laboratories) and kept at - 20° C. At least 15 cells were imaged for each condition.

Unscheduled DNA Synthesis (UDS)

MRC5-SV40 immortalized human fibroblasts, were grown on 18 mm coverslips. After local irradiation (100 J/m^2 UV-C) through a 5 µm pore polycarbonate membrane filter, cells were incubated for 3 hours with ethynyldeoxyuridine, washed, fixed and permeabilized. Fixed cells were treated with a PBS-blocking solution (PBS+: PBS containing 0.15% glycine and 0.5% bovine serum albumin) for 30 min, subsequently incubated with primary antibodies mouse monoclonal anti-yH2AX (Ser139) (Upstate, clone JBW301) 1/500 diluted in PBS+ for 1h, followed by extensive washes with Tween20 in PBS. Cells were then incubated for 1h with secondary antibodies conjugated with Alexa Fluor 594 fluorescent dyes (Molecular Probes, 1:400 dilution in PBS+). Then, cells were incubated for 30 min with the Click-iT reaction cocktail containing Alexa Fluor Azide 488. After washing, the coverslips were mounted with Vectashield containing DAPI (Vector). Images of the cells were obtained with the same microscopy system and constant acquisition parameters. Images were analysed using ImageJ as follows: (i) a ROI outlining the locally damaged area was defined by using the yH2AX staining, (ii) a second ROI of comparable size was defined in the nucleus (avoiding nucleoli and other non-specific signals) to estimate background signal, (iii)

the ‘local damage’ ROI was then used to measure the average fluorescence correlated to the EdU incorporation, which is an estimate of DNA synthesis after repair once the nuclear background signal obtained during step (ii) is subtracted. For each sample three independent experiments were performed.

Fluorescent imaging and analysis

Imaging has been performed on a Zeiss LSM 780 NLO confocal laser-scanning microscope (Zeiss), using a 60x/1.4 oil objective. Images were analyzed with ImageJ software. For all images of this study, nuclei and nucleoli were delimited with dashed and dotted line respectively, using DAPI staining or transmitted light.

Statistical analysis

Error bars represent the Standard Error of the Mean (SEM) of the biological replicates.

Draft

Unravelling the molecular role of XAB2 during transcription and DNA repair

Elena CERUTTI, Lise-Marie DONNIO, Damien NEUILLET, Pierre-Olivier MARI, Giuseppina GIGLIA-MARI

Institut NeuroMyoGène (INMG), CNRS UMR 5310, INSERM U1217, Université de Lyon, Université Claude Bernard Lyon1, 16 rue Dubois, 69622 Villeurbanne CEDEX France

Keywords: XPA-binding protein 2; CSA; CSB; pre-mRNA splicing; Transcription-coupled Repair; RNA polymerase 2

Introduction

The DNA contained in the nucleus of our cells constitutes the instruction manual for proper cellular functioning. Unfortunately, the integrity of DNA is continuously challenged by a variety of endogenous and exogenous agents (e.g. ultraviolet light, cigarette smoke, environmental pollution, oxidative damage, etc …) that cause DNA lesions which interfere with proper cellular functions, leading to aging or premature aging of the tissue and eventually of the whole organism.

To prevent the deleterious consequences of persisting DNA lesions, all organisms are equipped with a network of efficient DNA repair systems. One of these systems is the Nucleotide Excision Repair (NER). NER removes helix-distorting DNA adducts such as UV-induced lesions (Cyclo-Pyrimidine Dimers and 6-4 Photoproducts, CPD and 6-4PP) in a coordinated multi-step process (1).

The NER system has been linked to rare human diseases classically grouped into three distinct NER-related syndromes. These include the highly cancer prone disorder xeroderma pigmentosum (XP) and the two progeroid diseases: Cockayne syndrome (CS) and trichothiodystrophy (TTD). Importantly, CS and TTD patients are not cancer-prone but present severe neurological and developmental features (2).

NER exists in two distinct sub-pathways depending where DNA lesions are located within the genome. Global Genome Repair (GG-NER or GGR) will repair DNA lesion located on non-transcribed DNA. The second sub-pathway is directly coupled to transcription elongation and repairs DNA lesions located on the transcribed strand of active genes. This second sub-pathway is designated as Transcription Coupled Repair (TC-NER or TCR).

The clinical outcomes exhibited by patients affected by a NER-related syndrome present extensive differences depending which NER sub pathway is unpaired. The mostly neurological symptoms observed in CS patients (carrying mutations on genes involved in TCR repair) cannot solely be explained by a repair defect. The most likely explanation could be the involvement of the transcription-coupled mechanism in other cellular processes, or at least of one of its factors. Therefore, it is of great relevance the identification and the comprehension of mechanisms at the crossroads between transcription-coupled repair and other cellular processes. For this purpose, we investigated the molecular function of a poorly studied protein, which has been proposed to have a role in a variety of cellular mechanisms: the XPA-binding protein 2.

The XPA Binding Protein 2 (XAB2) is a 100 kDa protein composed of 855 amino acids. Sequence analysis revealed that XAB2 has 15 Tetratricopeptide repeats (TPR) of the class I located

all along the protein. XAB2 protein shows sequence homology with factors from different organisms, such as *Drosophila melanogaster*, *Caenorhabditis elegans*, *Schizosaccharomyces pombe,* and with the SYF1 protein in *Saccharomyces cerevisiae*. This strong conservation and the preimplantation lethality observed in XAB2 knockout mice (3) suggest the relevance of this protein in cellular functioning (4).

XAB2 has been first identified with XPA protein in a yeast two-hybrid screen and their interaction has been confirmed *in vitro*. Actually, a small fraction of XAB2 has been co-immunoprecipitated with both CSA and CSB and with elongating RNAP2 and micro-injection of anti-XAB2 antisera in XPC cells (defective for GGR) results in a significant reduction of UV-induced Unscheduled DNA Synthesys during repair (4). In light of this finding, a role of XAB2 in TCR reaction has been proposed. In addition, XAB2 has been purified as part of a complex containing multiple pre-mRNA splicing factors: hAquarius, hPRP19, CCDC16, hISY1 and PPIE, then suggesting for XAB2 an involvement in cellular functions connected to splicing events (5).

In this study, we confirm, in living cells, the XAB2 involvement in the TCR repair process and the consequent failure of Recovery of RNA Synthesis (RRS) after UV damage in absence of XAB2. Furthermore, we analyze the molecular dynamic of XAB2 during TCR, revealing that, unlike all the other NER protein studied so far, XAB2 is released from the damaged site and its mobility before and during repair is CSA and CSB-dependent. We then investigate in living cells XAB2 interaction with the pre-mRNA splicing complex before and during the repair process. Finally, we focus on the XAB2 role in RNAP2 dynamic and our results suggests that XAB2 plays a role in keeping RNAP2 on the chromatin during the pause of transcription.

Results

XAB2 involvement in DNA repair

In light of the demonstrated UV-hypersensitivity due to XAB2 depletion (5) and other results obtained within the same study, we decided to explore the role of XAB2 in DNA Repair and particularly within the Nucleotide Excision Repair system. This repair pathway can be subdivided into GGR (Global Genome Repair) and TCR (Transcription Couple Repair). The well-known standard to quantify GGR is the measure of the Unscheduled DNA Synthesis (UDS). This technique allow the quantification of the new DNA strand synthetized to fill the single strand DNA gap left by NER repair mechanism. In order to discriminate between replicative and not replicative cells, we locally irradiated cells, through a 5 µm pores filter. As we expected, XPF siRNA treated cells showed a reduction in UDS level, due to the inability to repair UV lesions. XAB2 siRNA treated cells did not present a decreased level of UDS, as for mock-treated cells (Figure 1A and S1). This result show that XAB2 is not involved in GGR, but do not exclude an involvement of XAB2 in TCR. Actually, since the TCR mechanism is confined to actively transcribed genes, the amount of TCR events strongly depend on the number of active transcription sites and their number is significantly lower than the GGR events. Actually, TCR represents only the 10% of the total NER acting on UV-lesion (6).

The standard experiment to evaluate the TCR efficiency on globally irradiated cells is the measure of RNA Recovery Synthesis (RRS). This technique allow the quantification of the newly transcribed RNA by incorporation of a fluorophore-coupled nucleoside analog. Furthermore, the experiment is conducted at different time point after UV irradiation, allowing to follow the transcriptional activity all along the DNA repair process and the restart of transcription after DNA repair completion. We then conducted this test in siRNA treated cells. As expected, XPF siRNA treated cells did not present any restart of transcription, due to the inability to repair UV lesions. XAB2 siRNA treated cell did not present the restart of transcription either, while mock treated cells showed, 24 h hours after UVC exposure, a transcription level similar to the no UV condition (Figure 1C). This result demonstrated an XAB2 involvement in the repair process, but did not discriminate a role in the mechanism of restart of transcription or in the repair process.

In order to discern between these two possibilities, we performed an assay previously designed in our group, which specifically measures repair replication during TCR: the TCR-UDS assay (6). We treated a XPC-deficient cell line (defective for GGR) with siRNA and we locally irradiated cells, through a 5 µm pores filter. We exactly localized the damaged area by co-immunofluorescence labeling of γ-H2AX and we quantified the newly synthetized DNA. XPF siRNA

treated cells presented, as expected, low DNA synthesis related to repair since cells are defective for both the sub pathways. In addition, XAB2 siRNA treated cells presented a low TCR-UDS level compared to the mock-treated condition (Figure 1B). This result confirms the XAB2 involvement in the TCR repair process, but not in the GGR.

We have recently published a study in which we demonstrate that a fully functional NER mechanism is necessary for repair of ribosomal DNA transcribed by the RNAP1 (7). Due to the nature of the rDNA containing region, the nucleolus, and of the rDNA itself, the only way to visualize the efficacy of NER mechanism is by RNA fluorescence in situ hybridization (RNAfish). For this experiment, we use a RNA probe coupled to a fluorophore, which recognize the 5' end of the 47S pre-rRNA, upstream from the first cleavage site that is rapidly processed during rRNA maturation. We performed this experiment at different time point after UVC exposure, in order to follow the rRNA transcription. CSB siRNA treated cells presented a low level of rRNA synthesis even 40h after UVC exposure, when repair of rDNA performed by the GGR is completed, due to TCR deficiency. On the contrary, XAB2 siRNA treated cells, as the mock-treated condition, showed a total recovery of rRNA transcription 40h after UVC exposure (Figure 1D). This result demonstrated a function of XAB2 in the TCR process specific for RNAP2 transcribed genes.

XAB2 dynamic during TC-NER

Because of the XAB2 involvement in the TCR mechanism, we decided to explore its localization during DNA repair. We locally irradiated WT cells through a 5 µm pores filter and we performed a co-immunofluorescence against both γ-H2AX, to exactly visualize the damaged area, and XAB2 at different time point after UVC exposure. Thanks to the XAB2 staining we have also been able to quantify the amount of fluorescence in the damaged area compared to the rest of the nucleus (Figure 2B). Unexpectedly, in contrast with all the other NER protein studied so far, we observed a transiently release of XAB2 from the damaged area that last until the completion of DNA repair 16h after UVC irradiation (Figure 2A upper left panel and 2B). This surprising observation, prompt us to investigate the localization of XAB2 during repair in CSA and CSB deficient cell lines (defective for TCR). We observed that in CSA and CSB deficient cells, XAB2 is released from the damage area and, interestingly, this release did not decrease even after 16h after UVC exposure, due to defective TCR (Figure 2A upper right and lower panels).

With the aim of explore more deeply XAB2 dynamic during repair, we generated stably expressing GFP tagged XAB2 (XAB2-GFP) (Figure S2A and S2B) SV40-immortalized human fibroblasts MRC5, CS3BE and CS1AN (WT, CSA and CSB-deficient respectively). Initially, we defined the minimum sufficient UV dose allowing us to observe a significant difference in XAB2 dynamic

after UVC exposure. To do so, we exposed MRC5 XAB2-GFP-tagged cells to different UVC doses, ranging from 2 J/m² to 16 J/m² and then we applied the Spot-FRAP method at different time point after UVC irradiation (Figure 2C). Spot-FRAP (Fluorescence Recovery After Photobleaching) is a technique (8) in which fluorescent molecules are photo-bleached in a small spot by a high intensity laser pulse and then the subsequent recovery of fluorescence is monitored in time within the bleached area. In absence of DNA damage, this fluorescence recovery measure provides us information about the protein's immobile fraction in living cells and, also, about its mobility profile, conceived as the sum of binding events and inertial diffusion (Figure S2C). On the other hand, after perturbation of the nuclear environment, e. g. after DNA damage induction, the recovery of fluorescence can be reduced, e. g. if the protein interacts with a new substrate that was absent before (like NER proteins), enhanced, e. g. if the protein is released from a previously present complex, or even unchanged, e. g. if the perturbation does not concern the protein of interest. Thanks to this technique we have been able to identify 8 J/m^2 as the minimum UVC dose necessary to induce a significant increase in XAB2 mobility during repair (3h post UV) and the following return to the normal condition once repair is completed (16h post UV) (Figure 2C). Thanks to this technique, we observed an increased mobility of XAB2 during repair, confirming our previous observation by immunofluorescence on local damage. Then, we performed Spot-FRAP experiment on XAB2-GFP expressing cells deficient for the TCR factors CSA or CSB. We observed an increasing XAB2 mobility lasting in time in both CSA and CSB cell lines, from induction of UVC lesion to even 24h after UVC exposure. This result further confirms our previous finding. Nevertheless, we also unexpectedly observed that in absence of lesions, in TCR deficient cell lines, XAB2 mobility was reduced compared to the WT condition. These results, taken together, demonstrate that XAB2 mobility is CSA and CSB-dependent, during both transcription and DNA repair.

XAB2 pre-mRNA splicing complex during repair

The XAB2 protein has been purified, thanks to a FLAG fusion protein, as a multimeric protein complex containing several factors known to be involved in pre-mRNA splicing (5). The XAB2 complex includes: hAquarius, which is an intron-binding protein and has been reported as the linking factor between snRNP formation and pre-mRNA splicing (9); PRP19, which forms itself a spicing complex, also known as NineTeen Complex (NTC), involved in splicing, transcription and mRNA export (10); CCDC16, which belong to a family of zinc finger proteins detected in RNA-binding proteins (11); PPIE which is a nuclear RNA-binding cyclophilin; and ISY1, which associates with SYF1 (yeast XAB2 homologue) and snRNAs (12, 13). In light of our observations involving XAB2 in the TCR process, we decided to explore the potential role of XAB2 complex factors in the NER

mechanism. We then applied the previously described techniques of Unscheduled DNA Synthesis (Figure S3B), RNA Recovery Synthesis (Figure S3D) and TCR-Unscheduled DNA Synthesis (Figure S3C) in absence of each component factor of the XAB2 complex. XPF siRNA and mock-treated cells validate our results as positive and negative control. We observe, in our experimental condition, that XAB2 partners are not involved neither in GGR nor in TCR repair mechanism. These results indicated that XAB2 is the only complex component involved in DNA repair and this could be due to the nature of XAB2 structure. The presence of 15 tandem arrays of tetratricopeptide repeats all along the amino acidic sequence allow the simultaneous interaction with multiple proteins, by employing specific combination of TPR motif within the superhelix. This structural feature could explain the simultaneous role of XAB2 in multiple processes.

Interestingly, we observed that depletion of a XAB2 complex factor by siRNA could strongly influence the protein level of the others complex factors (Figure S3A). This observation demonstrates that the expression levels of XAB2, hAQR, PRP19, CCDC16, PPIE and ISY1 are highly interconnected.

In order to investigate the physical interaction between XAB2 and XAB2 complex factors during repair, we performed an immunoprecipitation against XAB2 and RNAP2 on the nuclear fraction of MRC5 cells before and after UVC exposure (Figure 3A). We obtained an interesting result showing that the amount of RNAP2 decrease during repair and increase to a level comparable to the No UV condition 16 h after UVC exposure, when transcription restarts. This observation suggest that RNAP2 molecules present in the nuclear fraction are degraded in response to UV global irradiation. Concerning the interaction of XAB2 complex, in our experimental conditions, we co-immunoprecipitate with XAB2 the hAQR protein and PPIE factor. Interestingly, the amount of the XAB2 interacting complex seems to increase 3h and 16 h after UVC exposure, but this result has to be confirmed. Furthermore, we observed that XAB2 co-immunoprecipitates with RNAP2 during transcription and 1h after UV lesion induction. We could speculate that XAB2 could be involved in the recognition of the damage.

In light of our results involving CSA and CSB in XAB2 dynamic regulation, we performed the co-immunoprecipitation analysis in CSA and CSB-deficient cell lines (Figure 3B). In both this cell lines, we observed that RNAP2 amount decrease after UVC exposure and it is not restored even 16h after damage induction, likely because of the defective repair on actively transcribed genes in these cell lines (TCR-deficient). Furthermore, we unexpectedly co-immunoprecipitates with XAB2 also the CCDC16 factor, together with hAQR and PPIE. This interaction could be due to the absence of CSA and CSB. Finally, we did not reproduce in these cell lines, the interaction between XAB2 and RNAP2 during transcription and the first steps of DNA repair, observed in WT cells. This

result could confirm the XAB2 involvement in the lesion recognition step of TCR, essential for a proficient repair.

RNAP2 dynamic in absence of XAB2

Tanaka's research group demonstrated that a small fraction of XAB2 interacts with the elongating form of RNAP2 during transcription (5). This specific RNAP2 form involves, among a series of protein interaction, posttranscriptional modification of the CTD tail of RNAP2 biggest subunit. Several evidences associate CTD posttranslational modification to the recruitment of splicing factors, underling a link between RNAP2 transcription and splicing. In light of these results and considering the XAB2 involvement in TCR, we investigated whether the absence of XAB2 would affect the mobility of the RNAP2 during the repair reaction. For that purpose, we applied the Strip-FRAP technique on stably expressing GFP tagged RNAP2 (GFP-RNAP2) SV40-immortalized human fibroblasts MRC5 previously generated and validated in our group and we achieved XAB2 knockdown through siRNA transfection. In mock-treated cells, Strip-FRAP assays showed that GFP-RNAP2 is largely immobilized, showing only a limited fraction of recovered protein after the photo-bleach. This immobile fraction represents the RNAP2 molecules engaged in the process of transcription and therefore retained on the chromatin. After UVC exposure, in mock-treated cells, there is no measurable change of the mobility of GFP-RNAP2 (Figure 4A), as already observed in a previous study in our group (6). However, in absence of DNA damage and in absence of XAB2, the RNAP2 immobile fraction significantly decreases (Figure 4C). Moreover, after UVC exposure and XAB2 depletion, RNAP2 immobile fraction decreases even more (Figure 4D). These results could be explained by an involvement of XAB2 in the pause of transcription for RNAP2. The more prominent effect of XAB2 depletion on RNAP2 after UVC exposure could be due to a role of XAB2 in the TCR first step of lesion recognition by blocked RNAP2. In order to confirm this observation, we decided to investigate RNAP2 binding on the chromatin fraction in absence of XAB2. For this purpose, we depleted XAB2 from MRC5 cells by siRNA transfection, we cross-linked proteins to DNA and we evaluated the amount of bound RNAP2 on the sonicated chromatin by western blot (Figure 4E). The result we obtained confirm our previous observation by showing a reduced amount of RNAP2 bound to the chromatin fraction in absence of XAB2.

Material and Methods

Cell culture and treatments

The cells used in this study were: (i) wild-type SV40-immortalized human fibroblasts (MRC5); (ii) GG-NER–deficient SV40-immortalized human fibroblast: XPC (XP4PA); (iii) TC-NER–deficient SV40-immortalized human fibroblast: CSA (CS3BE) and CSB (CS1AN); (iv) MRC5-SV stably expressing XAB2-GFP (G418 selected 0.2 mg/ml); (v) CSA-SV stably expressing XAB2-GFP (G418 selected 0.2 mg/ml); (vi) CSB-SV stably expressing XAB2-GFP (G418 selected 0.2 mg/ml); (vii) MRC5-SV stably expressing GFP-RNAP2 (G418 selected 0.2 mg/ml).

Immortalized human fibroblasts were cultured in a 1:1 mixture of Ham's F10 and DMEM (Lonza) supplemented with 1% antibiotics (penicillin and streptomycin; Lonza) and 10% fetal bovine serum (Gibco) and incubated at 37°C with 20% O_2 and 5% CO_2.

DNA damage was inflicted by UV-C light (254 nm, 6-Watt lamp). Cells were globally irradiated with a UV-C dose of 2, 4, 8 or 16 J/m^2 or locally irradiated with a 60 or 100 J/m^2 dose of UV-C through a Millipore filter (holes of 5 µm of diameter).

Transfection of small interfering RNAs (siRNAs)

On day 0, 100 000 cells were seeded in a 6-wells plate and/or on 18 mm coverslips. The first and second transfections were performed on day 1 and day 2, using Lipofectamine® RNAiMAX reagent (Invitrogen; 13778150) or Gen Jet (Tebu-Bio), according to the manufactures' protocols. Experiments were performed between 24h or 72h after the second transfection. SiRNA efficiency was confirmed by western blot on whole cell extracts. siRNAs sequences are described in Table 1.

Target	Final Concentration	Reference/Sequence
siMock	10 nM	D-001206-14
siXAB2	20 nM	L-004914-01
siXPF	10 nM	M-019946-00
siCSB	10 nM	L-004888-00
sihAquarius	10 nM	CCAGACCACUUCCCAUUCU
siPRP19	10 nM	GGUGUACAUGGACAUCAAG
siCCDC16	5 nM	GCGAUCUAGUUUCAUUAAA
siPPIE	5 nM	GGCUAUGAGGCAAGUCAAC

siISY1	5 nM	GGAAAUCGAGGUUACAAGU

Table 1. siRNAs references

Whole cell extracts

Cells were collected using trypsin and centrifuged 10 min at 1400 rpm. Firstly, cell pellet was washed with PBS supplemented with the Protease Inhibitor Cocktail (Roche) and spinned down 10 min at 1400 rpm. Secondly, cell pellet was incubated with Lysis buffer (ProteoJETTM Mammalian Cell Lysis Reagent, Fermentas) complemented with the Protease Inhibitor Cocktail (Roche), for 10 min at room temperature on a shaker (500 rpm). Finally, samples were centrifuged at 16000 g for 15 min and supernatant was freezed at - 80° C. Protein concentration was determined using the Bradford method, samples were diluted with 1X Laemmli buffer and heated 10 min at 95° C.

Nuclear Extracts

Cells were cultured in 10 cm dishes. After irradiation as described above, cells were harvested by scraping. The extraction of proteins has been performed by using the kit CelLytic™ NuCLEAR™ Extraction (Sigma-Aldrich). The concentration of proteins has been determined by using the Bradford method.

Recovery of RNA synthesis (RRS)

MRC5-SV40 cells were grown on 18 mm coverslips. siRNA (siMock/siXAB2/siXPF) transfections were performed 24h before RRS assays. RNA detection was performed using a Click-iT RNA Alexa Fluor Imaging kit (Invitrogen), according to the manufacturer's instructions. Briefly, cells were UV-C irradiated (16 J/m^2) and incubated for 0, 3, 16 and 24 h at 37°C. Then, cells were incubated for 2 hours with 5-ethynyl uridine, fixed and permeabilized. Cells were incubated for 30 min with the Click iT reaction cocktail containing Alexa Fluor Azide 594. After washing, the coverslips were mounted with Vectashield containing DAPI (Vector). Images of the cells were obtained with the same setup and constant acquisition parameters, then the average fluorescence intensity per nucleus was estimated after background subtraction (using ImageJ) and normalized to not treated cells. For each sample, at least 50 nuclei were analysed from three independent experiments.

Unscheduled DNA synthesis (UDS or TCR-UDS)

MRC5-SV40 or XPC deficient SV40-immortalized human fibroblasts (XP4PA GGR-deficient cell line), were grown on 18 mm coverslips. siRNA (siMock/siXAB2/siXPF) transfections were

performed 24h before UDS assays. After local irradiation (100 J/m^2 UV-C) through a 5 µm pore polycarbonate membrane filter, cells were incubated for 3 or 8 hours with ethynyldeoxyuridine, washed, fixed and permeabilized. Fixed cells were treated with a PBS-blocking solution (PBS+: PBS containing 0.15% glycine and 0.5% bovine serum albumin) for 30 min, subsequently incubated with primary antibody mouse monoclonal anti-yH2AX (Ser139) (Upstate, clone JBW301) 1/500 diluted in PBS+ for 1h, followed by extensive washes with Tween20 in PBS. Cells were then incubated for 1h with secondary antibodies conjugated with Alexa Fluor 594 fluorescent dyes (Molecular Probes, 1:400 dilution in PBS+). Then, cells were incubated for 30 min with the Click-iT reaction cocktail containing Alexa Fluor Azide 488. After washing, the coverslips were mounted with Vectashield containing DAPI (Vector). Images of the cells were obtained with the same microscopy system and constant acquisition parameters. Images were analysed using ImageJ as follows: (i) a ROI outlining the locally damaged area was defined by using the yH2AX staining, (ii) a second ROI of comparable size was defined in the nucleus (avoiding nucleoli and other non-specific signals) to estimate background signal, (iii) the 'local damage' ROI was then used to measure the average fluorescence correlated to the EdU incorporation, which is an estimate of DNA synthesis after repair, once the nuclear background signal obtained during step (ii) is subtracted. For each sample three independent experiments were performed.

RNA Fluorescence In Situ Hybridization (RNAfish)

Cells were grown on 18 mm coverslips, washed with warm (37°C) PBS and fixed with 4% paraformaldehyde for 15 min at 37° C. Coverslips were washed twice with PBS. Cells were permeabilized by washing with PBS 0.4 % Triton X-100 for 7 min at 4° C. Cells were washed rapidly with PBS before incubating them with pre-hybridization buffer (2X SSPE and 15 % formamide) (20X SSPE, [pH 8.0]: 3 M NaCl, 157 mM NaH2PO4.H2O and 25 mM EDTA) for at least 30 min. 3.5 µl of probe (10 ng/ml) was diluted in 70 µl of hybridization mix (2X SSPE, 15 % formamide, 10 % dextran sulphate, 0.5 mg/ml tRNA) and heated at 90° C for 1 min. Hybridization of the probe was conducted overnight at 37° C in a humidified environment. Subsequently, cells were washed twice for 20 min with pre-hybridization buffer, then once for 20 min with 1X SSPE and finally mounted with Vectashield (Vector Laboratories) and kept at -20° C. The probe sequence (5' to 3') is: Cy5-AGACGAGAACGCCTGACACGCACGGCAC. At least 30 cells were imaged for each condition.

Immunofluorescence

Cells were grown on 18 mm coverslips and after local irradiation (60 J/m^2 UV-C) through a 5 µm pore polycarbonate membrane filter, cells were incubated for 1, 3 or 16h hours at 37° C. Cells were then washed with warm (37° C) PBS and fixed with 2% paraformaldehyde for 15 min at 37°

C. Cells were permeabilized with PBS 0.1 % Triton X-100 (3X short + 2X 10 min washes). Blocking of non-specific signal was performed with PBS+ (PBS, 0.5 % BSA, 0.15 % glycine) for at least 30 min. Then, coverslips were incubated with 70 µl of primary antibody mix in PBS+ (Rabbit anti-γH2AX (ab2893) 1/500 in PBS+ and Mouse anti-XAB2 (sc-271037) 1/400 in PBS+) for 2 h at RT in a moist chamber, washed with PBS (3X short + 2X 10 min), quickly washed with PBS+ before incubating with 70 µl of secondary antibody mix (Goat anti-mouse Alexa Fluor® 488 and Goat anti-rabbit Alexa Fluor® 594, 1/400 in PBS+,Invitrogen) for 1 h at RT in a moist chamber. After the same washing procedure, coverslips were finally mounted using Vectashield with DAPI (Vector Laboratories) and kept at - 20° C. At least 15 cells were imaged for each condition. Imaging has been performed on a Zeiss LSM 780 NLO confocal laser-scanning microscope (Zeiss), using a 60x/1.4 oil objective. Images were analyzed with ImageJ software. The variation of fluorescence in the locally irradiated zone has been calculated as for the UDS experiment (see above).

Fluorescence Recovery after Photobleaching (FRAP)

FRAP experiments were performed on a Zeiss LSM 780 NLO confocal laser scanning microscope (Zeiss), using a 40x/1.3 oil objective, under a controlled environment (37°C, 5% CO_2). Briefly, a narrow region of interest (ROI) centered across the nucleus of a living cell was monitored every 20 ms (1% laser intensity of the 488 nm line of a 25 mW Argon laser) until the fluorescence signal reached a steady state level (after ≈ 2 s). The same region was then photobleached for 20 ms at 100% laser intensity. Recovery of fluorescence in the bleached ROI was then monitored (1% laser intensity) every 20 ms for about 20 seconds. Analysis of raw data was performed with the ImageJ software. All FRAP data were normalized to the average pre-bleached fluorescence after background removal. Every plotted FRAP curve is an average of at least twenty measured cells.

Analysis of SPOT FRAP data was performed as follows (Figure S2D). The average fluorescence (over all cells) of the No UV condition was subtracted from the average fluorescence of the UV treated conditions. The obtained difference between the two FRAP curves was then summed point by point, starting from the bleach up to the following 100 measurements i.e. the area between the curve of interest and the untreated condition curve.

Co-immunoprecipitation

For co-immunoprecipitation, 10 µl of protein G magnetic bead (Bio-adembead, Ademtech) were used per IP. 1 µg of anti-RANP2 antibody (rabbit, A300-653A, Bethyl) or 1 µg of anti-XAB2 antibody (rabbit, A303-638A, Bethyl) were bound to the beads in PBS with BSA (3%) during 2h at 4°C with rotation. 100 µg of nuclear extracts were then incubated with beads-antibodies complex

for 2h at 4°C with rotation. After 2 washes at 100 mM salt, 2 washes at 150 mM and 1 wash at 100 mM, beads were boiled in 2x Laemmli buffer and eluted samples loaded on a SDS PAGE gel.

Chromatin extracts

All procedures were carried out on ice unless otherwise stated. Cells were grown in 10 cm dish. After treatments, cells were washed twice with PBS and cross-linked with a solution of 1 % formaldehyde in PBS (10 min at RT, shaking) prepared from a 37 % stock (Sigma-Aldrich, F1635). Cross-linking was neutralized by adding glycine for a final concentration of 0.14 M, followed by a wash with cold PBS. Cells were collected by scraping in PBS supplemented with the EDTA-free protease inhibitor tablets (Roche) and centrifuged 10 min at 2000 rpm and 4° C.

All buffers used for chromatin extraction contained, among others, the EDTA-free protease inhibitor tablets (Roche).

Cell pellet was suspended in Swelling buffer (25 mM Hepes-KOH [pH 7.6], 1.5 mM $MgCl_2$, 10 mM KCl, 0.5 % NP-40) freshly completed with 1 mM DTT and incubated 10 min rotating at 4° C. The suspension was centrifuged 10 min at 5000 rpm and 4° C. Cell pellet was then incubated in Sonication buffer (50 mM Hepes-KOH [pH 7.6], 1 mM EDTA, 140 mM NaCl, 1 % Triton X-100, 0.1 % Na-deoxycholate, 0.1 % SDS) 30 min before sonication. The nuclear suspension was sonicated using the Bioruptor (Diagenode) (60 cycles: 30" ON + 60" OFF, high power) to yield DNA fragments with an average size of 250 bp. Samples were then centrifuged (14.000 rpm, 10 min, 4° C) and the supernatant containing the cross-linked chromatin was freezed at -80° C. DNA concentration was quantified using the NanoDropTM 2000 Spectrophotometer (Termo Scientific). 20 ng of chromatin were then boiled in 2x Laemmli buffer, to allow reverse of the crosslink reaction, and load on a SDS PAGE gel.

Western-blot

Proteins were separated on a SDS-PAGE gel composed of bisacrylamide (37:5:1) and blotted onto a polyvinylidene difluoride membrane (PVDF, 0.45 µm Millipore.) The membrane was blocked in 5 % milk in PBS 0.1 % Tween 20 (PBS-T) solution and incubated for 1.5 h RT or overnight at 4° C with the following primary antibodies in milk PBS-T : Rabbit anti-RNAP2 Rpb1 Bethyl A300-653A 1/1000; Rabbit anti-hAQR Bethyl A302-547A 1/2000; Rabbit anti-XAB2 Bethyl A303-638A 1/1000; Rabbit anti-CCDC16 Bethyl A301-419A 1/2000; Rabbit anti-PPIE ab154865 1/1000; Rabbit anti-PRP19 ab27692 1/1000; Rabbit anti-ISY1 ab121523 1/500; Mouse anti-XPF NeoMarkers MS-1351-P1 1/500; Mouse anti-α-Tubulin Sigma-Aldrich T6074 1/50000; Rabbit anti-TBP Cell Signaling 8515 1/500. Subsequently, membrane was washed repeatedly with PBS-T and incubated 1 h RT with the secondary antibody in milk PBS-T (Goat anti-mouse IgG HRP conjugate (170-6516;

BioRad); Goat anti-rabbit IgG HRP conjugate (170-6515; BioRad)). After the same washing procedure, protein bands were visualized via chemiluminescence (ECL Enhanced Chemo Luminescence; Pierce ECL Western Blotting Substrate) using the ChemiDoc MP system (BioRad).

Statistical analysis

Error bars represent the Standard Error of the Mean (SEM) of the biological replicates.

Discussion

Helix distorting lesions continuously challenge the cell survival by blocking fundamental cellular functions, such as transcription and replication. In order to prevent the deleterious effects of this events, cells have developed a series of focused repaired mechanism. The importance of rapidly reestablish perturbed cellular functions is underlined by the presence of a repair mechanism directly coupled with transcription.

Within this study, we demonstrated in living cells that the XPA binding protein 2 is involved in the repair process of lesions located on the transcribed strand of active genes (TCR). It has to be taken in account that XAB2 is part of a pre-mRNA splicing complex and that increasing evidences support the idea that transcription and splicing are physically and functionally coupled. Our findings can thus provide a specific role in TCR repair to a splicing factor. Although its involvement in TCR, we demonstrated that the XAB2 protein is released from the damage induced by UVC exposure, unlike all the other NER protein studied so far. This observation could be explained by the importance for the cell to rapidly recognize the site of damage, to limit local transcription and to provide access to the repair machinery. Actually, it has been demonstrated that DNA lesions that block transcription rapidly decrease the localization of U2 and U5/U6 snRNPs at irradiated sites (14). Furthermore, we show that XAB2 dynamic is CSA and CSB-dependent during both transcription and repair.

XAB2 has been found as part of the pre-mRNA splicing complex composed of hAQR, PRP19, CCDC16, PPIE and ISY1 (5). In our experimental conditions, we have been able to confirm XAB2 interaction with only three partners: hAQR, CCDC16 and PPIE. We then investigate the involvement of each factor of the XAB2 complex in NER repair. None of them seems to take part in the repair process, underlying the peculiar function of XAB2. We hypothesized that XAB2 structure may explain its multiple role. The presence of 15 tandem arrays of tetratricopeptide repeats all along the amino acidic sequence allow the simultaneous interaction with multiple proteins, by employing specific combination of TPR motif within the superhelix.

In light of XAB2 role in TCR and splicing, we investigated if it could influence RNAP2 mobility. Our finding demonstrated that RNAP2 immobile fraction significantly decreases in absence of XAB2 and the amount of RNAP2 bound to the chromatin fraction is also reduced. We speculate that XAB2 could have a role in the pause of transcription by RNAP2. Furthrmore, we co-immunoprecipitates a fraction of XAB2 with RNAP2 during transcription and during the first hour after UVC exposure; this same observation has not been reproduced in TCR-deficient cell lines.

We speculate that the possible XAB2 role in pausing of transcription could also involve the recognition of the damaged site by RNAP2.

In order to have a complete picture of XAB2 involvement in transcription and DNA repair and confirm some of our results, other experiments have to be conducted. At the moment, the results we obtained shed light on a protein having multiple roles, which could provide a new link between multiple mechanism occurring during RNAP2 transcription.

Figures

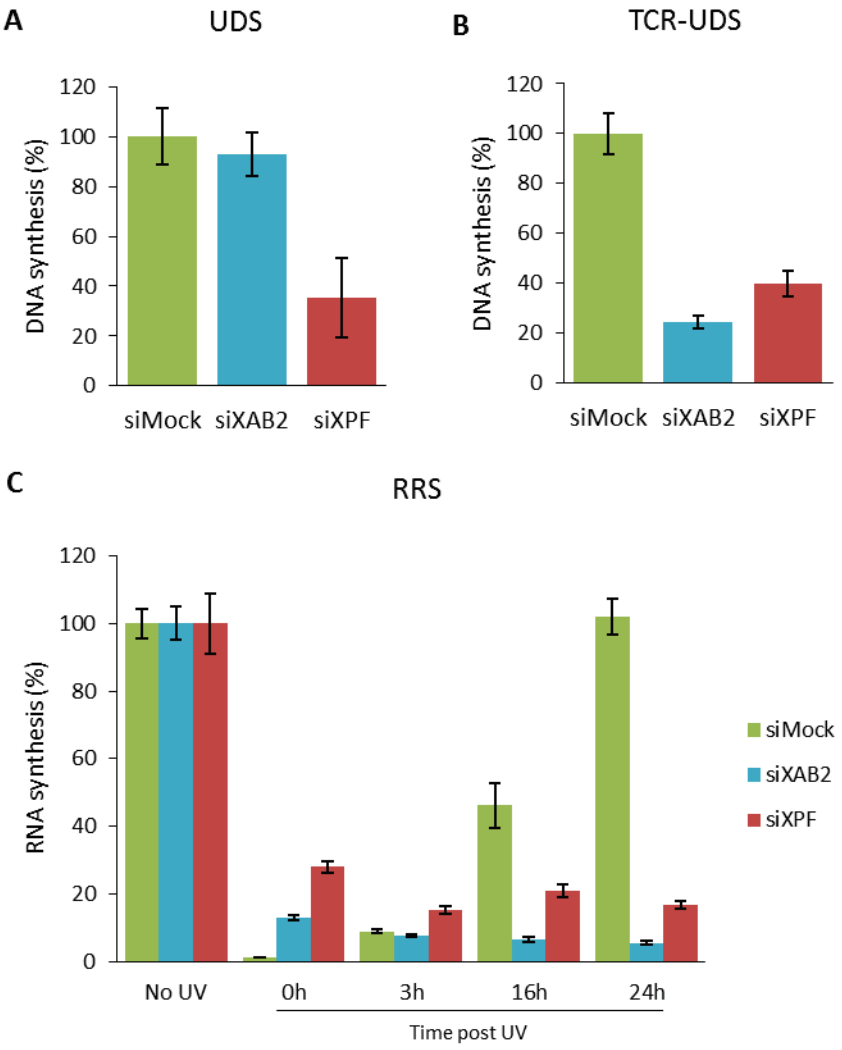

Figure 1. XAB2 involvement in DNA repair

A) Unscheduled DNA Synthesis determined by EdU incorporation after local damage induction with UV-C in MRC5 cells treated with siRNAs against indicated factors. **B)** Unscheduled DNA Synthesis determined by EdU incorporation after local damage induction with UV-C in GG-NER deficient cells treated with siRNAs against indicated factors. **C)** RNA Recovery Synthesis determined by EU incorporation after UV-C exposure in MRC5 cells treated with siRNAs against indicated factors. **D)** Quantification of RNA FISH assay showing the 47S pre-rRNA level after UV-C exposure in MRC5 cells treated with siRNAs against indicated factors.

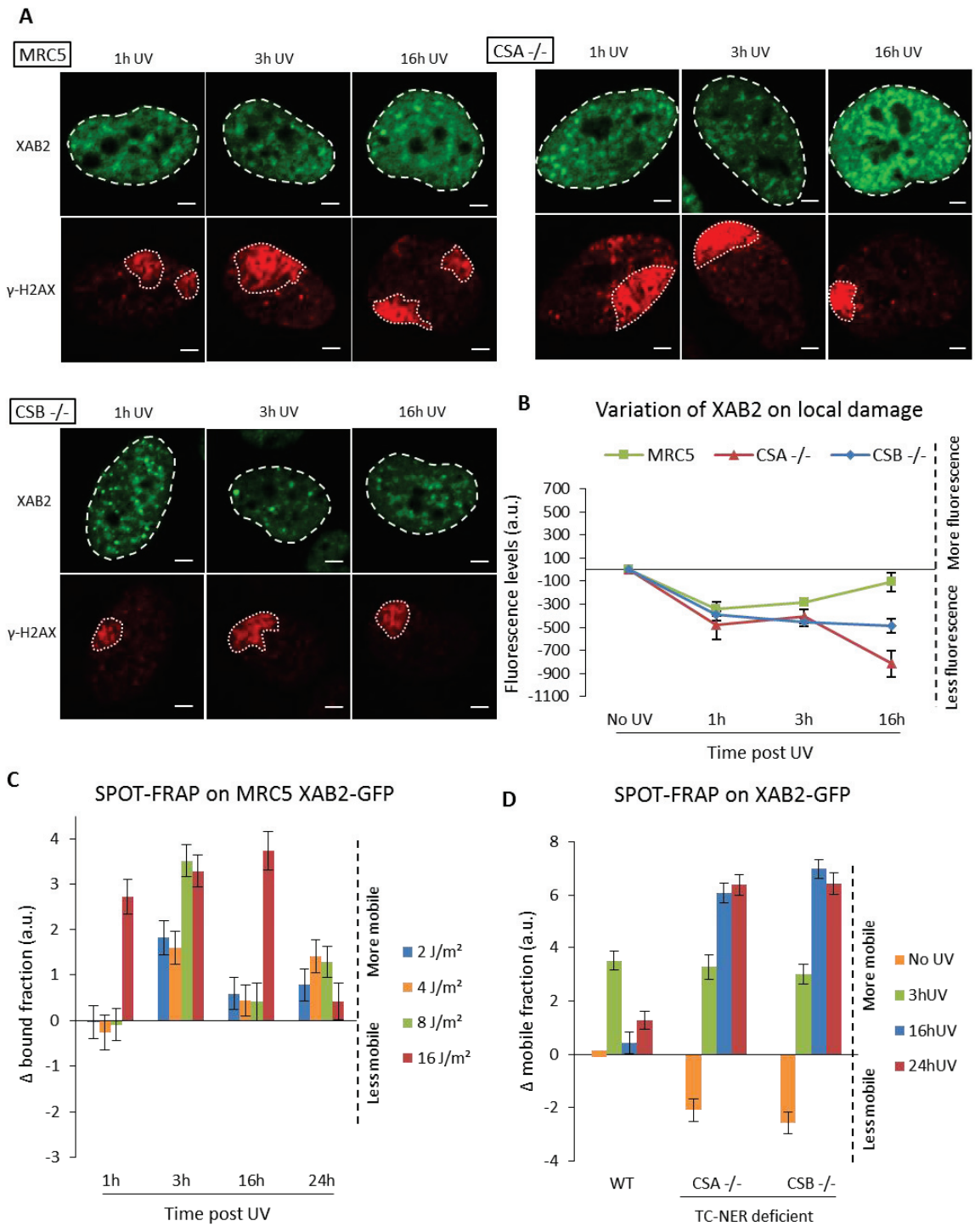

Figure 2. XAB2 dynamic during TC-NER

A) Confocal images of immunofluorescence against XAB2 (green) after local damage induction with UV-C (γ-H2AX staining in red) in different cell lines. Nuclei and LD are indicated by dashed and dotted lines respectively. **B)** Quantification of XAB2-GFP on local damage in different cell lines. Data has been subtracted from the background of each cell. **C)** Dose-response data**.** FRAP analysis of XAB2-GFP expressing cells treated or not with different UV-C doses and at different time points after UV-C exposure. **D)** FRAP analysis of XAB2-GFP expressing cells (WT) and TC-NER deficient XAB2-GFP expressing cells (CSA -/- and CSB -/-) treated or not with UV-C at 8 J/m². Data were calculated with respect to the No UV condition of the WT cell line.

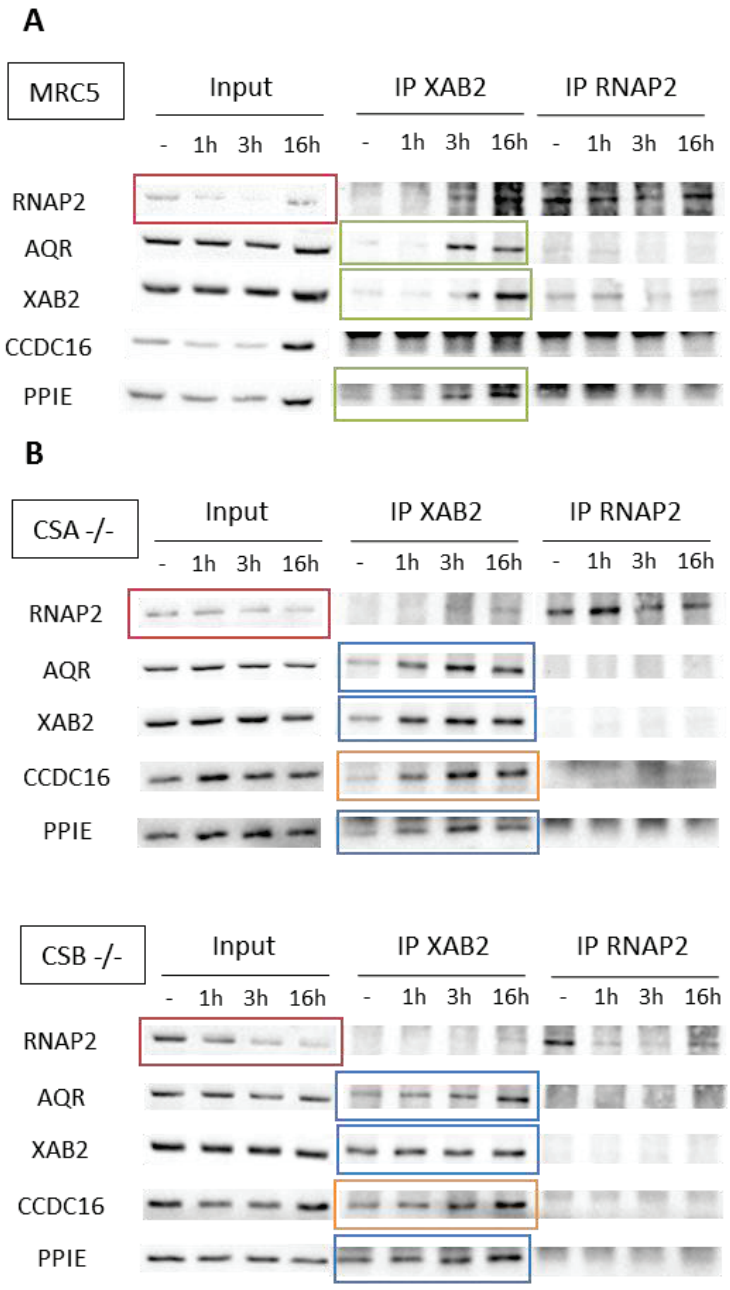

Figure 3. XAB2 pre-mRNA splicing complex during repair
A) Immunoprecipitation of XAB2 and RNAP2 in MRC5 cells nuclear extracts treated or not with UV-C. Bound proteins were revealed by Western blot using antibodies against RNAP2, hAquarius, XAB2, PRP19, CCDC16, PPIE and ISY1. INPUT corresponds to 20% of the lysate used for IP reactions. **B)** Immunoprecipitation of XAB2 and RNAP2 in CSB -/- and CSA -/- cells. Bound proteins were revealed by Western blot using antibodies against RNAP2, hAquarius, XAB2, CCDC16 and PPIE. INPUT corresponds to 20% of the lysate used for IP reactions.

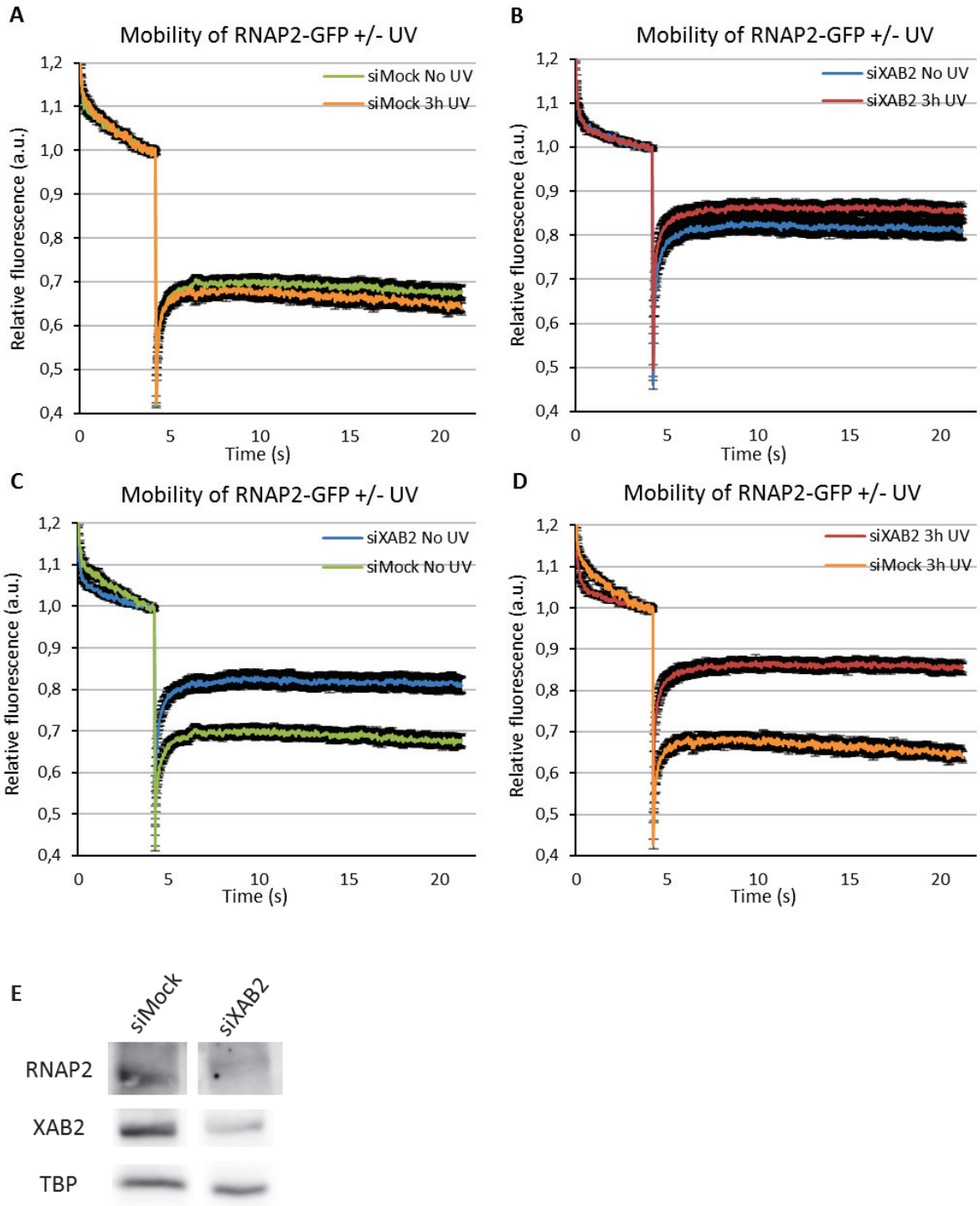

Figure 4. RNAP2 dynamic in absence of XAB2

A) Strip-FRAP analysis of RNAP2-GFP expressing cells treated or not with UV-C after siRNA mediated knockdown of the indicated factors. Each panel **(A, B, C, D)** represents the conditions treated or not with siRNA and/or treated or not with UV-C. **E)** Western Blot on Chromatin Extract of MRC5 treated with siRNA against indicated factors.

Supplementary Information

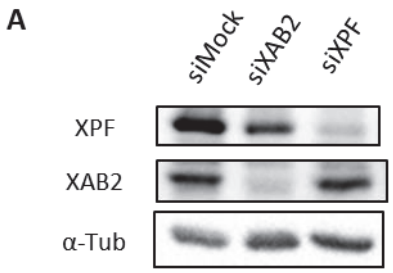

Figure S1.
A) Western Blot on whole cell extracts of cells treated with siRNA against indicated factors

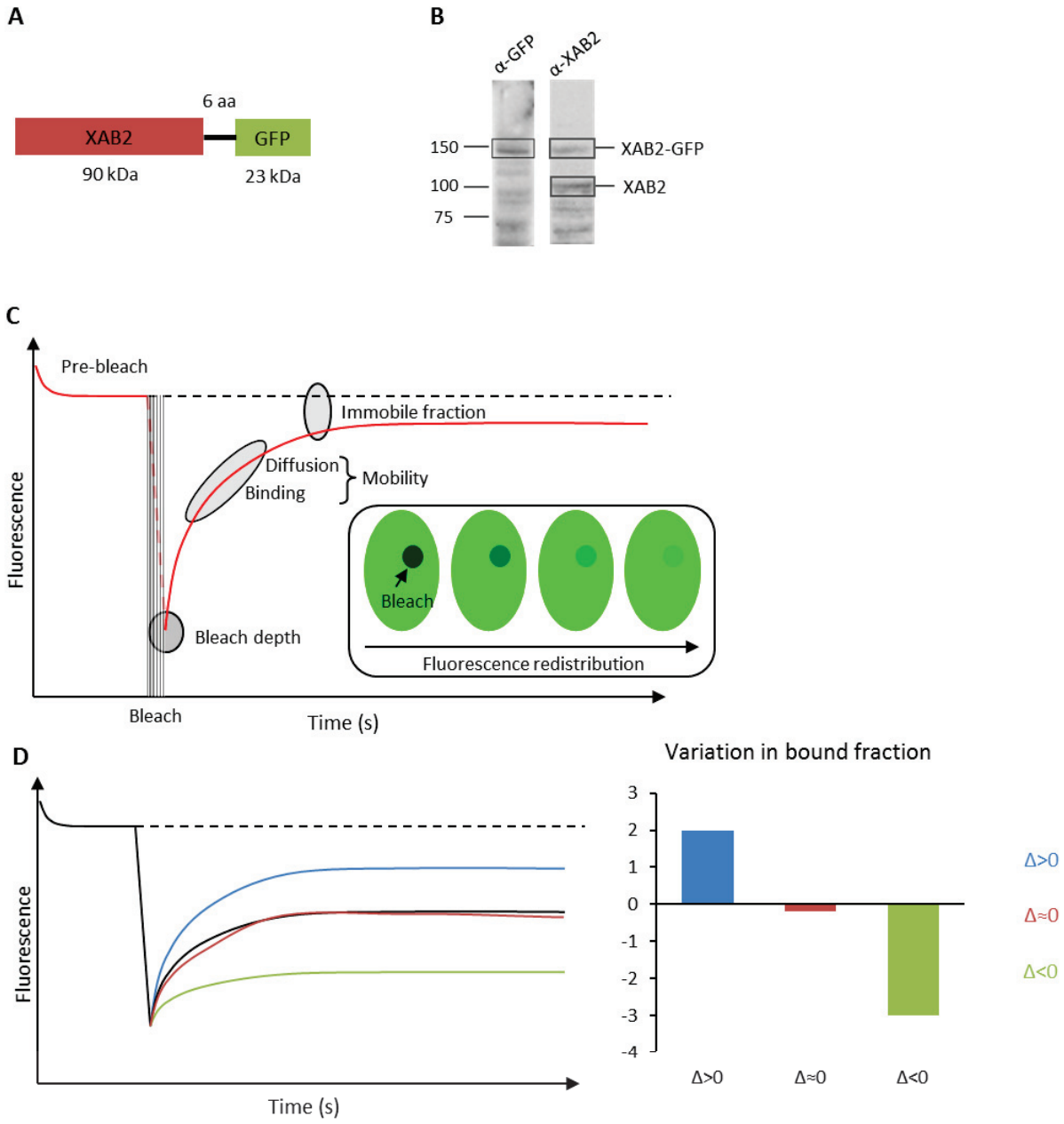

Figure S2.
A) Schematic representation of the XAB2-GFP construct. **B)** Western Blot on whole cell extracts of MRC5 transfected with the XAB2-GFP plasmid. **C)** Schematic representation of the FRAP experiment. **D)** Schematic representation of the calculation method used to represent FRAP data in figures 2C and 2D. The average fluorescence (over all cells) of the No UV condition (black line) was subtracted from the average fluorescence of the UV treated conditions. The obtained difference between the two FRAP curves was then summed point by point, starting from the bleach up to the following 100 measurements i.e. the area between the curve of interest and the untreated condition curve. When proteins have more or less the same mobility, there is no difference (red line), when the protein is more mobile than the control, it results in a positive difference (blue line), when the protein is less mobile, the difference is negative (green line).

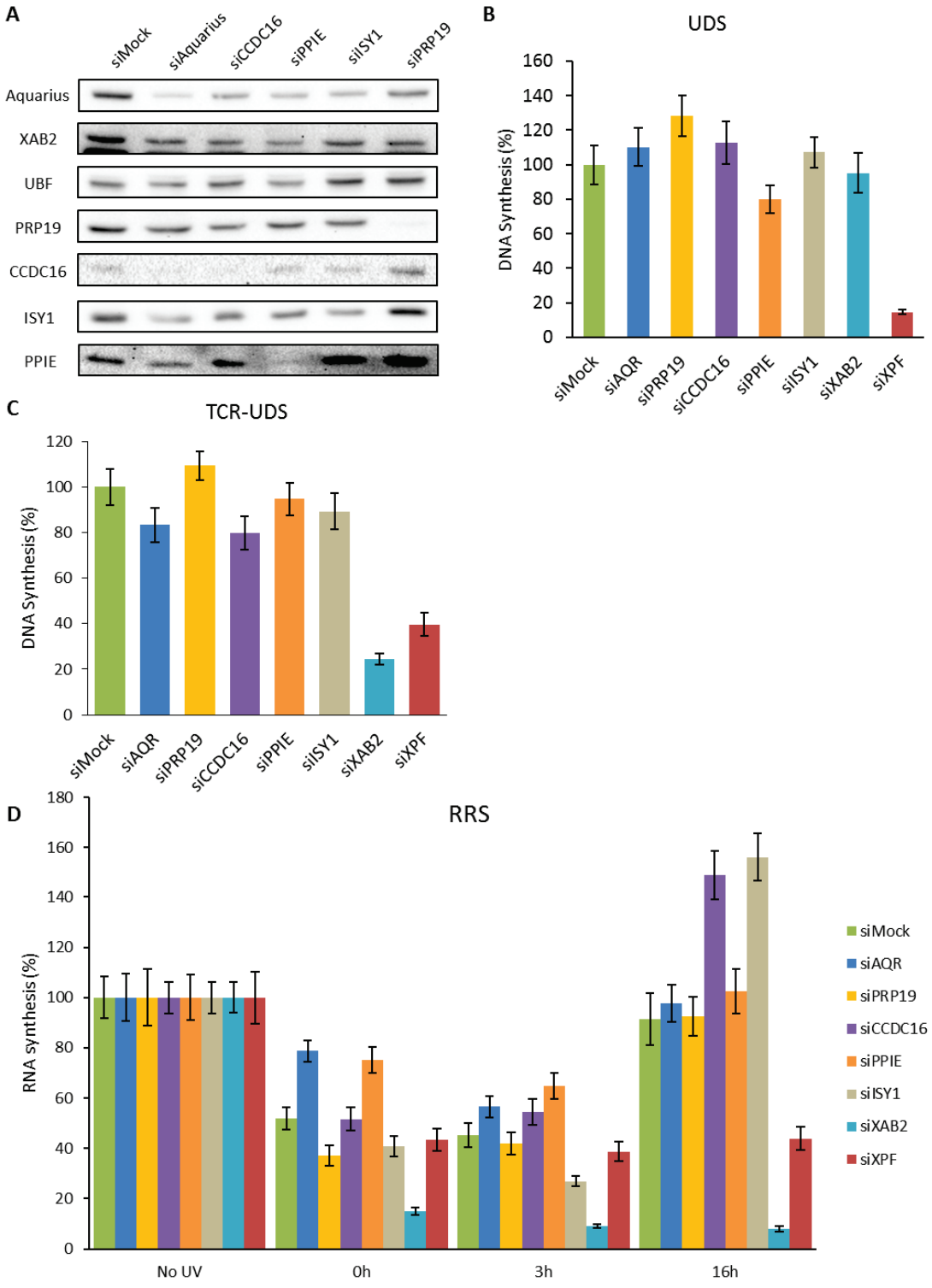

Figure S3.
A) Western Blot on whole cell extracts of cells treated with siRNA against indicated factors. **B)** Unscheduled DNA Synthesis determined by EdU incorporation after local damage induction with UV-C in MRC5 cells treated with siRNAs against indicated factors. **C)** Unscheduled DNA Synthesis determined by EdU incorporation after local damage induction with UV-C in GG-NER deficient cells treated with siRNAs against indicated factors. **D)** RNA Recovery Synthesis determined by EU incorporation after UV-C exposure in MRC5 cells treated with siRNAs against indicated factors

Bibliography

1. Giglia-Mari G, Zotter A, Vermeulen W. DNA damage response. Cold Spring Harb Perspect Biol. 2011;3(1):a000745. doi: 10.1101/cshperspect.a000745. PubMed PMID: 20980439; PubMed Central PMCID: PMCPMC3003462.

2. Kraemer KH, Patronas NJ, Schiffmann R, Brooks BP, Tamura D, DiGiovanna JJ. Xeroderma pigmentosum, trichothiodystrophy and Cockayne syndrome: a complex genotype-phenotype relationship. Neuroscience. 2007;145(4):1388-96. Epub 2007/02/01. doi: 10.1016/j.neuroscience.2006.12.020. PubMed PMID: 17276014; PubMed Central PMCID: PMCPMC2288663.

3. Yonemasu R, Minami M, Nakatsu Y, Takeuchi M, Kuraoka I, Matsuda Y, et al. Disruption of mouse XAB2 gene involved in pre-mRNA splicing, transcription and transcription-coupled DNA repair results in preimplantation lethality. DNA Repair (Amst). 2005;4(4):479-91. Epub 2005/01/19. doi: 10.1016/j.dnarep.2004.12.004. PubMed PMID: 15725628.

4. Nakatsu Y, Asahina H, Citterio E, Rademakers S, Vermeulen W, Kamiuchi S, et al. XAB2, a novel tetratricopeptide repeat protein involved in transcription-coupled DNA repair and transcription. J Biol Chem. 2000;275(45):34931-7. doi: 10.1074/jbc.M004936200. PubMed PMID: 10944529.

5. Kuraoka I, Ito S, Wada T, Hayashida M, Lee L, Saijo M, et al. Isolation of XAB2 complex involved in pre-mRNA splicing, transcription, and transcription-coupled repair. J Biol Chem. 2008;283(2):940-50. Epub 2007/11/02. doi: 10.1074/jbc.M706647200. PubMed PMID: 17981804.

6. Mourgues S, Gautier V, Lagarou A, Bordier C, Mourcet A, Slingerland J, et al. ELL, a novel TFIIH partner, is involved in transcription restart after DNA repair. Proc Natl Acad Sci U S A. 2013;110(44):17927-32. doi: 10.1073/pnas.1305009110. PubMed PMID: 24127601; PubMed Central PMCID: PMCPMC3816466.

7. Daniel L, Cerutti E, Donnio LM, Nonnekens J, Carrat C, Zahova S, et al. Mechanistic insights in transcription-coupled nucleotide excision repair of ribosomal DNA. Proc Natl Acad Sci U S A. 2018;115(29):E6770-E9. Epub 2018/07/02. doi: 10.1073/pnas.1716581115. PubMed PMID: 29967171; PubMed Central PMCID: PMCPMC6055190.

8. Giglia-Mari G, Miquel C, Theil AF, Mari PO, Hoogstraten D, Ng JM, et al. Dynamic interaction of TTDA with TFIIH is stabilized by nucleotide excision repair in living cells. PLoS Biol. 2006;4(6):e156. PubMed PMID: 16669699.

9. Hirose T, Ideue T, Nagai M, Hagiwara M, Shu MD, Steitz JA. A spliceosomal intron binding protein, IBP160, links position-dependent assembly of intron-encoded box C/D snoRNP to pre-mRNA splicing. Mol Cell. 2006;23(5):673-84. doi: 10.1016/j.molcel.2006.07.011. PubMed PMID: 16949364.

10. Chanarat S, Sträßer K. Splicing and beyond: the many faces of the Prp19 complex. Biochim Biophys Acta. 2013;1833(10):2126-34. Epub 2013/06/03. doi: 10.1016/j.bbamcr.2013.05.023. PubMed PMID: 23742842.

11. Matsushima Y, Matsumura K, Kitagawa Y. Zinc finger-like motif conserved in a family of RNA binding proteins. Biosci Biotechnol Biochem. 1997;61(5):905-6. doi: 10.1271/bbb.61.905. PubMed PMID: 9178570.

12. Dix I, Russell C, Yehuda SB, Kupiec M, Beggs JD. The identification and characterization of a novel splicing protein, Isy1p, of Saccharomyces cerevisiae. RNA. 1999;5(3):360-8. PubMed PMID: 10094305; PubMed Central PMCID: PMCPMC1369765.

13. Ben-Yehuda S, Dix I, Russell CS, McGarvey M, Beggs JD, Kupiec M. Genetic and physical interactions between factors involved in both cell cycle progression and pre-mRNA splicing in Saccharomyces cerevisiae. Genetics. 2000;156(4):1503-17. PubMed PMID: 11102353; PubMed Central PMCID: PMCPMC1461362.

14. Shkreta L, Chabot B. The RNA Splicing Response to DNA Damage. Biomolecules. 2015;5(4):2935-77. Epub 2015/10/29. doi: 10.3390/biom5042935. PubMed PMID: 26529031; PubMed Central PMCID: PMCPMC4693264.

CONCLUSIONS AND PERSPECTIVES

During my PhD, we add some molecular pieces to the complex puzzle of the NER repair process and RNA transcription.

First, we demonstrated that a fully functional TC-NER mechanism is required for repair of UV lesions on transcribed ribosomal DNA (187), partially confirming, in human cells, previous studies conducted in yeast. Actually, some differences have been observed, such as the CSB-independent TCR mechanism observed in yeast (188).

Furthermore, we observed that the ribosomal DNA together with RNAP1 is displaced at the periphery of the nucleolus during repair and that rDNA/RNAP1 is relocated within the nucleolus when repair process is completed. This displacement/repositioning process has been previously observed concerning the repair of DSBs on the rDNA (189-191) and DNA replication (192).

Therefore, it seems to be essential for the completion of the repair process allowing some repair protein, excluded from the nucleolus, to access and repair the lesion. We have proposed two factor as responsible for the re-establishment of the proper rDNA position after DNA repair: Nuclear Beta Actin and Nuclear Myosin I. We showed that ACTβ and NMI do not have a role in the repair process and that they are specifically involved in the UV-dependent repositioning mechanism. Furthermore, we provide evidences suggesting that ACTβ and NMI could work synergistically to bind rDNA/RNAP1 and assure its repositioning upon repair.

The two phases of this displacement, exit and re-entry, might imply different proteins set, different interactions with the chromatin or the transcriptional machinery. Different stress conditions might also involve different set of proteins and could be governed by different mechanisms. Furthermore, the proper chromatin position re-establishment may be essential for the cellular viability and in the long term for the organism survival.

For this reason and in light of our results, it will be of great interest to look for other factors involved in the displacement/repositioning mechanism. In order to identify new factors, we will set up an unbiased siRNA bank screening containing proteins involved in transcription, chromatin remodelling and DNA Damage Response and the read-out will be based on RNAP1 immunofluorescence at different time point after UVC exposure. Once new factors will be identified, we will investigate their involvement in basal rRNA transcription and rRNA transcription recovery after DNA damage. Furthermore, we will evaluate whether they can have an impact on the repair process *per se* through the UDS experiment. In complement to the unbiased screening analysis, we will continue to perform the “best candidate approach” and we will determine whether nucleolar proteins such as fibrillarin (193), nucleophosmine (194), etc. are involved into the DNA dependent nucleolar reorganization. Actually, we have already obtained some

preliminary results revealing that the fibrillarin undergoes the same displacement/repositioning mechanism after UVC exposure as the rDNA/RNAP1 complex. Furthermore, we observed, as for ACTβ and NMI, a UV-specific involvement of the fibrillarin in the repositioning phase of rDNA/RNAP1 nucleolar rearrangement.

Furthermore, it could be interesting to analyse the involvement in this process of the Centrin2 protein, an XPC partner, which belongs to a superfamily of Calmodulin proteins, and, together with Calcium, modulate movements in cells (37, 195). Our preliminary results reveal a Centrin2 involvement in rDNA/RNAP1 repositioning, independent from its role in damage recognition and GGR. In addition, we have also observed, for the first time in human fibroblast, that a Calcium depletion affects RNAP1 transcriptional rate. This calcium effect has already been observed for RNAP2 transcription (196), but not for RNAP1 and it would be interesting to investigate its possible role in the nucleolar reorganization.

Concerning RNAP1 mobility, it could be of great interest to follow in time and in living cells, RNAP1 displacement/repositioning movements during rDNA repair and, in the meantime, to observe the reorganization of RNAP1 foci using a super resolution technique, which is already available within the Ciqle microscopy platform.

Another aspect that we would like to analyse in order to answer to many questions regarding the interesting mechanism of rDNA/RNAP1 displacement/repositioning is the composition of the genetic and proteomic environment of the rDNA before, during and after repair. We will set up a CRISPR/Cas9-based purification method that allow the identification of molecules associated with a genomic region of interest in living cells (197). In this technique, called CLASP, catalytically inactive dCas9 is used to purify genomic DNA bound by a guideRNA (gRNA), programmable for different genomic loci. After purification of the locus, molecules associated with the locus can be identified by mass spectrometry, RNA-sequencing and next generation sequencing.

During my thesis, we also work on RNAP2 transcription and the related NER repair process. We demonstrated, in living cells, that the XPA binding protein 2 (XAB2) is involved in the TCR repair mechanism, but not in GGR. Furthermore, we observe that XAB2 dynamic during both transcription and TCR is CSA and CSB-dependent. We partially confirm the presence of XAB2 in a pre-mRNA splicing complex, which was previously observed by Dr. Tanaka's research group (198). Furthermore, our findings demonstrate the involvement of XAB2 in RNAP2 chromatin binding during transcription. This result suggests a role of the XAB2 protein during the pause of transcription by RNAP2.

In order to depict a clearer framework for the XAB2 role in transcription and DNA repair, this work has to be completed with further experiments. It could be interesting to further develop the involvement of XAB2 in the splicing process *per se*, by applying a specific splicing test and by RNA-seq in absence of XAB2. Furthermore, in light of our findings on RNAP2 dynamic, we will evaluate the RNAP2 binding to the chromatin fraction in absence of XAB2 and in XPC cell (GGR deficient). The completion of this study could provide a useful link between transcription, DNA repair and splicing, which could be a piece of the bigger puzzle about the understanding of the markedly different clinical symptoms affecting GGR and TCR-deficient patients, respectively.

BIBLIOGRAPHY

1. Hoeijmakers JH. Genome maintenance mechanisms for preventing cancer. Nature. 2001;411(6835):366-74. Epub 2001/05/18. doi: 10.1038/35077232. PubMed PMID: 11357144.

2. Lindahl T. Instability and decay of the primary structure of DNA. Nature. 1993;362(6422):709-15. doi: 10.1038/362709a0. PubMed PMID: 8469282.

3. Hoeijmakers JH. DNA damage, aging, and cancer. N Engl J Med. 2009;361(15):1475-85. doi: 10.1056/NEJMra0804615. PubMed PMID: 19812404.

4. B. L. Genes VIII2003.

5. Lindahl T, Nyberg B. Rate of depurination of native deoxyribonucleic acid. Biochemistry. 1972;11(19):3610-8. PubMed PMID: 4626532.

6. van Loon B, Markkanen E, Hübscher U. Oxygen as a friend and enemy: How to combat the mutational potential of 8-oxo-guanine. DNA Repair (Amst). 2010;9(6):604-16. doi: 10.1016/j.dnarep.2010.03.004. PubMed PMID: 20399712.

7. Zaludová R, Zákovská A, Kasparková J, Balcarová Z, Kleinwächter V, Vrána O, et al. DNA interactions of bifunctional dinuclear platinum(II) antitumor agents. Eur J Biochem. 1997;246(2):508-17. PubMed PMID: 9208945.

8. Fu D, Calvo JA, Samson LD. Balancing repair and tolerance of DNA damage caused by alkylating agents. Nat Rev Cancer. 2012;12(2):104-20. Epub 2012/01/12. doi: 10.1038/nrc3185. PubMed PMID: 22237395; PubMed Central PMCID: PMCPMC3586545.

9. Lindahl T, Barnes DE. Repair of endogenous DNA damage. Cold Spring Harb Symp Quant Biol. 2000;65:127-33. PubMed PMID: 12760027.

10. Cannan WJ, Pederson DS. Mechanisms and Consequences of Double-Strand DNA Break Formation in Chromatin. J Cell Physiol. 2016;231(1):3-14. doi: 10.1002/jcp.25048. PubMed PMID: 26040249; PubMed Central PMCID: PMCPMC4994891.

11. Vilenchik MM, Knudson AG. Endogenous DNA double-strand breaks: production, fidelity of repair, and induction of cancer. Proc Natl Acad Sci U S A. 2003;100(22):12871-6. Epub 2003/10/17. doi: 10.1073/pnas.2135498100. PubMed PMID: 14566050; PubMed Central PMCID: PMCPMC240711.

12. Zhou BB, Elledge SJ. The DNA damage response: putting checkpoints in perspective. Nature. 2000;408(6811):433-9. doi: 10.1038/35044005. PubMed PMID: 11100718.

13. Whitaker AM, Schaich MA, Smith MR, Flynn TS, Freudenthal BD. Base excision repair of oxidative DNA damage: from mechanism to disease. Front Biosci (Landmark Ed). 2017;22:1493-522. Epub 2017/03/01. PubMed PMID: 28199214; PubMed Central PMCID: PMCPMC5567671.

14. Krokan HE, Bjørås M. Base excision repair. Cold Spring Harb Perspect Biol. 2013;5(4):a012583. Epub 2013/04/01. doi: 10.1101/cshperspect.a012583. PubMed PMID: 23545420; PubMed Central PMCID: PMCPMC3683898.

15. Jiricny J. The multifaceted mismatch-repair system. Nat Rev Mol Cell Biol. 2006;7(5):335-46. doi: 10.1038/nrm1907. PubMed PMID: 16612326.

16. Bak ST, Sakellariou D, Pena-Diaz J. The dual nature of mismatch repair as antimutator and mutator: for better or for worse. Front Genet. 2014;5:287. Epub 2014/08/21. doi: 10.3389/fgene.2014.00287. PubMed PMID: 25191341; PubMed Central PMCID: PMCPMC4139959.

17. Jasin M, Rothstein R. Repair of strand breaks by homologous recombination. Cold Spring Harb Perspect Biol. 2013;5(11):a012740. Epub 2013/11/01. doi: 10.1101/cshperspect.a012740. PubMed PMID: 24097900; PubMed Central PMCID: PMCPMC3809576.

18. Mladenov E, Magin S, Soni A, Iliakis G. DNA double-strand-break repair in higher eukaryotes and its role in genomic instability and cancer: Cell cycle and proliferation-dependent regulation. Semin Cancer Biol. 2016;37-38:51-64. Epub 2016/03/22. doi: 10.1016/j.semcancer.2016.03.003. PubMed PMID: 27016036.

19. Wright WD, Shah SS, Heyer WD. Homologous recombination and the repair of DNA double-strand breaks. J Biol Chem. 2018;293(27):10524-35. Epub 2018/03/29. doi: 10.1074/jbc.TM118.000372. PubMed PMID: 29599286; PubMed Central PMCID: PMCPMC6036207.

20. Bhargava R, Onyango DO, Stark JM. Regulation of Single-Strand Annealing and its Role in Genome Maintenance. Trends Genet. 2016;32(9):566-75. Epub 2016/07/19. doi: 10.1016/j.tig.2016.06.007. PubMed PMID: 27450436; PubMed Central PMCID: PMCPMC4992407.

21. Davis AJ, Chen DJ. DNA double strand break repair via non-homologous end-joining. Transl Cancer Res. 2013;2(3):130-43. doi: 10.3978/j.issn.2218-676X.2013.04.02. PubMed PMID: 24000320; PubMed Central PMCID: PMCPMC3758668.

22. Chang HHY, Pannunzio NR, Adachi N, Lieber MR. Non-homologous DNA end joining and alternative pathways to double-strand break repair. Nat Rev Mol Cell Biol. 2017;18(8):495-506. Epub 2017/05/17. doi: 10.1038/nrm.2017.48. PubMed PMID: 28512351.

23. BOYCE RP, HOWARD-FLANDERS P. RELEASE OF ULTRAVIOLET LIGHT-INDUCED THYMINE DIMERS FROM DNA IN E. COLI K-12. Proc Natl Acad Sci U S A. 1964;51:293-300. PubMed PMID: 14124327; PubMed Central PMCID: PMCPMC300064.

24. PETTIJOHN D, HANAWALT P. EVIDENCE FOR REPAIR-REPLICATION OF ULTRAVIOLET DAMAGED DNA IN BACTERIA. J Mol Biol. 1964;9:395-410. PubMed PMID: 14202275.

25. SETLOW RB, CARRIER WL. THE DISAPPEARANCE OF THYMINE DIMERS FROM DNA: AN ERROR-CORRECTING MECHANISM. Proc Natl Acad Sci U S A. 1964;51:226-31. PubMed PMID: 14124320; PubMed Central PMCID: PMCPMC300053.

26. Menoni H, Hoeijmakers JH, Vermeulen W. Nucleotide excision repair-initiating proteins bind to oxidative DNA lesions in vivo. The Journal of cell biology. 2012;199(7):1037-46. Epub 2012/12/21. doi: 10.1083/jcb.201205149. PubMed PMID: 23253478; PubMed Central PMCID: PMC3529521.

27. Wood RD. Mammalian nucleotide excision repair proteins and interstrand crosslink repair. Environ Mol Mutagen. 2010;51(6):520-6. doi: 10.1002/em.20569. PubMed PMID: 20658645; PubMed Central PMCID: PMCPMC3017513.

28. Spivak G. Nucleotide excision repair in humans. DNA Repair (Amst). 2015;36:13-8. Epub 2015/09/10. doi: 10.1016/j.dnarep.2015.09.003. PubMed PMID: 26388429; PubMed Central PMCID: PMCPMC4688078.

29. de Laat WL, Jaspers NG, Hoeijmakers JH. Molecular mechanism of nucleotide excision repair. Genes Dev. 1999;13(7):768-85. PubMed PMID: 10197977.

30. Reardon JT, Sancar A. Recognition and repair of the cyclobutane thymine dimer, a major cause of skin cancers, by the human excision nuclease. Genes Dev. 2003;17(20):2539-51. Epub 2003/10/01. doi: 10.1101/gad.1131003. PubMed PMID: 14522951; PubMed Central PMCID: PMCPMC218148.

31. Tang JY, Hwang BJ, Ford JM, Hanawalt PC, Chu G. Xeroderma pigmentosum p48 gene enhances global genomic repair and suppresses UV-induced mutagenesis. Mol Cell. 2000;5(4):737-44. PubMed PMID: 10882109; PubMed Central PMCID: PMCPMC2894271.

32. Scrima A, Konícková R, Czyzewski BK, Kawasaki Y, Jeffrey PD, Groisman R, et al. Structural basis of UV DNA-damage recognition by the DDB1-DDB2 complex. Cell. 2008;135(7):1213-23. doi: 10.1016/j.cell.2008.10.045. PubMed PMID: 19109893; PubMed Central PMCID: PMCPMC2676164.

33. Schärer OD, Campbell AJ. Wedging out DNA damage. Nat Struct Mol Biol. 2009;16(2):102-4. doi: 10.1038/nsmb0209-102. PubMed PMID: 19190661; PubMed Central PMCID: PMCPMC2745198.

34. Mu H, Zhang Y, Geacintov NE, Broyde S. Lesion Sensing during Initial Binding by Yeast XPC/Rad4: Toward Predicting Resistance to Nucleotide Excision Repair. Chem Res Toxicol. 2018;31(11):1260-8. Epub 2018/10/22. doi: 10.1021/acs.chemrestox.8b00231. PubMed PMID: 30284444; PubMed Central PMCID: PMCPMC6247245.

35. Ng JM, Vermeulen W, van der Horst GT, Bergink S, Sugasawa K, Vrieling H, et al. A novel regulation mechanism of DNA repair by damage-induced and RAD23-dependent stabilization of xeroderma pigmentosum group C protein. Genes Dev. 2003;17(13):1630-45. Epub 2003/06/18. doi: 10.1101/gad.260003. PubMed PMID: 12815074; PubMed Central PMCID: PMCPMC196135.

36. Bergink S, Toussaint W, Luijsterburg MS, Dinant C, Alekseev S, Hoeijmakers JH, et al. Recognition of DNA damage by XPC coincides with disruption of the XPC-RAD23 complex. J Cell Biol. 2012;196(6):681-8. doi: 10.1083/jcb.201107050. PubMed PMID: 22431748; PubMed Central PMCID: PMCPMC3308700.

37. Nishi R, Okuda Y, Watanabe E, Mori T, Iwai S, Masutani C, et al. Centrin 2 stimulates nucleotide excision repair by interacting with xeroderma pigmentosum group C protein. Mol Cell Biol. 2005;25(13):5664-74. doi: 10.1128/MCB.25.13.5664-5674.2005. PubMed PMID: 15964821; PubMed Central PMCID: PMCPMC1156980.

38. Nishi R, Sakai W, Tone D, Hanaoka F, Sugasawa K. Structure-function analysis of the EF-hand protein centrin-2 for its intracellular localization and nucleotide excision repair. Nucleic Acids Res. 2013;41(14):6917-29. Epub 2013/05/28. doi: 10.1093/nar/gkt434. PubMed PMID: 23716636; PubMed Central PMCID: PMCPMC3737541.

39. Okuda M, Kinoshita M, Kakumu E, Sugasawa K, Nishimura Y. Structural Insight into the Mechanism of TFIIH Recognition by the Acidic String of the Nucleotide Excision Repair Factor XPC. Structure. 2015;23(10):1827-37. Epub 2015/08/13. doi: 10.1016/j.str.2015.07.009. PubMed PMID: 26278177.

40. Spivak G. Transcription-coupled repair: an update. Arch Toxicol. 2016;90(11):2583-94. Epub 2016/08/22. doi: 10.1007/s00204-016-1820-x. PubMed PMID: 27549370; PubMed Central PMCID: PMCPMC5065778.

41. Sarker AH, Tsutakawa SE, Kostek S, Ng C, Shin DS, Peris M, et al. Recognition of RNA polymerase II and transcription bubbles by XPG, CSB, and TFIIH: insights for transcription-coupled repair and Cockayne Syndrome. Mol Cell. 2005;20(2):187-98. doi: 10.1016/j.molcel.2005.09.022. PubMed PMID: 16246722.

42. Charlet-Berguerand N, Feuerhahn S, Kong SE, Ziserman H, Conaway JW, Conaway R, et al. RNA polymerase II bypass of oxidative DNA damage is regulated by transcription elongation factors. EMBO J. 2006;25(23):5481-91. Epub 2006/11/16. doi: 10.1038/sj.emboj.7601403. PubMed PMID: 17110932; PubMed Central PMCID: PMCPMC1679758.

43. Saxowsky TT, Meadows KL, Klungland A, Doetsch PW. 8-Oxoguanine-mediated transcriptional mutagenesis causes Ras activation in mammalian cells. Proc Natl Acad Sci U S A. 2008;105(48):18877-82. Epub 2008/11/19. doi: 10.1073/pnas.0806464105. PubMed PMID: 19020090; PubMed Central PMCID: PMCPMC2596238.

44. Harreman M, Taschner M, Sigurdsson S, Anindya R, Reid J, Somesh B, et al. Distinct ubiquitin ligases act sequentially for RNA polymerase II polyubiquitylation. Proc Natl Acad Sci U S A. 2009;106(49):20705-10. Epub 2009/11/17. doi: 10.1073/pnas.0907052106. PubMed PMID: 19920177; PubMed Central PMCID: PMCPMC2778569.

45. Tornaletti S, Reines D, Hanawalt PC. Structural characterization of RNA polymerase II complexes arrested by a cyclobutane pyrimidine dimer in the transcribed strand of template DNA. J Biol Chem. 1999;274(34):24124-30. PubMed PMID: 10446184; PubMed Central PMCID: PMCPMC3371614.

46. Hanawalt PC, Spivak G. Transcription-coupled DNA repair: two decades of progress and surprises. Nat Rev Mol Cell Biol. 2008;9(12):958-70. doi: 10.1038/nrm2549. PubMed PMID: 19023283.

47. Lans H, Marteijn JA, Vermeulen W. ATP-dependent chromatin remodeling in the DNA-damage response. Epigenetics Chromatin. 2012;5:4. Epub 2012/01/30. doi: 10.1186/1756-8935-5-4. PubMed PMID: 22289628; PubMed Central PMCID: PMCPMC3275488.

48. Chiou YY, Hu J, Sancar A, Selby CP. RNA polymerase II is released from the DNA template during transcription-coupled repair in mammalian cells. J Biol Chem. 2018;293(7):2476-86. Epub 2017/12/27. doi: 10.1074/jbc.RA117.000971. PubMed PMID: 29282293; PubMed Central PMCID: PMCPMC5818198.

49. Beerens N, Hoeijmakers JH, Kanaar R, Vermeulen W, Wyman C. The CSB protein actively wraps DNA. J Biol Chem. 2005;280(6):4722-9. Epub 2004/11/16. doi: 10.1074/jbc.M409147200. PubMed PMID: 15548521.

50. Selby CP, Sancar A. Cockayne syndrome group B protein enhances elongation by RNA polymerase II. Proc Natl Acad Sci U S A. 1997;94(21):11205-9. PubMed PMID: 9326587; PubMed Central PMCID: PMCPMC23417.

51. Sin Y, Tanaka K, Saijo M. The C-terminal Region and SUMOylation of Cockayne Syndrome Group B Protein Play Critical Roles in Transcription-coupled Nucleotide Excision Repair. J Biol Chem. 2016;291(3):1387-97. Epub 2015/11/30. doi: 10.1074/jbc.M115.683235. PubMed PMID: 26620705; PubMed Central PMCID: PMCPMC4714222.

52. Iyama T, Wilson DM. Elements That Regulate the DNA Damage Response of Proteins Defective in Cockayne Syndrome. J Mol Biol. 2016;428(1):62-78. Epub 2015/11/23. doi: 10.1016/j.jmb.2015.11.020. PubMed PMID: 26616585; PubMed Central PMCID: PMCPMC4738086.

53. Groisman R, Polanowska J, Kuraoka I, Sawada J, Saijo M, Drapkin R, et al. The ubiquitin ligase activity in the DDB2 and CSA complexes is differentially regulated by the COP9 signalosome in response to DNA damage. Cell. 2003;113(3):357-67. PubMed PMID: 12732143.

54. Brooks PJ. Blinded by the UV light: how the focus on transcription-coupled NER has distracted from understanding the mechanisms of Cockayne syndrome neurologic disease. DNA Repair (Amst). 2013;12(8):656-71. Epub 2013/05/16. doi: 10.1016/j.dnarep.2013.04.018. PubMed PMID: 23683874; PubMed Central PMCID: PMCPMC4240003.

55. Fei J, Chen J. KIAA1530 protein is recruited by Cockayne syndrome complementation group protein A (CSA) to participate in transcription-coupled repair (TCR). J Biol Chem. 2012;287(42):35118-26. Epub 2012/08/17. doi: 10.1074/jbc.M112.398131. PubMed PMID: 22902626; PubMed Central PMCID: PMCPMC3471710.

56. Nakazawa Y, Sasaki K, Mitsutake N, Matsuse M, Shimada M, Nardo T, et al. Mutations in UVSSA cause UV-sensitive syndrome and impair RNA polymerase IIo processing in transcription-

coupled nucleotide-excision repair. Nat Genet. 2012;44(5):586-92. doi: 10.1038/ng.2229. PubMed PMID: 22466610.

57. Schwertman P, Lagarou A, Dekkers DH, Raams A, van der Hoek AC, Laffeber C, et al. UV-sensitive syndrome protein UVSSA recruits USP7 to regulate transcription-coupled repair. Nat Genet. 2012;44(5):598-602. doi: 10.1038/ng.2230. PubMed PMID: 22466611.

58. Zhang X, Horibata K, Saijo M, Ishigami C, Ukai A, Kanno S, et al. Mutations in UVSSA cause UV-sensitive syndrome and destabilize ERCC6 in transcription-coupled DNA repair. Nat Genet. 2012;44(5):593-7. doi: 10.1038/ng.2228. PubMed PMID: 22466612.

59. Okuda M, Nakazawa Y, Guo C, Ogi T, Nishimura Y. Common TFIIH recruitment mechanism in global genome and transcription-coupled repair subpathways. Nucleic Acids Res. 2017;45(22):13043-55. doi: 10.1093/nar/gkx970. PubMed PMID: 29069470; PubMed Central PMCID: PMCPMC5727438.

60. Giglia-Mari G, Miquel C, Theil AF, Mari PO, Hoogstraten D, Ng JM, et al. Dynamic interaction of TTDA with TFIIH is stabilized by nucleotide excision repair in living cells. PLoS Biol. 2006;4(6):e156. PubMed PMID: 16669699.

61. Mathieu N, Kaczmarek N, Rüthemann P, Luch A, Naegeli H. DNA quality control by a lesion sensor pocket of the xeroderma pigmentosum group D helicase subunit of TFIIH. Curr Biol. 2013;23(3):204-12. Epub 2013/01/24. doi: 10.1016/j.cub.2012.12.032. PubMed PMID: 23352696.

62. Coin F, Oksenych V, Mocquet V, Groh S, Blattner C, Egly JM. Nucleotide excision repair driven by the dissociation of CAK from TFIIH. Mol Cell. 2008;31(1):9-20. doi: 10.1016/j.molcel.2008.04.024. PubMed PMID: 18614043.

63. Schärer OD. Nucleotide excision repair in eukaryotes. Cold Spring Harb Perspect Biol. 2013;5(10):a012609. Epub 2013/10/01. doi: 10.1101/cshperspect.a012609. PubMed PMID: 24086042; PubMed Central PMCID: PMCPMC3783044.

64. Nakatsu Y, Asahina H, Citterio E, Rademakers S, Vermeulen W, Kamiuchi S, et al. XAB2, a novel tetratricopeptide repeat protein involved in transcription-coupled DNA repair and transcription. J Biol Chem. 2000;275(45):34931-7. doi: 10.1074/jbc.M004936200. PubMed PMID: 10944529.

65. Fagbemi AF, Orelli B, Schärer OD. Regulation of endonuclease activity in human nucleotide excision repair. DNA Repair (Amst). 2011;10(7):722-9. Epub 2011/05/17. doi: 10.1016/j.dnarep.2011.04.022. PubMed PMID: 21592868; PubMed Central PMCID: PMCPMC3139800.

66. Ogi T, Limsirichaikul S, Overmeer RM, Volker M, Takenaka K, Cloney R, et al. Three DNA polymerases, recruited by different mechanisms, carry out NER repair synthesis in human cells. Mol Cell. 2010;37(5):714-27. doi: 10.1016/j.molcel.2010.02.009. PubMed PMID: 20227374.

67. Overmeer RM, Gourdin AM, Giglia-Mari A, Kool H, Houtsmuller AB, Siegal G, et al. Replication factor C recruits DNA polymerase delta to sites of nucleotide excision repair but is not required for PCNA recruitment. Mol Cell Biol. 2010;30(20):4828-39. Epub 2010/08/16. doi: 10.1128/MCB.00285-10. PubMed PMID: 20713449; PubMed Central PMCID: PMCPMC2950542.

68. Lehmann AR. DNA polymerases and repair synthesis in NER in human cells. DNA Repair (Amst). 2011;10(7):730-3. Epub 2011/05/20. doi: 10.1016/j.dnarep.2011.04.023. PubMed PMID: 21601536.

69. Mourgues S, Gautier V, Lagarou A, Bordier C, Mourcet A, Slingerland J, et al. ELL, a novel TFIIH partner, is involved in transcription restart after DNA repair. Proc Natl Acad Sci U S A. 2013;110(44):17927-32. doi: 10.1073/pnas.1305009110. PubMed PMID: 24127601; PubMed Central PMCID: PMCPMC3816466.

70. Dutta A, Babbarwal V, Fu J, Brunke-Reese D, Libert DM, Willis J, et al. Ccr4-Not and TFIIS Function Cooperatively To Rescue Arrested RNA Polymerase II. Mol Cell Biol. 2015;35(11):1915-25. Epub 2015/03/16. doi: 10.1128/MCB.00044-15. PubMed PMID: 25776559; PubMed Central PMCID: PMCPMC4420917.

71. Oksenych V, Zhovmer A, Ziani S, Mari PO, Eberova J, Nardo T, et al. Histone methyltransferase DOT1L drives recovery of gene expression after a genotoxic attack. PLoS Genet. 2013;9(7):e1003611. doi: 10.1371/journal.pgen.1003611. PubMed PMID: 23861670; PubMed Central PMCID: PMCPMC3701700.

72. Andrade-Lima LC, Veloso A, Ljungman M. Transcription Blockage Leads to New Beginnings. Biomolecules. 2015;5(3):1600-17. Epub 2015/07/21. doi: 10.3390/biom5031600. PubMed PMID: 26197343; PubMed Central PMCID: PMCPMC4598766.

73. de Boer J, Hoeijmakers JH. Nucleotide excision repair and human syndromes. Carcinogenesis. 2000;21(3):453-60. Epub 2000/02/26. PubMed PMID: 10688865.

74. Kraemer KH, Patronas NJ, Schiffmann R, Brooks BP, Tamura D, DiGiovanna JJ. Xeroderma pigmentosum, trichothiodystrophy and Cockayne syndrome: a complex genotype-phenotype relationship. Neuroscience. 2007;145(4):1388-96. Epub 2007/02/01. doi: 10.1016/j.neuroscience.2006.12.020. PubMed PMID: 17276014; PubMed Central PMCID: PMCPMC2288663.

75. Smerdon MJ, Lieberman MW. Nucleosome rearrangement in human chromatin during UV-induced DNA- reapir synthesis. Proc Natl Acad Sci U S A. 1978;75(9):4238-41. PubMed PMID: 279912; PubMed Central PMCID: PMCPMC336087.

76. Peterson CL, Almouzni G. Nucleosome dynamics as modular systems that integrate DNA damage and repair. Cold Spring Harb Perspect Biol. 2013;5(9). Epub 2013/09/01. doi: 10.1101/cshperspect.a012658. PubMed PMID: 24003210; PubMed Central PMCID: PMCPMC3753706.

77. Soria G, Polo SE, Almouzni G. Prime, repair, restore: the active role of chromatin in the DNA damage response. Mol Cell. 2012;46(6):722-34. doi: 10.1016/j.molcel.2012.06.002. PubMed PMID: 22749398.

78. Jiang Y, Wang X, Bao S, Guo R, Johnson DG, Shen X, et al. INO80 chromatin remodeling complex promotes the removal of UV lesions by the nucleotide excision repair pathway. Proc Natl Acad Sci U S A. 2010;107(40):17274-9. Epub 2010/09/20. doi: 10.1073/pnas.1008388107. PubMed PMID: 20855601; PubMed Central PMCID: PMCPMC2951448.

79. Zhao Q, Wang QE, Ray A, Wani G, Han C, Milum K, et al. Modulation of nucleotide excision repair by mammalian SWI/SNF chromatin-remodeling complex. J Biol Chem. 2009;284(44):30424-32. Epub 2009/09/08. doi: 10.1074/jbc.M109.044982. PubMed PMID: 19740755; PubMed Central PMCID: PMCPMC2781597.

80. Luijsterburg MS, Dinant C, Lans H, Stap J, Wiernasz E, Lagerwerf S, et al. Heterochromatin protein 1 is recruited to various types of DNA damage. J Cell Biol. 2009;185(4):577-86. doi: 10.1083/jcb.200810035. PubMed PMID: 19451271; PubMed Central PMCID: PMCPMC2711568.

81. Polo SE, Roche D, Almouzni G. New histone incorporation marks sites of UV repair in human cells. Cell. 2006;127(3):481-93. doi: 10.1016/j.cell.2006.08.049. PubMed PMID: 17081972.

82. Adam S, Polo SE, Almouzni G. Transcription Recovery after DNA Damage Requires Chromatin Priming by the H3.3 Histone Chaperone HIRA. Cell. 2013;155(1):94-106. Epub 2013/10/01. doi: 10.1016/j.cell.2013.08.029. PubMed PMID: 24074863.

83. Bushnell DA, Kornberg RD. Complete, 12-subunit RNA polymerase II at 4.1-A resolution: implications for the initiation of transcription. Proc Natl Acad Sci U S A. 2003;100(12):6969-73.

Epub 2003/05/13. doi: 10.1073/pnas.1130601100. PubMed PMID: 12746498; PubMed Central PMCID: PMCPMC165814.

84. Armache KJ, Kettenberger H, Cramer P. Architecture of initiation-competent 12-subunit RNA polymerase II. Proc Natl Acad Sci U S A. 2003;100(12):6964-8. Epub 2003/05/13. doi: 10.1073/pnas.1030608100. PubMed PMID: 12746495; PubMed Central PMCID: PMCPMC165813.

85. Dahmus ME. Phosphorylation of the C-terminal domain of RNA polymerase II. Biochim Biophys Acta. 1995;1261(2):171-82. PubMed PMID: 7711060.

86. Bentley D. The mRNA assembly line: transcription and processing machines in the same factory. Curr Opin Cell Biol. 2002;14(3):336-42. PubMed PMID: 12067656.

87. Gershenzon NI, Ioshikhes IP. Synergy of human Pol II core promoter elements revealed by statistical sequence analysis. Bioinformatics. 2005;21(8):1295-300. Epub 2004/11/30. doi: 10.1093/bioinformatics/bti172. PubMed PMID: 15572469.

88. Smale ST, Kadonaga JT. The RNA polymerase II core promoter. Annu Rev Biochem. 2003;72:449-79. Epub 2003/03/19. doi: 10.1146/annurev.biochem.72.121801.161520. PubMed PMID: 12651739.

89. Hahn S. Structure and mechanism of the RNA polymerase II transcription machinery. Nat Struct Mol Biol. 2004;11(5):394-403. doi: 10.1038/nsmb763. PubMed PMID: 15114340; PubMed Central PMCID: PMCPMC1189732.

90. He Y, Fang J, Taatjes DJ, Nogales E. Structural visualization of key steps in human transcription initiation. Nature. 2013;495(7442):481-6. Epub 2013/02/27. doi: 10.1038/nature11991. PubMed PMID: 23446344; PubMed Central PMCID: PMCPMC3612373.

91. Kim YJ, Björklund S, Li Y, Sayre MH, Kornberg RD. A multiprotein mediator of transcriptional activation and its interaction with the C-terminal repeat domain of RNA polymerase II. Cell. 1994;77(4):599-608. PubMed PMID: 8187178.

92. Murakami KS, Masuda S, Campbell EA, Muzzin O, Darst SA. Structural basis of transcription initiation: an RNA polymerase holoenzyme-DNA complex. Science. 2002;296(5571):1285-90. doi: 10.1126/science.1069595. PubMed PMID: 12016307.

93. Coin F, Bergmann E, Tremeau-Bravard A, Egly JM. Mutations in XPB and XPD helicases found in xeroderma pigmentosum patients impair the transcription function of TFIIH. EMBO J. 1999;18(5):1357-66. doi: 10.1093/emboj/18.5.1357. PubMed PMID: 10064601; PubMed Central PMCID: PMCPMC1171225.

94. Liu X, Bushnell DA, Kornberg RD. RNA polymerase II transcription: structure and mechanism. Biochim Biophys Acta. 2013;1829(1):2-8. Epub 2012/09/18. doi: 10.1016/j.bbagrm.2012.09.003. PubMed PMID: 23000482; PubMed Central PMCID: PMCPMC4244541.

95. Ohkuma Y, Roeder RG. Regulation of TFIIH ATPase and kinase activities by TFIIE during active initiation complex formation. Nature. 1994;368(6467):160-3. doi: 10.1038/368160a0. PubMed PMID: 8166891.

96. Bentley DL. Coupling mRNA processing with transcription in time and space. Nat Rev Genet. 2014;15(3):163-75. Epub 2014/02/11. doi: 10.1038/nrg3662. PubMed PMID: 24514444; PubMed Central PMCID: PMCPMC4304646.

97. Lei L, Ren D, Burton ZF. The RAP74 subunit of human transcription factor IIF has similar roles in initiation and elongation. Mol Cell Biol. 1999;19(12):8372-82. PubMed PMID: 10567562; PubMed Central PMCID: PMCPMC84928.

98. Yamaguchi Y, Takagi T, Wada T, Yano K, Furuya A, Sugimoto S, et al. NELF, a multisubunit complex containing RD, cooperates with DSIF to repress RNA polymerase II elongation. Cell. 1999;97(1):41-51. PubMed PMID: 10199401.

99. Peng J, Marshall NF, Price DH. Identification of a cyclin subunit required for the function of Drosophila P-TEFb. J Biol Chem. 1998;273(22):13855-60. PubMed PMID: 9593731.

100. Marshall NF, Peng J, Xie Z, Price DH. Control of RNA polymerase II elongation potential by a novel carboxyl-terminal domain kinase. J Biol Chem. 1996;271(43):27176-83. PubMed PMID: 8900211.

101. Fujinaga K, Irwin D, Huang Y, Taube R, Kurosu T, Peterlin BM. Dynamics of human immunodeficiency virus transcription: P-TEFb phosphorylates RD and dissociates negative effectors from the transactivation response element. Mol Cell Biol. 2004;24(2):787-95. PubMed PMID: 14701750; PubMed Central PMCID: PMCPMC343783.

102. Yamada T, Yamaguchi Y, Inukai N, Okamoto S, Mura T, Handa H. P-TEFb-mediated phosphorylation of hSpt5 C-terminal repeats is critical for processive transcription elongation. Mol Cell. 2006;21(2):227-37. doi: 10.1016/j.molcel.2005.11.024. PubMed PMID: 16427012.

103. Chen FX, Smith ER, Shilatifard A. Born to run: control of transcription elongation by RNA polymerase II. Nat Rev Mol Cell Biol. 2018;19(7):464-78. doi: 10.1038/s41580-018-0010-5. PubMed PMID: 29740129.

104. Bartkowiak B, Greenleaf AL. Phosphorylation of RNAPII: To P-TEFb or not to P-TEFb? Transcription. 2011;2(3):115-9. doi: 10.4161/trns.2.3.15004. PubMed PMID: 21826281; PubMed Central PMCID: PMCPMC3149687.

105. Sims RJ, Belotserkovskaya R, Reinberg D. Elongation by RNA polymerase II: the short and long of it. Genes Dev. 2004;18(20):2437-68. doi: 10.1101/gad.1235904. PubMed PMID: 15489290.

106. Schweikhard V, Meng C, Murakami K, Kaplan CD, Kornberg RD, Block SM. Transcription factors TFIIF and TFIIS promote transcript elongation by RNA polymerase II by synergistic and independent mechanisms. Proc Natl Acad Sci U S A. 2014;111(18):6642-7. Epub 2014/04/14. doi: 10.1073/pnas.1405181111. PubMed PMID: 24733897; PubMed Central PMCID: PMCPMC4020062.

107. Zhou Q, Li T, Price DH. RNA polymerase II elongation control. Annu Rev Biochem. 2012;81:119-43. Epub 2012/03/09. doi: 10.1146/annurev-biochem-052610-095910. PubMed PMID: 22404626; PubMed Central PMCID: PMCPMC4273853.

108. Kuehner JN, Pearson EL, Moore C. Unravelling the means to an end: RNA polymerase II transcription termination. Nat Rev Mol Cell Biol. 2011;12(5):283-94. Epub 2011/04/13. doi: 10.1038/nrm3098. PubMed PMID: 21487437.

109. Lykke-Andersen S, Jensen TH. Overlapping pathways dictate termination of RNA polymerase II transcription. Biochimie. 2007;89(10):1177-82. Epub 2007/06/02. doi: 10.1016/j.biochi.2007.05.007. PubMed PMID: 17629387.

110. Park NJ, Tsao DC, Martinson HG. The two steps of poly(A)-dependent termination, pausing and release, can be uncoupled by truncation of the RNA polymerase II carboxyl-terminal repeat domain. Mol Cell Biol. 2004;24(10):4092-103. PubMed PMID: 15121832; PubMed Central PMCID: PMCPMC400489.

111. Nag A, Narsinh K, Martinson HG. The poly(A)-dependent transcriptional pause is mediated by CPSF acting on the body of the polymerase. Nat Struct Mol Biol. 2007;14(7):662-9. Epub 2007/06/17. doi: 10.1038/nsmb1253. PubMed PMID: 17572685.

112. Kazerouninia A, Ngo B, Martinson HG. Poly(A) signal-dependent degradation of unprocessed nascent transcripts accompanies poly(A) signal-dependent transcriptional pausing in vitro. RNA. 2010;16(1):197-210. Epub 2009/11/19. doi: 10.1261/rna.1622010. PubMed PMID: 19926725; PubMed Central PMCID: PMCPMC2802029.

113. West S, Gromak N, Proudfoot NJ. Human 5' --> 3' exonuclease Xrn2 promotes transcription termination at co-transcriptional cleavage sites. Nature. 2004;432(7016):522-5. doi: 10.1038/nature03035. PubMed PMID: 15565158.

114. Steinmetz EJ, Conrad NK, Brow DA, Corden JL. RNA-binding protein Nrd1 directs poly(A)-independent 3'-end formation of RNA polymerase II transcripts. Nature. 2001;413(6853):327-31. doi: 10.1038/35095090. PubMed PMID: 11565036.

115. Steinmetz EJ, Warren CL, Kuehner JN, Panbehi B, Ansari AZ, Brow DA. Genome-wide distribution of yeast RNA polymerase II and its control by Sen1 helicase. Mol Cell. 2006;24(5):735-46. doi: 10.1016/j.molcel.2006.10.023. PubMed PMID: 17157256.

116. Gilbert W. Why genes in pieces? Nature. 1978;271(5645):501. PubMed PMID: 622185.

117. Wang Y, Liu J, Huang BO, Xu YM, Li J, Huang LF, et al. Mechanism of alternative splicing and its regulation. Biomed Rep. 2015;3(2):152-8. Epub 2014/12/17. doi: 10.3892/br.2014.407. PubMed PMID: 25798239; PubMed Central PMCID: PMCPMC4360811.

118. Nilsen TW, Graveley BR. Expansion of the eukaryotic proteome by alternative splicing. Nature. 2010;463(7280):457-63. doi: 10.1038/nature08909. PubMed PMID: 20110989; PubMed Central PMCID: PMCPMC3443858.

119. Mercer TR, Clark MB, Andersen SB, Brunck ME, Haerty W, Crawford J, et al. Genome-wide discovery of human splicing branchpoints. Genome Res. 2015;25(2):290-303. Epub 2015/01/05. doi: 10.1101/gr.182899.114. PubMed PMID: 25561518; PubMed Central PMCID: PMCPMC4315302.

120. Herzel L, Ottoz DSM, Alpert T, Neugebauer KM. Splicing and transcription touch base: co-transcriptional spliceosome assembly and function. Nat Rev Mol Cell Biol. 2017;18(10):637-50. Epub 2017/08/09. doi: 10.1038/nrm.2017.63. PubMed PMID: 28792005; PubMed Central PMCID: PMCPMC5928008.

121. Fabrizio P, Dannenberg J, Dube P, Kastner B, Stark H, Urlaub H, et al. The evolutionarily conserved core design of the catalytic activation step of the yeast spliceosome. Mol Cell. 2009;36(4):593-608. doi: 10.1016/j.molcel.2009.09.040. PubMed PMID: 19941820.

122. Will CL, Lührmann R. Spliceosome structure and function. Cold Spring Harb Perspect Biol. 2011;3(7). Epub 2011/07/01. doi: 10.1101/cshperspect.a003707. PubMed PMID: 21441581; PubMed Central PMCID: PMCPMC3119917.

123. Reed R, Maniatis T. Intron sequences involved in lariat formation during pre-mRNA splicing. Cell. 1985;41(1):95-105. PubMed PMID: 3888410.

124. Beyer AL, Bouton AH, Miller OL. Correlation of hnRNP structure and nascent transcript cleavage. Cell. 1981;26(2 Pt 2):155-65. PubMed PMID: 6174239.

125. Montes M, Becerra S, Sánchez-Álvarez M, Suñé C. Functional coupling of transcription and splicing. Gene. 2012;501(2):104-17. Epub 2012/04/17. doi: 10.1016/j.gene.2012.04.006. PubMed PMID: 22537677.

126. Abruzzi KC, Lacadie S, Rosbash M. Biochemical analysis of TREX complex recruitment to intronless and intron-containing yeast genes. EMBO J. 2004;23(13):2620-31. Epub 2004/06/10. doi: 10.1038/sj.emboj.7600261. PubMed PMID: 15192704; PubMed Central PMCID: PMCPMC449771.

127. David CJ, Boyne AR, Millhouse SR, Manley JL. The RNA polymerase II C-terminal domain promotes splicing activation through recruitment of a U2AF65-Prp19 complex. Genes Dev. 2011;25(9):972-83. doi: 10.1101/gad.2038011. PubMed PMID: 21536736; PubMed Central PMCID: PMCPMC3084030.

128. McCracken S, Fong N, Yankulov K, Ballantyne S, Pan G, Greenblatt J, et al. The C-terminal domain of RNA polymerase II couples mRNA processing to transcription. Nature. 1997;385(6614):357-61. doi: 10.1038/385357a0. PubMed PMID: 9002523.

129. Merkhofer EC, Hu P, Johnson TL. Introduction to cotranscriptional RNA splicing. Methods Mol Biol. 2014;1126:83-96. doi: 10.1007/978-1-62703-980-2_6. PubMed PMID: 24549657; PubMed Central PMCID: PMCPMC4102251.

130. Ip JY, Schmidt D, Pan Q, Ramani AK, Fraser AG, Odom DT, et al. Global impact of RNA polymerase II elongation inhibition on alternative splicing regulation. Genome Res. 2011;21(3):390-401. Epub 2010/12/16. doi: 10.1101/gr.111070.110. PubMed PMID: 21163941; PubMed Central PMCID: PMCPMC3044853.

131. de la Mata M, Alonso CR, Kadener S, Fededa JP, Blaustein M, Pelisch F, et al. A slow RNA polymerase II affects alternative splicing in vivo. Mol Cell. 2003;12(2):525-32. PubMed PMID: 14536091.

132. Howe KJ, Kane CM, Ares M. Perturbation of transcription elongation influences the fidelity of internal exon inclusion in Saccharomyces cerevisiae. RNA. 2003;9(8):993-1006. PubMed PMID: 12869710; PubMed Central PMCID: PMCPMC1370465.

133. Chathoth KT, Barrass JD, Webb S, Beggs JD. A splicing-dependent transcriptional checkpoint associated with prespliceosome formation. Mol Cell. 2014;53(5):779-90. Epub 2014/02/20. doi: 10.1016/j.molcel.2014.01.017. PubMed PMID: 24560925; PubMed Central PMCID: PMCPMC3988880.

134. Orphanides G, LeRoy G, Chang CH, Luse DS, Reinberg D. FACT, a factor that facilitates transcript elongation through nucleosomes. Cell. 1998;92(1):105-16. PubMed PMID: 9489704.

135. Saunders A, Werner J, Andrulis ED, Nakayama T, Hirose S, Reinberg D, et al. Tracking FACT and the RNA polymerase II elongation complex through chromatin in vivo. Science. 2003;301(5636):1094-6. doi: 10.1126/science.1085712. PubMed PMID: 12934007.

136. Teves SS, Weber CM, Henikoff S. Transcribing through the nucleosome. Trends Biochem Sci. 2014;39(12):577-86. doi: 10.1016/j.tibs.2014.10.004. PubMed PMID: 25455758.

137. Fontana F. Traité sur le venin de la vipère, avec des observations sur la structure primitive du corps animale. 1781.

138. Mélèse T, Xue Z. The nucleolus: an organelle formed by the act of building a ribosome. Curr Opin Cell Biol. 1995;7(3):319-24. PubMed PMID: 7662360.

139. BROWN DD, GURDON JB. ABSENCE OF RIBOSOMAL RNA SYNTHESIS IN THE ANUCLEOLATE MUTANT OF XENOPUS LAEVIS. Proc Natl Acad Sci U S A. 1964;51:139-46. PubMed PMID: 14106673; PubMed Central PMCID: PMCPMC300879.

140. Andersen JS, Lyon CE, Fox AH, Leung AK, Lam YW, Steen H, et al. Directed proteomic analysis of the human nucleolus. Curr Biol. 2002;12(1):1-11. PubMed PMID: 11790298.

141. Politz JC, Hogan EM, Pederson T. MicroRNAs with a nucleolar location. RNA. 2009;15(9):1705-15. Epub 2009/07/23. doi: 10.1261/rna.1470409. PubMed PMID: 19628621; PubMed Central PMCID: PMCPMC2743059.

142. Sirri V, Urcuqui-Inchima S, Roussel P, Hernandez-Verdun D. Nucleolus: the fascinating nuclear body. Histochem Cell Biol. 2008;129(1):13-31. Epub 2007/11/29. doi: 10.1007/s00418-007-0359-6. PubMed PMID: 18046571; PubMed Central PMCID: PMCPMC2137947.

143. Tsekrekou M, Stratigi K, Chatzinikolaou G. The Nucleolus: In Genome Maintenance and Repair. Int J Mol Sci. 2017;18(7). Epub 2017/07/01. doi: 10.3390/ijms18071411. PubMed PMID: 28671574; PubMed Central PMCID: PMCPMC5535903.

144. Christensen MO, Barthelmes HU, Boege F, Mielke C. The N-terminal domain anchors human topoisomerase I at fibrillar centers of nucleoli and nucleolar organizer regions of mitotic chromosomes. J Biol Chem. 2002;277(39):35932-8. Epub 2002/07/15. doi: 10.1074/jbc.M204738200. PubMed PMID: 12119295.

145. Henderson AS, Warburton D, Atwood KC. Location of ribosomal DNA in the human chromosome complement. Proc Natl Acad Sci U S A. 1972;69(11):3394-8. PubMed PMID: 4508329; PubMed Central PMCID: PMCPMC389778.

146. Gautier T, Fomproix N, Masson C, Azum-Gélade MC, Gas N, Hernandez-Verdun D. Fate of specific nucleolar perichromosomal proteins during mitosis: cellular distribution and association with U3 snoRNA. Biol Cell. 1994;82(2-3):81-93. PubMed PMID: 7606218.

147. Roussel P, André C, Comai L, Hernandez-Verdun D. The rDNA transcription machinery is assembled during mitosis in active NORs and absent in inactive NORs. J Cell Biol. 1996;133(2):235-46. PubMed PMID: 8609158; PubMed Central PMCID: PMCPMC2120807.

148. Gébrane-Younès J, Fomproix N, Hernandez-Verdun D. When rDNA transcription is arrested during mitosis, UBF is still associated with non-condensed rDNA. J Cell Sci. 1997;110 (Pt 19):2429-40. PubMed PMID: 9410881.

149. Dousset T, Wang C, Verheggen C, Chen D, Hernandez-Verdun D, Huang S. Initiation of nucleolar assembly is independent of RNA polymerase I transcription. Mol Biol Cell. 2000;11(8):2705-17. doi: 10.1091/mbc.11.8.2705. PubMed PMID: 10930464; PubMed Central PMCID: PMCPMC14950.

150. Hernandez-Verdun D, Roussel P, Thiry M, Sirri V, Lafontaine DL. The nucleolus: structure/function relationship in RNA metabolism. Wiley Interdiscip Rev RNA. 2010;1(3):415-31. Epub 2010/09/22. doi: 10.1002/wrna.39. PubMed PMID: 21956940.

151. Dundr M, Misteli T, Olson MO. The dynamics of postmitotic reassembly of the nucleolus. J Cell Biol. 2000;150(3):433-46. PubMed PMID: 10931858; PubMed Central PMCID: PMCPMC2175201.

152. Savino TM, Gébrane-Younès J, De Mey J, Sibarita JB, Hernandez-Verdun D. Nucleolar assembly of the rRNA processing machinery in living cells. J Cell Biol. 2001;153(5):1097-110. PubMed PMID: 11381093; PubMed Central PMCID: PMCPMC2174343.

153. Miller OL, Beatty BR. Visualization of nucleolar genes. Science. 1969;164(3882):955-7. PubMed PMID: 5813982.

154. Long EO, Dawid IB. Repeated genes in eukaryotes. Annu Rev Biochem. 1980;49:727-64. doi: 10.1146/annurev.bi.49.070180.003455. PubMed PMID: 6996571.

155. Lam YW, Trinkle-Mulcahy L. New insights into nucleolar structure and function. F1000Prime Rep. 2015;7:48. Epub 2015/04/02. doi: 10.12703/P7-48. PubMed PMID: 26097721; PubMed Central PMCID: PMCPMC4447046.

156. Floutsakou I, Agrawal S, Nguyen TT, Seoighe C, Ganley AR, McStay B. The shared genomic architecture of human nucleolar organizer regions. Genome Res. 2013;23(12):2003-12. Epub

2013/08/29. doi: 10.1101/gr.157941.113. PubMed PMID: 23990606; PubMed Central PMCID: PMCPMC3847771.

157. Moore PB, Steitz TA. The involvement of RNA in ribosome function. Nature. 2002;418(6894):229-35. doi: 10.1038/418229a. PubMed PMID: 12110899.

158. Moss T, Stefanovsky VY. At the center of eukaryotic life. Cell. 2002;109(5):545-8. Epub 2002/06/14. PubMed PMID: 12062097.

159. Dundr M, Hoffmann-Rohrer U, Hu Q, Grummt I, Rothblum LI, Phair RD, et al. A kinetic framework for a mammalian RNA polymerase in vivo. Science. 2002;298(5598):1623-6. doi: 10.1126/science.1076164. PubMed PMID: 12446911.

160. Russell J, Zomerdijk JC. The RNA polymerase I transcription machinery. Biochem Soc Symp. 2006(73):203-16. PubMed PMID: 16626300; PubMed Central PMCID: PMCPMC3858827.

161. Haag JR, Pikaard CS. RNA polymerase I: a multifunctional molecular machine. Cell. 2007;131(7):1224-5. doi: 10.1016/j.cell.2007.12.005. PubMed PMID: 18160031.

162. Kuhn CD, Geiger SR, Baumli S, Gartmann M, Gerber J, Jennebach S, et al. Functional architecture of RNA polymerase I. Cell. 2007;131(7):1260-72. doi: 10.1016/j.cell.2007.10.051. PubMed PMID: 18160037.

163. Beckouet F, Labarre-Mariotte S, Albert B, Imazawa Y, Werner M, Gadal O, et al. Two RNA polymerase I subunits control the binding and release of Rrn3 during transcription. Mol Cell Biol. 2008;28(5):1596-605. Epub 2007/12/17. doi: 10.1128/MCB.01464-07. PubMed PMID: 18086878; PubMed Central PMCID: PMCPMC2258765.

164. Albert B, Léger-Silvestre I, Normand C, Ostermaier MK, Pérez-Fernández J, Panov KI, et al. RNA polymerase I-specific subunits promote polymerase clustering to enhance the rRNA gene transcription cycle. J Cell Biol. 2011;192(2):277-93. doi: 10.1083/jcb.201006040. PubMed PMID: 21263028; PubMed Central PMCID: PMCPMC3172167.

165. Goodfellow SJ, Zomerdijk JC. Basic mechanisms in RNA polymerase I transcription of the ribosomal RNA genes. Subcell Biochem. 2013;61:211-36. doi: 10.1007/978-94-007-4525-4_10. PubMed PMID: 23150253; PubMed Central PMCID: PMCPMC3855190.

166. Comai L, Tanese N, Tjian R. The TATA-binding protein and associated factors are integral components of the RNA polymerase I transcription factor, SL1. Cell. 1992;68(5):965-76. PubMed PMID: 1547496.

167. Friedrich JK, Panov KI, Cabart P, Russell J, Zomerdijk JC. TBP-TAF complex SL1 directs RNA polymerase I pre-initiation complex formation and stabilizes upstream binding factor at the rDNA promoter. J Biol Chem. 2005;280(33):29551-8. Epub 2005/06/21. doi: 10.1074/jbc.M501595200. PubMed PMID: 15970593; PubMed Central PMCID: PMCPMC3858828.

168. Schmitz KM, Schmitt N, Hoffmann-Rohrer U, Schäfer A, Grummt I, Mayer C. TAF12 recruits Gadd45a and the nucleotide excision repair complex to the promoter of rRNA genes leading to active DNA demethylation. Mol Cell. 2009;33(3):344-53. doi: 10.1016/j.molcel.2009.01.015. PubMed PMID: 19217408.

169. Miller G, Panov KI, Friedrich JK, Trinkle-Mulcahy L, Lamond AI, Zomerdijk JC. hRRN3 is essential in the SL1-mediated recruitment of RNA Polymerase I to rRNA gene promoters. EMBO J. 2001;20(6):1373-82. doi: 10.1093/emboj/20.6.1373. PubMed PMID: 11250903; PubMed Central PMCID: PMCPMC145519.

170. Cavanaugh AH, Hirschler-Laszkiewicz I, Hu Q, Dundr M, Smink T, Misteli T, et al. Rrn3 phosphorylation is a regulatory checkpoint for ribosome biogenesis. J Biol Chem.

2002;277(30):27423-32. Epub 2002/05/15. doi: 10.1074/jbc.M201232200. PubMed PMID: 12015311.

171. Bierhoff H, Dundr M, Michels AA, Grummt I. Phosphorylation by casein kinase 2 facilitates rRNA gene transcription by promoting dissociation of TIF-IA from elongating RNA polymerase I. Mol Cell Biol. 2008;28(16):4988-98. Epub 2008/06/16. doi: 10.1128/MCB.00492-08. PubMed PMID: 18559419; PubMed Central PMCID: PMCPMC2519707.

172. Lin CY, Navarro S, Reddy S, Comai L. CK2-mediated stimulation of Pol I transcription by stabilization of UBF-SL1 interaction. Nucleic Acids Res. 2006;34(17):4752-66. Epub 2006/09/13. doi: 10.1093/nar/gkl581. PubMed PMID: 16971462; PubMed Central PMCID: PMCPMC1635259.

173. Panova TB, Panov KI, Russell J, Zomerdijk JC. Casein kinase 2 associates with initiation-competent RNA polymerase I and has multiple roles in ribosomal DNA transcription. Mol Cell Biol. 2006;26(16):5957-68. doi: 10.1128/MCB.00673-06. PubMed PMID: 16880508; PubMed Central PMCID: PMCPMC1592790.

174. Jantzen HM, Admon A, Bell SP, Tjian R. Nucleolar transcription factor hUBF contains a DNA-binding motif with homology to HMG proteins. Nature. 1990;344(6269):830-6. doi: 10.1038/344830a0. PubMed PMID: 2330041.

175. Panov KI, Panova TB, Gadal O, Nishiyama K, Saito T, Russell J, et al. RNA polymerase I-specific subunit CAST/hPAF49 has a role in the activation of transcription by upstream binding factor. Mol Cell Biol. 2006;26(14):5436-48. doi: 10.1128/MCB.00230-06. PubMed PMID: 16809778; PubMed Central PMCID: PMCPMC1592716.

176. Russell J, Zomerdijk JC. RNA-polymerase-I-directed rDNA transcription, life and works. Trends Biochem Sci. 2005;30(2):87-96. PubMed PMID: 15691654.

177. Hirschler-Laszkiewicz I, Cavanaugh AH, Mirza A, Lun M, Hu Q, Smink T, et al. Rrn3 becomes inactivated in the process of ribosomal DNA transcription. J Biol Chem. 2003;278(21):18953-9. Epub 2003/03/19. doi: 10.1074/jbc.M301093200. PubMed PMID: 12646563.

178. Iben S, Tschochner H, Bier M, Hoogstraten D, Hozak P, Egly JM, et al. TFIIH plays an essential role in RNA polymerase I transcription. Cell. 2002;109(3):297-306. PubMed PMID: 12015980.

179. Panov KI, Friedrich JK, Zomerdijk JC. A step subsequent to preinitiation complex assembly at the ribosomal RNA gene promoter is rate limiting for human RNA polymerase I-dependent transcription. Mol Cell Biol. 2001;21(8):2641-9. doi: 10.1128/MCB.21.8.2641-2649.2001. PubMed PMID: 11283244; PubMed Central PMCID: PMCPMC86895.

180. Jansa P, Burek C, Sander EE, Grummt I. The transcript release factor PTRF augments ribosomal gene transcription by facilitating reinitiation of RNA polymerase I. Nucleic Acids Res. 2001;29(2):423-9. PubMed PMID: 11139612; PubMed Central PMCID: PMCPMC29675.

181. El Hage A, Koper M, Kufel J, Tollervey D. Efficient termination of transcription by RNA polymerase I requires the 5' exonuclease Rat1 in yeast. Genes Dev. 2008;22(8):1069-81. doi: 10.1101/gad.463708. PubMed PMID: 18413717; PubMed Central PMCID: PMCPMC2335327.

182. Pontvianne F, Blevins T, Chandrasekhara C, Mozgová I, Hassel C, Pontes OM, et al. Subnuclear partitioning of rRNA genes between the nucleolus and nucleoplasm reflects alternative epiallelic states. Genes Dev. 2013;27(14):1545-50. doi: 10.1101/gad.221648.113. PubMed PMID: 23873938; PubMed Central PMCID: PMCPMC3731543.

183. McStay B, Grummt I. The epigenetics of rRNA genes: from molecular to chromosome biology. Annu Rev Cell Dev Biol. 2008;24:131-57. doi: 10.1146/annurev.cellbio.24.110707.175259. PubMed PMID: 18616426.

184. Santoro R, Grummt I. Epigenetic mechanism of rRNA gene silencing: temporal order of NoRC-mediated histone modification, chromatin remodeling, and DNA methylation. Mol Cell Biol. 2005;25(7):2539-46. doi: 10.1128/MCB.25.7.2539-2546.2005. PubMed PMID: 15767661; PubMed Central PMCID: PMCPMC1061655.

185. Zhou Y, Santoro R, Grummt I. The chromatin remodeling complex NoRC targets HDAC1 to the ribosomal gene promoter and represses RNA polymerase I transcription. EMBO J. 2002;21(17):4632-40. PubMed PMID: 12198165; PubMed Central PMCID: PMCPMC126197.

186. Moss T, Mars JC, Tremblay MG, Sabourin-Felix M. The chromatin landscape of the ribosomal RNA genes in mouse and human. Chromosome Res. 2019;27(1-2):31-40. Epub 2019/01/08. doi: 10.1007/s10577-018-09603-9. PubMed PMID: 30617621.

187. Daniel L, Cerutti E, Donnio LM, Nonnekens J, Carrat C, Zahova S, et al. Mechanistic insights in transcription-coupled nucleotide excision repair of ribosomal DNA. Proc Natl Acad Sci U S A. 2018;115(29):E6770-E9. Epub 2018/07/02. doi: 10.1073/pnas.1716581115. PubMed PMID: 29967171; PubMed Central PMCID: PMCPMC6055190.

188. Conconi A, Bespalov VA, Smerdon MJ. Transcription-coupled repair in RNA polymerase I-transcribed genes of yeast. Proc Natl Acad Sci U S A. 2002;99(2):649-54. Epub 2002/01/10. doi: 10.1073/pnas.022373099. PubMed PMID: 11782531; PubMed Central PMCID: PMC117360.

189. Franek M, Kovarikova A, Bartova E, Kozubek S. Nucleolar Reorganization Upon Site-Specific Double-Strand Break Induction. J Histochem Cytochem. 2016;64(11):669-86. doi: 10.1369/0022155416668505. PubMed PMID: 27680669; PubMed Central PMCID: PMCPMC5084524.

190. Larsen DH, Stucki M. Nucleolar responses to DNA double-strand breaks. Nucleic Acids Res. 2016;44(2):538-44. doi: 10.1093/nar/gkv1312. PubMed PMID: 26615196; PubMed Central PMCID: PMCPMC4737151.

191. van Sluis M, McStay B. A localized nucleolar DNA damage response facilitates recruitment of the homology-directed repair machinery independent of cell cycle stage. Genes Dev. 2015;29(11):1151-63. doi: 10.1101/gad.260703.115. PubMed PMID: 26019174; PubMed Central PMCID: PMCPMC4470283.

192. Dimitrova DS. DNA replication initiation patterns and spatial dynamics of the human ribosomal RNA gene loci. J Cell Sci. 2011;124(Pt 16):2743-52. doi: 10.1242/jcs.082230. PubMed PMID: 21807939.

193. Tessarz P, Santos-Rosa H, Robson SC, Sylvestersen KB, Nelson CJ, Nielsen ML, et al. Glutamine methylation in histone H2A is an RNA-polymerase-I-dedicated modification. Nature. 2014;505(7484):564-8. Epub 2013/12/20. doi: 10.1038/nature12819. PubMed PMID: 24352239; PubMed Central PMCID: PMC3901671.

194. Wu MH, Yung BY. UV stimulation of nucleophosmin/B23 expression is an immediate-early gene response induced by damaged DNA. J Biol Chem. 2002;277(50):48234-40. Epub 2002/10/08. doi: 10.1074/jbc.M206550200. PubMed PMID: 12374805.

195. Tourbez M, Firanescu C, Yang A, Unipan L, Duchambon P, Blouquit Y, et al. Calcium-dependent self-assembly of human centrin 2. J Biol Chem. 2004;279(46):47672-80. Epub 2004/09/08. doi: 10.1074/jbc.M404996200. PubMed PMID: 15356003.

196. West AE, Chen WG, Dalva MB, Dolmetsch RE, Kornhauser JM, Shaywitz AJ, et al. Calcium regulation of neuronal gene expression. Proc Natl Acad Sci U S A. 2001;98(20):11024-31. doi: 10.1073/pnas.191352298. PubMed PMID: 11572963; PubMed Central PMCID: PMCPMC58677.

197. Tsui C, Inouye C, Levy M, Lu A, Florens L, Washburn MP, et al. dCas9-targeted locus-specific protein isolation method identifies histone gene regulators. Proc Natl Acad Sci U S A.

2018;115(12):E2734-E41. Epub 2018/03/05. doi: 10.1073/pnas.1718844115. PubMed PMID: 29507191; PubMed Central PMCID: PMCPMC5866577.

198. Kuraoka I, Ito S, Wada T, Hayashida M, Lee L, Saijo M, et al. Isolation of XAB2 complex involved in pre-mRNA splicing, transcription, and transcription-coupled repair. J Biol Chem. 2008;283(2):940-50. Epub 2007/11/02. doi: 10.1074/jbc.M706647200. PubMed PMID: 17981804.